INSTITUTO POTOSINO DE INVESTIGACIÓN CIENTÍFICA Y TECNOLÓGICA, A.C.

POSGRADO EN CIENCIAS APLICADAS

Variability of carbon fluxes at different time-scales and their biotic and environmental controls on a short-grass steppe in Central Mexico

Tesis que presenta

Josué Delgado Balbuena

Para obtener el grado de

Doctor en Ciencias Aplicadas

En la opción de

Ciencias Ambientales

Codirectores de la Tesis:

Dr. José Tulio Arredondo Moreno

Dr. Henry W. Loescher

San Luis Potosí, S.L.P., abril de 2016

Constancia de aprobación de la tesis

La tesis **"Variability of carbon fluxes at different time-scales and their biotic and environmental controls on a short-grass steppe in Central Mexico"** presentada para obtener el Grado de Doctor en Ciencias Aplicadas en la opción de Ciencias Ambientales fue elaborada por **Josué Delgado Balbuena** y aprobada el **4 de abril de 2016** por los suscritos, designados por el Colegio de Profesores de la División de Ciencias Ambientales del Instituto Potosino de Investigación Científica y Tecnológica, A.C.

_____
Dr. José Tulio Arredondo Moreno
(Codirector)

_____
Dr. Henry W. Loescher
(Codirector)

_____
Dr. Felipe Pineda Martínez
(Asesor)

_____
Dr. José Noel Carbajal Pérez
(Asesor)

_____
Dra. Elisabet Huber-Sannwald
(Asesor)

Créditos Institucionales

Esta tesis fue elaborada en el Laboratorio de Ecología de la División de Ciencias Ambientales del Instituto Potosino de Investigación Científica y Tecnológica, A.C., bajo la codirección de los Doctores José Tulio Arredondo Moreno y Henry W. Loescher.

Durante la realización del trabajo el autor recibió una beca académica del Consejo Nacional de Ciencia y Tecnología (No. de registro **211819**) y del Instituto Potosino de Investigación Científica y Tecnológica, A. C.

La investigación de esta tesis fue financiada como parte del proyecto SEMARNAT-CONACYT num. ref.108000, CB 2008-01 102855, CB 2013 220788.

IPICYT

Instituto Potosino de Investigación Científica y Tecnológica, A.C.

Acta de Examen de Grado

El Secretario Académico del Instituto Potosino de Investigación Científica y Tecnológica, A.C., certifica que en el Acta 030 del Libro Primero de Actas de Exámenes de Grado del Programa de Doctorado en Ciencias Aplicadas en la opción de Ciencias Ambientales está asentado lo siguiente:

En la ciudad de San Luis Potosí a los 4 días del mes de abril del año 2016, se reunió a las 13:00 horas en las instalaciones del Instituto Potosino de Investigación Científica y Tecnológica, A.C., el Jurado integrado por:

Dr. José Noel Carbajal Pérez	**Presidente**	**IPICYT**
Dr. Luis Felipe Pineda Martínez	**Secretario**	**UAZ**
Dr. José Tulio Arredondo Moreno	**Sinodal**	**IPICYT**

a fin de efectuar el examen, que para obtener el Grado de:

DOCTOR EN CIENCIAS APLICADAS
EN LA OPCION DE CIENCIAS AMBIENTALES

sustentó el C.

Josué Delgado Balbuena

sobre la Tesis intitulada:

Variability of carbon fluxes at different time-scales and their biotic and environmental controls on a short-grass steppe in Central Mexico

que se desarrolló bajo la dirección de

Dr. José Tulio Arredondo Moreno
Dr. Henry William Loescher (NEON)

El Jurado, después de deliberar, determinó

APROBARLO

Dándose por terminado el acto a las 16:04 horas, procediendo a la firma del Acta los integrantes del Jurado. Dando fe el Secretario Académico del Instituto.

A petición del interesado y para los fines que al mismo convengan, se extiende el presente documento en la ciudad de San Luis Potosí, S.L.P., México, a los 4 días del mes de abril de 2016.

Dr. Marcial Bonilla Marín
Secretario Académico

Mtra. Ivonne Lizette Cuevas Vélez
Jefa del Departamento del Posgrado

INSTITUTO POTOSINO DE INVESTIGACIÓN CIENTÍFICA Y TECNOLÓGICA, A.C.
IPICYT
SECRETARIA ACADEMICA

A Laura y Sara Yaretzi

Y a mis padres, Cecilia y Alfonso

Agradecimientos

Quiero agradecer al Dr. Tulio Arredondo Moreno por su apoyo en el trabajo de campo y por su asesoría y revisión durante el transcurso de esta tesis.

Al Dr. Henry W. Loescher por sus comentarios y el tiempo invertido en la revisión de este trabajo.

Al Dr. Felipe Pineda Martínez, Dr. J. Noel Carbajal Pérez y Dr. Rodrigo Vargas Ramos por sus comentarios y revisiones al trabajo de tesis.

A la Dra. Elisabeth Huber-Sannwald por sus valiosos comentarios.

A los técnicos académicos M. en C. Dulce Isela de Fátima Partida, M. en C. Guillermo Vidriales Escobar y M. en C. Juan Pablo Rodas Ortiz, por su apoyo y facilidades otorgadas en el laboratorio de Ecología.

Agradezco al Laboratorio de Ecología del IPICYT y al Campo Experimental "Vaquerías" del INIFAP por las facilidades otorgadas para el desarrollo del presente trabajo.

A los amigos de IPICYT que me acompañaron en esta "larga" estancia.

Table of Contents

Créditos Institucionales iii

Acta de Examen de Grado iv

Agradecimientos vi

List of Tables ix

Resumen xv

General Introduction 1

Chapter 1

Precipitation legacy effects and environmental drivers on C fluxes of a semiarid grassland in Mexico 4

Materials and Methods ***10***
Site description 10
Meteorological and soil measurements 11
Net ecosystem CO_2 exchange measurements 11
Data processing, gap filling methods and statistical analysis 12
Gap filling methods and flux partitioning 15
Environmental drivers 15
Enhanced vegetation index (EVI) data 17
Ecosystem water use efficiency 18
Hydroecological years 19

Results ***20***
Energy balance 20
Environmental variables 21
Diurnal and seasonal patterns of NEE 24
Using hydroecological years instead of calendar years 26
CO2 balance and precipitation legacy effects 26
Environmental drivers 30
Enhanced vegetation index (EVI) 33
Inherent water use efficiency 35

Discussion ***36***
Energy balance 36
Environmental drivers 37
Implications for the use of whole day data in light-response curve models 39
NEE responses to PPT 39
Precipitation legacies 40
Precipitation legacies: NEE components 45

Conclusions ***46***

Appendix ***47***
Phenological phases calculations with EVI 47

References ***52***

Chapter 2

Drivers and dynamics of CO_2 fluxes following precipitation events in the semiarid grassland **64**

Introduction ***65***

Materials and methods ***71***
Site description 71
Meteorological and soil measurements 72
Net ecosystem CO_2 exchange measurements 73
Data processing 74
Gap filling procedures and characterization of PPT events 76
Statistical analysis 77

Results ***77***
Precipitation pattern 78
Short-term effects of precipitation events on carbon fluxes. 81
Drivers of the priming NEE effect 84
Variable thresholds 90

Discussion ***90***
"Priming carbon flux effect" of precipitation events 91
Variable thresholds 92
Influence of event size and a priori conditions 94
Decaying NEE rates 96
About the application of the T-D model to describe the "priming NEE effect" 97

Conclusion ***97***

Appendix ***99***
Threshold-Delay Model equations 99

References ***105***

General conclusions **113**

List of Tables

Chapter 1

Table A 1. Calculated parameters for EVI curves from Eq. 10. A0 stands for basal EVI, A1 is the maximum EVI, t0 is the center of the curve (date), dt is related to the slope of the curve with larger slopes indicating shallower curves, and slope at t0 is the calculated slope at the center of the curve (EVI/day). Values are means ± 1 S.E. Uppercase acronyms after year mean S for summer and W for winter seasons, and lowercase *s* and *e* stand for the start and the end of the growing seasons, respectively. 50

Table A 2. Calculated parameters for bivariate curves among soil volumetric water content (VWC, v/v) at 2.5 cm depth, enhanced vegetation index (EVI), and nighttime NEE (g C m^{-2} s^{-1}) in the form, $NEE_{nighttime} = y_0 + a*VWC + b*EVI$. All regressions were significant at α = 0.05. 52

Chapter 2

Table 1. Results of bivariate regression analysis among ΔNEE (μmol m-2 s-1) and PPT event size (PPT_event, mm), inter-event period (DSLE, days), change of volumetric soil water content (ΔVWC, v/v), and previous volumetric soil water content (prevVWC, v/v). The selected model was ΔNEE =a+bx+cy+dx2+ey2+fxy, where a, b, c, d, e, and f are calculated parameters and x and y are any of the independent variables. 86

Table A1. Calculated parameters of exponential decay models (NEE= y0 + a * Exp(-k*t), means ± 1 S.E.) for the daytime NEE after a PPT event. Relationship between the PPT sulse size (mm) and the decaying rate of above regressions is presented in the last row with the same negative exponential equation form –k = y0 + a * Exp(-b*PPT_event), where -k = -b. 104

Table A2.Calculated coefficients of bivariate quadratic regressions of Eq. 2, where ΔNEE stands for the change in net ecosystem exchange (μmol m-2 s-1), PPT_event is the PPT event size (mm), DSLE is the inter-event period (days), ΔVWC is the change of volumetric soil water content (v/v), prevNEE is the net ecosystem exchange (μmol m-2 s-1) previous to the PPT event, and prevVWC is previous volumetric soil water content (v/v). 104

List of Figures

Chapter 1

Figure 1. Asymmetric sensitivity hypothesis. Differential responses of C uptake and respiration to PPT can cause the attenuation of the positive C balance response at wetter years, which coincides with lower slopes observed in temporal annual precipitation-productivity models when are compared to general spatial models (lower left panel). While ecosystem C uptake increases linearly, asymptotically, or stepper on wet years with precipitation, ecosystem respiration does it almost linearly but with a lower change rate. Temporally, C balances in ecosystems experiencing changes from pre-dry to wet years are lower than the expected by the spatial model, coinciding with Sala et al. (2012) legacy effects hypothesis (H1 and H3, see below). If C uptake and respiration equally respond to PPT change, no additional effect on C balance of previous year PPT should be expected (a). A stepper response of C uptake than respiration to PPT should induce similar additional effects on C balance (b); whereas asymptotic response of C uptake at extreme humid years should display lower positive effects on C balance of previous wet years (c); or if C uptake is more sensitive to wet than dry years, larger positive effect on C balance should be expected by previous wet years (d). 8

Figure 2.Energy balance for each year during the study period, including all available data. Points represent half hour energy flux data. The line represents the linear fitting between available energy and sensible and latent energy fluxes. The two lines for 2011 describe the energy balance without the addition of storage and soil heat flux (slope 1), and with the inclusion of both terms (slope 2). 21

Figure 3 Interannual variation of air temperature (°C), photosynthetic photon flux density (PPFD), and vapor pressure deficit (VPD) for the study period (values are daily means). Lines represent daily mean values (a – c) and points are the average daily cycle (annual means by hour ± 1 S.E.). 22

Figure 4.Seasonal and interannual variation of daily precipitation and cummulative precipitation (a), and volumetric soil water content at 2.5 cm and 15 cm depth (gray and black line, respectively, b). 24

Figure 5.Distribution of precipitation events (a) and cumulative precipitation by precipitation events classes (b). 24

Figure 6.Whole year averaged daily course of net ecosystem exchange among years (NEE, μmol m^{-2} s^{-1}, mean ± 1 S.E.). 25

Figure 7.Seasonal and interannual variation of integrated NEE (black bars, g C m^{-2} d^{-1}), and cumulative NEE for each hydroecological year (HEY, dashed lines) and across the calendar year (solid lines). Vertical solid lines represent the division between calendar years, whereas dashed vertical lines stand for HEY divisions. 28

Figure 8.Linear relationship between annual precipitation and annually integrated NEE (a) and NEE partitioned fluxes (GEE and ER) (b). 28

Figure 9.Legacy effects of previous precipitation year. Points represent legacies calculated with Eq. 9, and lines show the linear fitting between legacies and previous-year precipitation. 29

Figure 10.a) Relationship between NEE and current PPT for half hydroecological years (Dec – May, and Jun – Nov), and b) relationship between residuals of NEE-current PPT model and previous half-HEY period PPT. White dots stand for December-May period (winter-spring), and black dots stand for June-November periods (summer-fall). 29

Figure 11. a) Relationship between Ecosystem respiration (ER), gross ecosystem exchange (GEE) and current half-hydroecological year PPT, and b) relationships of residuals of ER and GEE and previous half-HEY period PPT. White dots refer to winter-spring and black dots refer to summer-fall periods. 30

Figure 12.Observed and modeled NEE fluxes for each year. Solid gray lines represent the linear fit between observed and modeled NEE whereas the dashed lines stand for the 1:1 relationship. 31

Figure 13.Seasonal and interannual variation of physiological parameters obtained from the modified light response curve (Eq. 8). Points are weekly mean values ± 1 S.E. of apparent quantum yield (α, a), maximum photosynthetic capacity (Amax, b), respiration sensitivity to temperature (Q_{10}, c), and basal respiration at 15 °C (R_b, d). Vertical dashed lines stand for the end of the hydroecological year (HEY, at week 48) and the beginning of the next year. 32

Figure 14.Relationship between Enhanced Vegetation Index (EVI) and gross ecosystem exchange (GEE, g C m^{-2} d^{-1}) for eachr year. Points indicate weekly means (±1 S.E.), and lines are the lineal fittings. The shortest line with steeper slope in light gray colour that stands out from the rest, describes the trend of the relationship observed during the winter growing season of 2012 and 2014. 34

Figure 15.Relationship between the growing season length (GSL, days) and the annual net ecosystem exchange (NEE, g C m^{-2} y^{-1}). 35

Figure 16.Seasonal and interannual variation of inherent water use efficiency (IWUE, g C hPa / kg H_2O, means by week ± 1 S.E.). Vertical dashed line in plot represents the division of hydroecological years (a). Relationship between the weekly averaged GEE * VPD (g C m^{-2} d^{-1}hPa ± S.E.) and ET (mm H_2O d^{-1} ± S.E.) for 2011 ___, 2012 _ _ _, 2013_._._, and 2014 …. (b). Only IWUE values for growing periods are shown. 36

Figure A 1. Linear relationship between annual precipitation and annually integrated NEE (a) and their partitioned fluxes (GEE and ER, b) by calendar years. 48

Figure A 2. Linear relationship between previous-year precipitation and residuals of current-year PPT - integrated NEE relationship (a) and their partitioned fluxes (GEE and ER, b) by calendar years. 49

Figure A 3. Cumulative seasonal precipitation, where *w* stands for winter and *s* for summer season. 49

Figure A 4. Enhanced vegetation index (EVI, uniteless) values for the entire measurement period.DOY stands for day of year since 01/01/2011. 50

Figure A 5. Bivariate relationship among weakly means of soil volumetric water content (VWC, v/v) at 2.5 cm depth, enhanced vegetation index (EVI), and nighttime NEE (g C m-2 s-1). The plane describes the fitting of the model NEEnighttime = y0 + a*VWC + b*EVI. Parameters of models in Table A2. 51

Chapter 2

Figure 1. The Threshold-Delay model (Ogle and Reynolds, 2004). a) The magnitude of the increase in the response variable (Δt, e.g. carbon flux, yt) is determined by the size of PPT event and by the previous state of the response variable. The decreasing rate of the response following the stimulus is denoted by –k. The low PPT threshold (RL) indicates the minimum size PPT event to stimulate a response, and the upper PPT threshold (RU) indicatesPPT events that do not cause additional increment in the response variable. The time interval between the stimulus and the response is described by τ. b) The response of the net ecosystem exchange (NEE), that is the balance between the gross ecosystem exchange (GEE) and ecosystem respiration (ER), vary in response to changes of GEE and ER. According to the T-D model, GEE and ER have different PPT thresholds (doted band and mesh stand for effective PPT events size for ER and GEE, respectively), with ER responding to smaller size PPT events than GEE, therefore, small PPT events favor C release whereas large PPT events stimulate net C uptake by the ecosystem. Differences of time responses between soil microorganisms and plants to soil wet up led GEE and ER to differ in time delays (τ), with shorter time delays for ER than GEE (Huxman et al., 2004a). The hypothetical curve for NEE and its components was calculated introducing arbitrary parameters in the T-D model equations of Ogle and Reynolds (2004). 69

Figure 2. Seasonal and interannual variation of daily precipitation and cummulative precipitation (a), and volumetric soil water content at 2.5 (black line) and 15 cm depth (gray line; b) 79

Figure 3. Distribution of precipitation events (a) and cumulative precipitation by precipitation events classes (b). c) Distribution of inter-event periods (days) for the four years study. 80

Figure 4.Relationship between size of precipitation event (mm) and the change in soil volumetric water content at 2.5 cm depth (v/v). The line stands for the linear regression such that ΔVWC = -0.0047 + 0.0028 * PPT event (mm), R2 = 0.72. 81

Figure 5. Net ecosystem exchange (NEE) after a precipitation event showing the decreasing effect through time (days). The decreasing effect rate was adjusted to an exponential negative model NEE = yo + a *exp(-k *t). The insert stands for the relationship between the decaying rate (-k) and the PPT event that originated the NEE change. This relationship was fitted with an exponential model (black line; -k = yo + a *exp(-b*PPT_event). Symbols indicate different PPT event sizes that originated the NEE change, 13.7mm d-1 (Δ), 16.74 mm d-1 (▼), 6.86 mm d-1 (○), 10.08 mm d-1 (■), and 2.52 mm d-1 (●). Parameters are reported in Table A1. 82

Figure 6. Dynamics of a) precipitation (mm d-1) and net ecosystem exchange (NEE, μmol m-2 s-1, daily means ± 1 S.E.) and its components, the gross ecosystem exchange (GEE, μmol m-2 s-1) and ecosystem respiration (ER, μmol m-2 s-1) for the transition from the dry (December – May) to the wet season (June – November) in 2013. b) volumetric soil water content dynamics (VWC, v/v) at two depths (2.5 cm and 15 cm). Arrows indicate apparent changes in GEE and ER trends. 84

Figure 7. Univariate relationships between change of averaged daytime NEE (ΔNEE, μmol m-2 s-1) and, a) PPT event size (mm), b) inter-event period (DSLE, days), c) previous VWC at 2.5 cm depth (v/v), d) previous VWC at 15 cm depth (v/v), e) change in VWC at 2.5 cm depth (v/v), and f) previous NEE (NEEt-1, μmol m-2 s-1). 86

Figure 8. Quadratic relationship among; a) the change of the averaged daytime NEE (ΔNEE, μmol m-2 s-1), the size of first PPT event (mm), and the inter-event period (DSLE, days), and b) ΔNEE and change of VWC at 2.5 cm depth (ΔVWC2.5,v/v), and previous VWC at 2.5 cm depth (PreVWC2.5, v/v). Parameters presented in Table A2. 87

Figure 9. Dynamics of, a) basal respiration (Rb), b) temperature sensitivity (Q10), and c) maximum C uptake at PPFD=2500 μmol m-2 s-1 and 25 °C (NEE2500,25) following a PPT event. Insets in Figs. 1 and 3 show the relationship between PPT size event and the exponential decaying rates (-k). 90

Figure A1. Dynamic of half an hour net ecosystem exchange (μmol m-2 s-1) after a precipitation event of 8.12 mm. the arrow indicates the time of PPT event occurrence. 100

Figure A2. Dynamic of volumetric soil water content (VWC, v/v) at two depths (2.5 and 15 cm) after a small PPT event of 5 mm. 101

Figure A3. Bivariate relationship between precipitation event size (mm d-1) and the inter-event period between PPT events (days). 101

Figure A4. Bivariate relationship among the change of soil VWC at 2.5 cm depth, the previous C flux and the change of NEE after the PPT event adjusted to a quadratic function. 102

Figure A5. Extrapolation of decaying rates (-k) in the full range of observed PPT events (mm d-1) through the exponential model –k = 0.3821+2.1674*EXP(-0.1785*PPT_event). Shadow section of the figure (diagonal lines) indicates the range of PPT event size used to calculate parameters of the model, and the gray area indicates the range of PPT event size where decaying rates reach a steady state. 103

Figure A6. Relationship between nighttime-NEE derived ER and a) the soil volumetric water content at 2.5 cm depth (VWC2.5, v/v), b) the soil volumetric water content at 15 cm depth (VWC15, v/v), c) the enhanced vegetation index (EVI), and d) the air temperature (T, °C). 103

Resumen

Variabilidad de los flujos de carbono a diferentes escalas de tiempo y sus controles bióticos y ambientales de un pastizal semiárido del Centro de México.

Los ecosistemas terrestres controlan la dinámica del carbono (C) atmosférico sobre la tierra, removiendo hasta el 25% de las emisiones de C antropogénicas. Sin embargo, la alta variabilidad estacional e interanual de los flujos de C genera gran incertidumbre acerca de su capacidad de captura de C. El entendimiento de los factores que afectan las tasas de captura y liberación de C nos ayudará a mejorar las predicciones de los efectos del cambio climático sobre los procesos ecosistémicos, así como sus efectos de retroalimentación. El objetivo de este trabajo fue determinar los controles bióticos y ambientales sobre el intercambio neto de C a nivel ecosistema (NEE) y sus componentes para entender cuáles condiciones ambientales favorecen la captura de C en el pastizal semiárido, con énfasis en los efectos de "legado" de la precipitación (PPT) y los pulsos de C generados después de los eventos de PPT. Cuatro años continuos de mediciones del NEE con un sistema de covarianza de vórtices (EC) fueron analizados. Los flujos de C mostraron ciclos diarios y estacionales típicos con la temperatura del aire y la densidad de flujo fotónico fotosintético como controles diarios y la humedad del suelo y la dinámica de la vegetación (medida como EVI) controlando el NEE a escala estacional. El pastizal semiárido fue una fuente (16.37 and 93.83 g C m^{-2} a^{-1}) y un sumidero de C ((-15.85 and -121.02g C m^{-2} a^{-1}). Se identificaron efecto de legado de la PPT a escala estacional. La PPT invernal afectó positivamente la captura de C durante el verano; mientras que la PPT del verano no tuvo efectos sobre la productividad invernal. Cien mm de PPT invernal y 200 durante el verano fueron necesarios para convertir al pastizal en un sumidero neto de C. Por otra parte, la respiración del ecosistema (ER) respondió pocas horas después del evento de PPT, mientras que pasaron hasta 5 días para observar una respuesta de la productividad del ecosistema (GEE). Eventos de PPT tan bajos como 0.25mm incrementaron ER, pero PPT acumulada mayor a 40mm

estimularon GEE. En general, los pulsos de C estuvieron relacionados con la magnitud del estímulo (ej. tamaño del evento de PPT) y las condiciones previas del ecosistema (ej. contenido de humedad del suelo previo al evento de PPT). Los resultados de este estudio demostraron la importancia de la PPT invernal y de los pulsos de C después de los eventos de PPT al balance de C anual en un pastizal semiárido con lluvias durante el verano.

PALABRAS CLAVE: Intercambio neto de C a nivel ecosistema, covarianza de vórtices, respiración del ecosistema, efectos de legado de la precipitación.

Abstract

Variability of carbon fluxes at different time-scales and their biotic and environmental controls on a short-grass steppe in Central Mexico.

Terrestrial ecosystems control the atmospheric carbon (C) dynamics on Earth, removing~25% of C emissions derived from anthropogenic activities. However, high seasonal and interannual variability generates large uncertainties about their C uptake capacity. Understanding environmental and biotic factors affecting C uptake and C release rates will help us to improve predictions of climate change impacts on ecosystem processes as well as its feedback effects. The aim of this study was to determine biotic and environmental drivers of the net ecosystem C exchange (NEE) and its components to understand which environmental conditions favor uptake or release of C in the semiarid grassland, with emphasis on precipitation (PPT) legacy effects and short term C fluxes following PPT events. Four years of continuous NEE measurements with an eddy covariance (EC) system were analyzed. Carbon fluxes showed typical diurnal and seasonal cycles with air temperature and photosynthetic photon flux density (PPFD) as the main diurnal drivers, whereas soil moisture and vegetation dynamics (the enhanced vegetation index, EVI) controlled NEE at seasonal scale. The semiarid grassland behaved as a source (16.37 and 93.83 g C m^{-2} y^{-1}), and a sink of C (-15.85 and -121.02g C m^{-2} y^{-1}). Precipitation legacy effects on NEE and its components were identified at seasonal scale. Winter precipitation positively affected C uptake of summer, however, summer precipitation did not have effects on winter C fluxes. One hundred mm of winter PPT and 200 mm of summer PPT were needed for turning the ecosystem into a C sink. On the other hand, Ecosystem respiration (ER) responded within few hours following a PPT event whereas it took five days for gross ecosystem exchange (GEE) to respond. Precipitation events as low as 0.25 mm increased ER, but cumulative PPT > 40 mm that infiltrated deeper into the soil profile stimulated GEE. Overall, ER fluxes following PPT events were related with the size of the stimulus (e.g. PPT event size) and previous soil conditions (e.g.

previous soil volumetric water content and inter PPT event period). Results of this study demonstrated the importance of winter precipitation and short term ER responses following PPT events to the annual C balance in a summer rain season semiarid grassland.

KEYWORDS: Eddy covariance, net ecosystem exchange, ecosystem respiration, precipitation legacy effects.

General Introduction

Terrestrial ecosystems are the main control of atmospheric CO_2 dynamics (Friend *et al*., 2007), and indirectly modify Earth surface temperatures (Kutsch *et al*., 2005). Rates of uptake and release of CO_2 by terrestrial ecosystems are 10 fold bigger than CO_2 emissions from fossil fuels burning (Houghton *et al*., 2007). Thus, the accuracy and precision of C exchange estimations between biosphere and atmosphere is crucial to assess the potential of ecosystems C sequestration. Moreover, a better understanding about controls and feedbacks regulating the interactions between carbon and water cycle and climate variability will help to improve predictions of climate change effects on vegetation dynamics and ecosystem processes (Schimel et al., 2001; Heimann and Reichstein, 2008; Thomas *et al*., 2009).

Roughly, it is estimated that terrestrial ecosystems absorb ≈25% of anthropogenic C emissions derived from fossil fuel burning (Running, 2008), with the tropical (-1.9 ± 1.3 Gt C $year^{-1}$), and both the temperate and the boreal forests (-1.3 ± 0.9 Gt C $year^{-1}$, for both) as the main documented carbon sinks (Grace, 2004). In contrast, arid ecosystems have shown to behave as either sources (Emmerich, 2003; Mielnick et al., 2005; Gilmanov et al., 2007), or neutral (Gilmanov et al., 2007; Archibald et al., 2009; Propastin and Kappas, 2009), and rarely as C sinks (Frank and Dugas, 2001; Gilmanov et al., 2003; Gilmanov et al., 2004; Hastings et al., 2005; Zhao et al., 2006; Wohlfahrt et al., 2008; Propastin and Kappas, 2009). Thus, currently there is not a clear role of drylands in the global carbon cycle due in part to its high sensitivity to climate variability, especially variation of both quantity and timing of precipitation (Jongen et al., 2011; Hao et al., 2010; Ma et al., 2007; Xu and Baldocchi, 2004; Flanagan et al., 2002; Sala et al., 1988).

Arid lands comprise a wide range of ecosystem types covering more than 30% of terrestrial land (Lal, 2004). Precipitation pattern on these ecosystems is characterized by a scarce and highly intra and inter-annual precipitation variability in which small rainfall events account for a large proportion of water inputs (Sala and Lauenroth, 1982). Precipitation variability is of such degree that they are

considered hot spot regions of interannual variability in carbon fluxes that are controlled by moisture supply (Jung et al., 2011), and moreover, they drive the trend and interannual variability of the global C sink (Ahlsröm et a., 2015) . However, a high correlation between PPT and productivity has been demonstrated spatially across ecosystems, but a low correlation has been observed temporally, with annual PPT explaining a low amount of interannual variability of intra-site productivity (Sala et al., 2012).

Global circulation models forecast for the end of the 21st Century a 10 and a 20% reduction of summer and winter precipitation, respectively, for the arid and semiarid regions (Christensen et al., 2007) under current CO2 emission scenarios. Moreover, stronger and more spaced precipitation events with long rainless periods, are expected within this overall annual precipitation decreased scenario (Houghton et al., 2001; Easterling et al., 2000). So that, changes in the characteristics and functioning of these ecosystems are likely to occur, in particular modifications to the carbon and water cycle as a consequence of alterations in the energy balance. This imposes new challenges for scientist to elucidate the role of arid lands as C sinks or C sources as well as the mechanisms controlling C and water fluxes at short and long temporal scales. In particular to predict how these ecosystems will respond to future scenarios of climate change.

The contribution of ecosystems as either C sources or C sinks as well as their environmental and biotic drivers at different timescales can be evaluated through net ecosystem C exchange (NEE) studies. The NEE represents the balance between the carbon captured by plants from the atmosphere through the process of photosynthesis (gross ecosystem production, GEE) and the carbon released to the atmosphere by respiration of roots and associated microorganism (autotrophic respiration, Ra), fungi and soil microorganisms, which altogether is named heterotrophic respiration (Rh; (Law et al., 2002; Reichstein et al., 2005; Chapin et al., 2002; Nieder and Benbi, 2008). The sum of Ra and Rh results in the total ecosystem respiration (ER), which in contrast to photosynthesis is a process that remains poorly understood (Trumbore, 2006).

In this study, four years of continuous EC measurements in the southernmost part of the semiarid grassland in North America were analyzed. The aim of the study was to determine biotic and environmental drivers of NEE and its components to explain the large seasonal and interannual variability of C fluxes in this ecosystem. In particular, to understand which environmental conditions favor the uptake or the release of C in the semiarid grassland. Special emphasis was paid to NEE responses to precipitation and time delays at different time scales.

In Chapter 1, annual C balances and biotic and environmental drivers of NEE at different timescales were determined. Also, delayed effects of precipitation on NEE, GEE and ER were analyzed under the legacy precipitation effect hypothesis (Sala et al., 2012).

In Chapter 2, short-term effects of precipitation events on NEE, GEE and ER were evaluated. The Threshold-Delay model (Ogle and Reynolds, 2004) was used as the framework for describing immediate C effluxes following PPT events. Under this framework, time delays, thresholds and *a priori* conditions (base of the T-D model) between the GEE and the ER were contrasted.

References

Ahlström, A., Raupach, M.R., Schurgers, G., Smith, B., Arneth, A., Jung, M., Reichstein, M., Canadell, J.G., Friedlingstein, P., Jain, A.K., Kato, E., Poulter, B., Sitch, S., Stocker, B.D., Viovy, N., Wang, Y.P., Wiltshire, A., Zaehle, S., Zeng, N., 2015.The dominant role of semi-arid ecosystems in the trend and variability of the land CO2 sink. Science 348, 895–899. doi:10.1126/science.aaa1668

Archibald, S.A., Kirton, A., Merwe, M.R., Scholes, R.J., Williams, C.A., Hanan, N., 2009.Drivers of inter-annual variability in Net Ecosystem Exchange in a semi-arid savanna ecosystem, South Africa. Biogeosciences 6, 251–266.

Chapin, F.S., Matson, P.A., Vitousek, P.M., 2002. Principles of Terrestrial Ecosystem Ecology, 1st ed. Springer Verlag, New York.

Christensen, J.H., B. Hewitson, A. Busuioc, A. Chen, X. Gao, I. Held, R. Jones, R.K. Kolli, W.-T. Kwon, R. Laprise, V. Magaña Rueda, L. Mearns, C.G. Menéndez, J. Räisänen, A. Rinke, A. Sarr and P. Whetton, 2007: Regional Climate Projections. In: Climate Change 2007: The Physical Science Basis. Contribution of Working Group I to the Fourth Assessment Report of the Intergovernmental Panel on Climate Change [Solomon, S., D. Qin, M. Manning, Z. Chen, M. Marquis, K.B. Averyt, M. Tignor and H.L. Miller (eds.)]. Cambridge University Press, Cambridge, United Kingdom and New York, NY, USA.

Easterling, D.R., Meehl, G.A., Parmesan, C., Changnon, S.A., Karl, T.R., Mearns, L.O., 2000. Climate Extremes: Observations, Modeling, and Impacts. Science 289, 2068–2074.

Emmerich, W.E., 2003. Carbon dioxide fluxes in a semiarid environment with high carbonate soils. Agric. For. Meteorol. 116, 91–102.

Flanagan, L.B., Wever, L.A., Carlson, P.J., 2002. Seasonal and interannual variation in carbon dioxide exchange and carbon balance in a northern temperate grassland. Glob. Change Biol. 8, 599–615.

Frank, A.., Dugas, W.., 2001. Carbon dioxide fluxes over a northern, semiarid, mixed-grass prairie. Agric. For. Meteorol. 108, 317–326. doi:10.1016/S0168-1923(01)00238-6

Friend, A.D., Arneth, A., Kiang, N.Y., Lomas, M., Ogee, J., Rödenbeck, C., Running, S.W., Santaren, J.D., Sitch, S., Viovy, N., Woodward, F.I., Zaehle, S., 2007. FLUXNET and modelling the global carbon cycle.Glob. Change Biol. 13, 610–633. doi:10.1111/j.1365-2486.2006.01223.x

Gilmanov, T.G., Johnson, D.A., Saliendra, N.Z., Svejcar, T.J., Angell, R.F., Clawson, K.L., 2004. Winter CO2 fluxes above sagebrush-steppe ecosystems in Idaho and Oregon. Agric. For. Meteorol. 126, 73–88. doi:10.1016/j.agrformet.2004.05.007

Gilmanov, T.G., Soussana, J.F., Aires, L., Allard, V., Ammann, C., Balzarolo, M., Barcza, Z., Bernhofer, C., Campbell, C.L., Cernusca, A., Cescatti, A., Clifton-Brown, J., Dirks, B.O.M., Dore, S., Eugster, W., Fuhrer, J., Gimeno,

C., Gruenwald, T., Haszpra, L., Hensen, A., Ibrom, A., Jacobs, A.F.G., Jones, M.B., Lanigan, G., Laurila, T., Lohila, A., G.Manca, Marcolla, B., Nagy, Z., Pilegaard, K., Pinter, K., Pio, C., Raschi, A., Rogiers, N., Sanz, M.J., Stefani, P., Sutton, M., Tuba, Z., Valentini, R., Williams, M.L., Wohlfahrt, G., 2007. Partitioning European grassland net ecosystem CO2 exchange into gross primary productivity and ecosystem respiration using light response function analysis. Agric. Ecosyst. Environ. 121, 93–120. doi:10.1016/j.agee.2006.12.008

Gilmanov, T.G., Verma, S.B., Sims, P.L., Meyers, T.P., Bradford, J.A., Burba, G.G., Suyker, A.E., 2003. Gross primary production and light response parameters of four Southern Plains ecosystems estimated using long-term CO2-flux tower measurements. Glob.Biogeochem Cycles 17, 1071.

Grace, J., 2004. Understanding and managing the global carbon cycle. J. Ecol. 92, 189–202.

Hao, Y., Wang, Y., Mei, X., Cui, X., Zhou, X., Huang, X., 2010.The sensitivity of temperate steppe CO2 exchange to the quantity and timing of natural interannual rainfall. Ecol. Inform. 5, 222–228. doi:10.1016/j.ecoinf.2009.10.002

Hastings, S.J., Oechel, W.C., Muhlia-Melo, A., 2005.Diurnal, seasonal and annual variation in the net ecosystem CO2 exchange of a desert shrub community (Sarcocaulescent) in Baja California, Mexico.Glob. Change Biol. 11, 927–939. doi:10.1111/j.1365-2486.2005.00951.x

Heimann, M., Reichstein, M., 2008.Terrestrial ecosystem carbon dynamics and climate feedbacks. Nature 451, 289–292. doi:10.1038/nature06591

Houghton, J.T., Intergovernmental Panel on Climate Change (Eds.), 2001. Climate change 2001: the scientific basis: contribution of Working Group I to the third assessment report of the Intergovernmental Panel on Climate Change. Cambridge University Press, Cambridge ; New York.

Houghton, R.A., 2007. Balancing the Global Carbon Budget. Clim. Change State Art 2001-2007 1, 313–347. doi:10.1146/annurev.earth.35.031306.140057

Jongen, M., Pereira, J.S., Aires, L.M.I., Pio, C.A., 2011. The effects of drought and timing of precipitation on the inter-annual variation in ecosystem-atmosphere exchange in a Mediterranean grassland. Agric. For. Meteorol. 151, 595–606. doi:10.1016/j.agrformet.2011.01.008

Jung, M., Reichstein, M., Margolis, H.A., Cescatti, A., Richardson, A.D., Arain, M.A., Arneth, A., Bernhofer, C., Bonal, D., Chen, J., Gianelle, D., Gobron, N., Kiely, G., Kutsch, W., Lasslop, G., Law, B.E., Lindroth, A., Merbold, L., Montagnani, L., Moors, E.J., Papale, D., Sottocornola, M., Vaccari, F., Williams, C., 2011. Global patterns of land-atmosphere fluxes of carbon dioxide, latent heat, and sensible heat derived from eddy covariance, satellite, and meteorological observations. J Geophys Res 116, G00J07.doi:10.1029/2010JG001566

Kutsch, W.L., Liu, C., Hörmann, G., Herbst, M., 2005. Spatial heterogeneity of ecosystem carbon fluxes in a broadleaved forest in Northern Germany. Glob. Change Biol. 11, 70–88.

Lal, R., 2004. Carbon Sequestration in Dryland Ecosystems. Environ. Manage. 33, 528–544. doi:10.1007/s00267-003-9110-9

Law, B.., Falge, E., Gu, L., Baldocchi, D.., Bakwin, P., Berbigier, P., Davis, K., Dolman, A.., Falk, M., Fuentes, J.., Goldstein, A., Granier, A., Grelle, A., Hollinger, D., Janssens, I.., Jarvis, P., Jensen, N.., Katul, G., Mahli, Y., Matteucci, G., Meyers, T., Monson, R., Munger, W., Oechel, W., Olson, R., Pilegaard, K., Paw U, K.., Thorgeirsson, H., Valentini, R., Verma, S., Vesala, T., Wilson, K., Wofsy, S., 2002. Environmental controls over carbon dioxide and water vapor exchange of terrestrial vegetation. Agric. For. Meteorol. 113, 97–120. doi:10.1016/S0168-1923(02)00104-1

Ma, S., Baldocchi, D.D., Xu, L., Hehn, T., 2007.Inter-annual variability in carbon dioxide exchange of an oak/grass savanna and open grassland in California. Agric. For. Meteorol. 147, 157–171. doi:10.1016/j.agrformet.2007.07.008

Mielnick, P., Dugas, W.A., Mitchell, K., Havstad, K., 2005. Long-term measurements of CO2 flux and evapotranspiration in a Chihuahuan desert grassland. J. Arid Environ. 60, 423–436. doi:10.1016/j.jaridenv.2004.06.001

Nieder, R., Benbi, D.K., 2008. Carbon and Nitrogen in the Terrestrial Environment.Springer Netherlands.

Ogle, K., Reynolds, J.F., 2004. Plant responses to precipitation in desert ecosystems: integrating functional types, pulses, thresholds, and delays. Oecologia 141, 282–294. doi:10.1007/s00442-004-1507-5

Propastin, P., Kappas, M., 2009.Modeling Net Ecosystem Exchange for Grassland in Central Kazakhstan by Combining Remote Sensing and Field Data. Remote Sens. 1, 159–183.

Reichstein, M., Falge, E., Baldocchi, D., Papale, D., Aubinet, M., Berbigier, P., Bernhofer, C., Buchmann, N., Gilmanov, T., Granier, A., Grünwald, T., Havránková, K., Ilvesniemi, H., Janous, D., Knohl, A., Laurila, T., Lohila, A., Loustau, D., Matteucci, G., Meyers, T., Miglietta, F., Ourcival, J.-M., Pumpanen, J., Rambal, S., Rotenberg, E., Sanz, M., Tenhunen, J., Seufert, G., Vaccari, F., Vesala, T., Yakir, D., Valentini, R., 2005. On the separation of net ecosystem exchange into assimilation and ecosystem respiration: review and improved algorithm. Glob. Change Biol. 11, 1424–1439. doi:10.1111/j.1365-2486.2005.001002.x

Running, S.W., 2008.Ecosystem Disturbance, Carbon, and Climate.Science 321, 652 –653. doi:10.1126/science.1159607

Sala, O.E., Gherardi, L.A., Reichmann, L., Jobbagy, E., Peters, D., 2012. Legacies of precipitation fluctuations on primary production: theory and data synthesis. Philos. Trans. R. Soc. B Biol. Sci. 367, 3135–3144. doi:10.1098/rstb.2011.0347

Sala, O.E., Lauenroth, W.K., 1982. Small rainfall events: An ecological role in semiarid regions. Oecologia 53, 301–304. doi:10.1007/BF00389004

Sala, O.E., Parton, W.J., Joyce, L.A., Lauenroth, W.K., 1988. Primary Production of the Central Grassland Region of the United States. Ecology 69, 40–45.

Schimel, D.S., House, J.I., Hibbard, K.A., Bousquet, P., Ciais, P., Peylin, P., Braswell, B.H., Apps, M.J., Baker, D., Bondeau, A., Canadell, J., Churkina, G., Cramer, W., Denning, A.S., Field, C.B., Friedlingstein, P., Goodale, C., Heimann, M., Houghton, R.A., Melillo, J.M., Moore, B., Murdiyarso, D., Noble, I., Pacala, S.W., Prentice, I.C., Raupach, M.R., Rayner, P.J., Scholes, R.J., Steffen, W.L., Wirth, C., 2001. Recent patterns and mechanisms of carbon exchange by terrestrial ecosystems. Nature 414, 169–172. doi:10.1038/35102500

Thomas, C.K., Law, B.E., Irvine, J., Martin, J.G., Pettijohn, J.C., Davis, K.J., 2009. Seasonal hydrology explains interannual and seasonal variation in carbon and water exchange in a semiarid mature ponderosa pine forest in central Oregon. J Geophys Res 114, G04006.

Trumbre, S., 2006. Carbon respired by terrestrial ecosystems - recent progress and challenges. Glob. Change Biol. - GLOB CHANGE BIOL 12, 141–153. doi:10.1111/j.1365-2486.2006.01067.x

Wohlfahrt, G., Fenstermaker, L.F., Arnone III, J.A., 2008. Large annual net ecosystem CO2 uptake of a Mojave Desert ecosystem.Glob. Change Biol. 14, 1475–1487. doi:10.1111/j.1365-2486.2008.01593.x

Xu, L., Baldocchi, D.D., 2004. Seasonal variation in carbon dioxide exchange over a Mediterranean annual grassland in California. Agric. For. Meteorol. 123, 79–96. doi:10.1016/j.agrformet.2003.10.004

Zhao, L., Li, Y., Xu, S., Zhou, H., Gu, S., Yu, G., Zhao, X., 2006. Diurnal, seasonal and annual variation in net ecosystem CO2 exchange of an alpine shrubland on Qinghai-Tibetan plateau.Glob. Change Biol. 12, 1940–1953. doi:10.1111/j.1365-2486.2006.01197.x

Chapter 1

Precipitation legacy effects and environmental drivers on C fluxes of a semiarid grassland in Mexico

Keywords: net ecosystem exchange, ecosystem respiration, gross ecosystem exchange, eddy covariance.

Introduction

Photosynthesis and respiration of terrestrial ecosystems are the largest carbon (C) fluxes between the biosphere and the atmosphere. Terrestrial plants take up globally about 120 Tg C y^{-1} from the atmosphere through photosynthesis, but release a similar amount of CO_2 to the atmosphere through ecosystem respiration (115 Tg C y^{-1}, Houghton and Woodwell, 1982, Raich and Schlesinger, 1992). Even though, the residual of this balance, a fraction of about 5 TgC y^{-1}, still counterbalances the growing anthropogenic emissions of C to the atmosphere coming from cement production, fossil fuel burning and land use change (~7 Tg C y^{-1}, Friedlingstein et al., 2010, Running, 2008). Nowadays, studies quantifying ecosystem C fluxes and their environmental drivers are relevant to provide data for model assessment and improve forecasting accuracy of climate change models in addition to understand their role in the regional and global C cycle balance.

Long term and wide spatial net ecosystem exchange (NEE) measurements by eddy covariance (EC, Baldocchi et al., 1996; Loescher et al., 2006) have allowed identify different set of environmental factors controlling C fluxes across biomes at different timescales. The NEE is the balance between C uptake by photosynthesis (GEE, gross ecosystem exchange) and the C released via respiration (ER, ecosystem respiration) in such way that gross primary productivity (GPP) is estimated as GPP ≈ GEE = -NEE + ER (Loescher et al., 2006). The NEE is mainly controlled by temperature in mid and high latitude ecosystems with mean annual temperatures (MAT) lower than 16 °C, whereas precipitation and water deficit are the dominant controls in warmer ecosystems (Yi et al., 2010). Quality of light, and the timing and magnitude of precipitation also have effects on ecosystems ability to take up C, by for instance doubling light use efficiency under diffuse light conditions (Hollinger et al., 1994; Gu et al., 2002), and allowing more soil water storage with larger or more frequent precipitation pulses (Knapp et al., 2002;Thomey et al., 2011). Because photosynthesis and respiration responds differentially to environmental drivers makes it difficult to understand how climate affects net

ecosystem C balance, thus it is imperative partitioning NEE into its components (Anderson-Teixeira et al., 2011). For instance, temperature has a secondary role controlling GPP in dryland ecosystems (Noy-Meir, 1978), ER is more responsive to air and soil temperatures but always modulated by soil water availability (Conant et al., 2003; Amudson et al., 1988).

Semiarid grasslands are water limited ecosystems where productivity is subjected to seasonal and annual variability of precipitation (Sala et al., 1988; Sala and Lauenroth1982). This imposes a strong seasonal pattern in plants and microorganism activity, restricting growth to the season with the largest occurrence of precipitation (summer in semiarid tropical grasslands with monsoon influence). A strong correlation between precipitation (PPT) and aboveground net primary productivity (ANPP) has been shown to occur spatially but not temporally in ecosystems (Lauenroth and Sala 1992, Briggs and Knapp 1995, Hsu and Adler 2014). These results are argued to be a consequence of precipitation lag effects of the previous year (Oesterheld et al., 2001). For instance, Sala et al. (2012) showed that a previous-dry year lead to a decrease in annual productivity in the following year, and a previous wet year amplified the expected productivity of the next growing season (Linear-positive legacy hypothesis, Sala et al., 2012, Lauenroth and Sala 1992). These legacies of either pre-dry or pre-wet years have been suggested to be caused by; 1) structural changes of the ecosystem due to either plant mortality following a severe drought or by the increase of tillers at the end of a wet year (Yahdjian & Sala 2006, Sherry et al., 2008, Reichmann et al. 2013), 2) throughout biogeochemical processes that increase nutrient availability due to larger litter inputs from previous wet years (Sala et al. 2012), or 3) some combination of the two.

The lack of temporal relationship is also observed when NEE data have been analyzed with respect to PPT (Archibald et al. 2009; Wu et al. 2011). In this case, lagged PPT effects are also plausible causes of the inability of PPT to explain NEE rates in arid systems. Following this logic, the capacity for ecosystem C uptake is enhanced by a previous wet year, or by the contrary, reduced by a previous dry

year. On the other hand, the asymmetric responses of NEE components, GPP and ER to precipitation, could potentially alter precipitation-productivity relationships as suggested by legacy effects hypothesis (Figure 1). First, both experimental and synthesis studies have shown that ecosystem C balance (NEE) is determined by differential responses of carbon uptake (GPP) and respiration (ER) to the environment, i.e. NEE, is more affected by precipitation reduction than ER alone, indicating a differential effect of PPT on GPP and ER (Anderson-Teixeira et al., 2011; Shi et al. 2014, Yang and Zhou 2013). Although respiration is highly correlated to productivity, with autotrophic respiration (R_a) dampening after the short-term photosynthesis substrates decline (Bahn et al. 2008). These studies also showed that C assimilation was more sensitive to changes of PPT than respiration. Thus, it is likely that the long-term soil C sources change slowly, preventing heterotrophic respiration (R_h; ER = R_h + R_a) to change just after a multi-year drought (Shi et al. 2014), in turn making ER less responsive to short-term PPT changes. However, in the sort-term, the large soil water availability on extreme wet years can suppress soil respiration due to CO_2 and O_2 diffusion mechanisms. Second, revisions of Knapp and Smith (2001) and Wu et al. (2011) have also showed that ecosystems are more sensitive to a PPT increment (event) than to an overall decrease in PPT relative to mean annual PPT (MAP), allowing ecosystems relatively to gain more C in wet favorable years than C losses on dry years. And third, nitrogen limited ecosystems are impeded to assimilate C in very wet years (LeBauer et al., 2008). Adaptations to dry environments such as a relative low growth rate (Grime, 1977) make ecosystems incapable to take advantage of extremely wet conditions. Thus, it is likely that C uptake remains asymptotic on very humid years, whereas respiration could remain ascending or also could dampen due to soil CO_2 and O_2 diffusion phenomena.

The response of C balance to PPT would coincide with the low PPT sensitivity observed in the temporal model in comparison with the general spatial model. Carbon uptake in ecosystems experiencing a transition from previous dry to wet years should be lower for a temporal compared to a spatial model, and C uptake should be larger than the expected due to a wet legacy when change occurs from

wet to dry years, coinciding with Sala et al. (2012) legacy effects hypothesis (H1 and H3-4, see below).

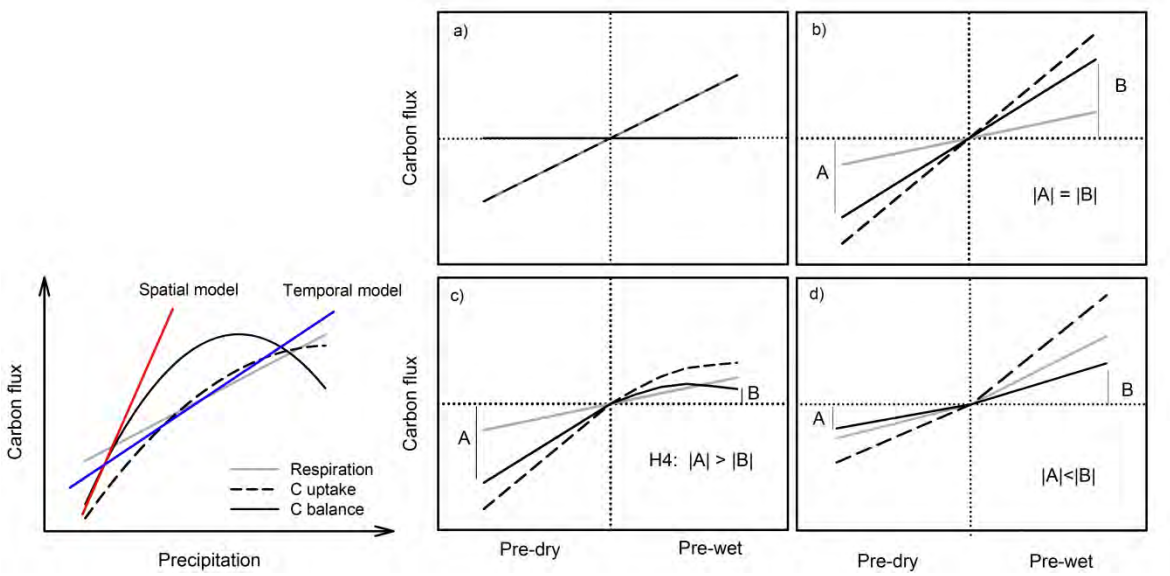

Figure 1.Asymmetric sensitivity hypothesis. Differential responses of C uptake and respiration to PPT can cause the attenuation of the positive C balance response at wetter years, which coincides with lower slopes observed in temporal annual precipitation-productivity models when are compared to general spatial models (lower left panel). While ecosystem C uptake increases linearly, asymptotically, or stepper on wet years with precipitation, ecosystem respiration does it almost linearly but with a lower change rate. Temporally, C balances in ecosystems experiencing changes from pre-dry to wet years are lower than the expected by the spatial model, coinciding with Sala et al. (2012) legacy effects hypothesis (H1 and H3, see below). If C uptake and respiration equally respond to PPT change, no additional effect on C balance of previous year PPT should be expected (a). A stepper response of C uptake than respiration to PPT should induce similar additional effects on C balance (b); whereas asymptotic response of C uptake at extreme humid years should display lower positive effects on C balance of previous wet years (c); or if C uptake is more sensitive to wet than dry years, larger positive effect on C balance should be expected by previous wet years (d).

Direct continuous measurements of net ecosystem C exchange (NEE) and remote

sensing have shown that semiarid grasslands annually exchange between -164 and 210 g C m^{-2} y^{-1} and behave as either small carbon sinks (Propastin and Kappas, 2009), net C sources (Emmerich, 2003;Mielnick et al., 2005), or even as both across years with contrasting precipitation rates (Archibald et al. 2009,Rajanet al., 2013). Thus, it is possible that semiarid grasslands at the interannual and decadal time scale (Sierra et al 2009) are carbon neutral, such that; i) the same amount of carbon captured via photosynthesis is released via respiration regardless of the abiotic environment, ii) in terms of the abiotic environment, in favorable growth years grasslands can behave as small C sinks, whereas in unfavorable environmental conditions, grasslands perform as small C sources. However, when we consider legacy effects of precipitation, it is likely that iii) precipitation of the previous year influences the annual C balance of the grassland, decreasing C uptake with previous dry year or increasing C uptake after previous wet years. Different sensitivities of the sum of -NEE + ER and ER to precipitation could lead semiarid grassland to release more C than expected at both severe dry or wet years.

Thus, the objectives of this study were; First, we hypothesized that the annual C balance of grasslands, as either a net C sink or C source will be mainly controlled by precipitation; however total precipitation from the previous year should modify this balance with respect to expected productivity under current year precipitation (H_1). Thus, when annual PPT changes from a severe drought to a wet year the grassland should exhibit a reduction on net C gain (H_2), whereas a transition from a wet year to a dry or similar wet year the grassland should display an increase on net C uptake rate (H_3).

Separation of NEE into its flux components should provide insights into mechanisms of precipitation legacies on C balance. If both GPP and ER respond equally to PPT, NEE and GPP should be related linearly to current and previous year precipitation (H_4) with equal slopes. Moreover, if NEE components respond asymmetrically to precipitation, we should expect GEE to be more sensitive to

reductions of PPT than ER (H_5), and behave exponentially or asymptotically in very wet years (*e.g.* wetter than the MAP).

Materials and Methods

Site description

The study site is located on a shortgrass steppe, within the Llanos de Ojuelos subprovince NE of Jalisco state, Mexico. The shortgrass biome in Mexico extends from the North American Midwest along a strip that follows the *Sierra Madre Occidental* through the *Chihuahuan* Desert into the sub-province *Llanos de Ojuelos*. Vegetation is dominated by grasses, with *Bouteloua gracilis* H.B.K. Lag ex Steud (blue grama) as the key grass species, forming under well preserved conditions near mono-specific stands. The region has a semiarid climate with mean annual precipitation of 424 mm ± 11 mm (last 30 years; INIFAP, Rancho experimental Vaquerías. Unpublished data) distributed mainly between June and September and exhibits 6 to 9 month period of no rain. Winter rains account for < 5% of the total annual precipitation (Aguado-Santacruz, 1993, García, 2004). Mean annual temperature was 17.5± 0.5 °C, with mean temperature extremes ranging from 2.2°C for the coldest to 26.8 °C for the warmest month, respectively. The topography is characterized by valleys and gentle rolling hills with soils classified as haplic xerosols (associated with lithosols and eutric planosols), and haplic phaeozems (associated with lithosols) (Aguado-Santacruz, 1993). Soils are shallow with average depth of 0.3-0.4 m containing a cemented layer at ~ 0.5 m in depth, with textures dominated by silty clay and sandy loam soils (Aguado, 1993, COTECOCA, 1979).

The study site is a fenced area of ~64 ha of semiarid grassland divided into 16 paddocks of ~4 ha each that are subjected to different grazing regimes and fire management. A 6 m high tower was placed at the center of the area of interest to estimate carbon-energy flux (NEE) and associated meteorological instruments. That location allowed an ever-changing and integrated measurement footprint of 320 m, 410 m, 580 m, and 260 m from the tower according to the N, E, S, and W orientations, respectively. The footprint model (Kormann and Meixner, 2001)

revealed that on average >80% of cumulative fluxes came from these integrated distances and area of interest. Eddy covariance (EC) instruments were placed at 3 m high to cover a fetch of 300 m.

Meteorological and soil measurements

Meteorological data was collected continuously at a rate of 1 s and averaged at 30 min intervals using a datalogger (CR3000, Campbell Scientific Inc., Logan, Utah). Variables measured included; air temperature and relative humidity (1000 Ω PRT, HMP45C, Vaisala, Helsinki, Finland) housed into a radiation shield (R.M. Young Company Inc., Traverse City, MI), incident and reflected shortwave and longwave solar radiation (NR01, Hukseflux, Netherlands), photosynthetic photon flux density (PARLITE, Kipp and Zonen, Delft, the Netherlands). Soil variables were measured at a 5 min frequency and averaged at 30 min intervals. These included soil heat flux with a self-calibrating system buried at 8 cm deep (HFP01SC, Hukseflux, Netherlands), volumetric soil water content (CS616, Campbell Sci., Logan, Utah) positioned horizontally to 2.5 cm and 15 cm deep, average soil temperature of the top 8 cm soil profile, and soil temperature at 5 cm deep (T108 temperature probes, Campbell Scientific Inc., Logan, Utah). Soil temperature variables were acquired by a CR510 datalogger (Campbell Scientific Inc., Logan, Utah). Precipitation was measured with a bucket rain gauge installed 5 m away from the tower (FTS, Victoria, British Columbia, Canada). When air temperature, relative humidity, solar radiation, or photosynthetic photon flux density variables were not available because of sensor or datalogger operational failures, they were calculated by linear regression using data from a weather station mounted on the same tower (FTS, Victoria, British Columbia, Canada) that acquired information at 10 s sampling rate, and averaged every 10 min.

Net ecosystem CO_2 exchange measurements

An open path EC system was used to measure NEE over the semiarid grassland. The system consisted of a three-dimensional sonic anemometer (CSAT-3D, Campbell Sci., Logan, Utah) for measuring wind velocity on each polar coordinate

(u, v, w) and sonic temperature (θs), and an open-path infrared gas analyzer (IRGA, Li-7500, LI-COR Inc., Lincoln, NE) to measure CO_2 and water vapor concentrations. Instruments were mounted in a tower at 3 m above soil surface oriented towards the prevailing winds. Because prevailing winds change along the year, EC was oriented SW in winter and turned East during summer on the last two years. The IRGA sensor was mounted at the same height as the midway between the two arms of the anemometer transducers, and tilted 45° to avoid dust and water accumulation in the IRGA optical path. Digital signal of both sensors were recorded at a sampling rate of 10 Hz in a datalogger (CR3000, Campbell Scientific Inc., Logan, Utah). Instruments were installed in December 2010 and were continuously operating during four years (2011-2014). Several episodes of power failure throughout the study period and a lightening in 2012 caused data gaps in the time series, but on average 60% of half-hour data periods per year were available (42247 30-min averaging periods after quality filtering were used)

NEE was estimated as:

$$NEE = \overline{w'CO_2'} \qquad (1)$$

Overbar denotes time averaging and primes are the deviations of instantaneous values (at 10 Hz) from a block-averaged mean (30 min) of vertical windspeed (*w*, m s^{-1}) and molar fraction of CO_2 (μmol CO_2 mol^{-1}), respectively. Micrometeorological convention was used, where negative NEE values stand for ecosystem C uptake. We did not estimate a storage flux because of the low ecosystem stature, and we assumed it would be 0 over a 24-h period (Loescher et al. 2006)

Data processing, gap filling methods and statistical analysis

Raw eddy covariance data were processed in EdiRe (v1.5.0.10, The University of Edinburgh). Wind velocities, sonic temperature, [CO_2], and [H_2O] signals were despiked, considering outliers those values with a deviation larger than 8 standard deviations. A 2-D coordinate rotation was applied to sonic anemometer wind

velocities to obtain turbulence statistics perpendicular to the local stream line. Lags among horizontal wind velocity and scalars were removed with a cross-correlation procedure to maximize the covariance among signals. Carbon and water vapor fluxes were estimated as molar fluxes (mol m^{-2} s^{-1}) at 30 min block averages, and then they were corrected for air density fluctuations (WPL correction, Webb et al. 1980). To account for frequency loss on NEE, frequency response correction was done considering the cospectra of *w'θ'* as ideal, and then comparing the summed cospectral density in the inertial subrange to that of the total spectra of *w'θ'* and *w'*CO_2*'* (Baldocchi and Meyers, 1989). Sensible heat flux was estimated from the covariance between fluctuations of horizontal wind velocity (w') and sonic temperature (θ'_s). This buoyancy flux was corrected for humidity effects (Schotanus et al. 1983, Foken et al., 2012) and momentum fluctuations (cross wind correction, Schotanus et al. 1983).

Fluxes were subjected to quality control procedures, i) stationarity (<50%), ii) integral turbulence characteristics (<50%), iii) flags of IRGA and sonic anemometer (AGC value < 75, Max CSAT diagnostic flag=63) which are strongly related with advices of problem measurement due to rain events, iv) range tests (±20 μmol CO_2 m^{-2} s^{-1}) (Taylor and Loescher 2013), and v) a threshold u*= 0.1 m s^{-1} was used to filter nighttime NEE under poor developed turbulence. This threshold was defined through the 99% threshold criterion after Reichstein et al. (2005), where data are split into six temperature classes of equal sample size, and then each temperature class is split into 20 u*-classes. The threshold is defined when the u* class average reaches the 99% of the night-time flux average of the higher u*-classes. The mean of u* thresholds of at least 6 temperature classes is defined as the final threshold. The procedure is done for subsets of three months per year (J-M, A-J, J-S, and O-D) to account for seasonal variation of vegetation structure.

Ecosystem measures of productivity were derived such that,

$$NEP \approx -NEE \qquad (2)$$

$$GPP \approx GEE = -NEE + RE \qquad (3)$$

where NEP is net ecosystem productivity (µmol CO_2 m^{-2} s^{-1}), GPP is gross primary productivity (µmol CO_2 m^{-2} s^{-1}), GEE is gross ecosystem exchange (µmol CO_2 m^{-2} s^{-1}), and ER is ecosystem respiration (µmol CO_2 m^{-2} s^{-1}).

The energy balance closure was the method used for assessing the reliability of the NEE measurements. The energy budget was estimated as:

$$H + LE = Rn + G + S \qquad (4)$$

Where *H* is the sensible heat flux (W m^{-2}), *LE* is the latent heat flux (W m^{-2}), Rn is the net radiation (W m^{-2}), *G* is the heat flux into the soil (W m^{-2}), and *S* is the energy stored in the soil (W m^{-2}).

Sensible and latent heat flux were calculated as:

$$H = \rho_a C_p \overline{w'T'} \qquad (5)$$

$$LE = \lambda \frac{M_w / M_a}{P} \rho_a \overline{w'e'} \qquad (6)$$

where ρ_a is the air density (g mol^{-1}), Cp is the specific heat of air at constant pressure (units), w', T' and e' are the instantaneous deviations from a running mean of vertical air velocity (m s^{-1}) and air temperature (°C), and the molar fraction of water vapor (mmol mol^{-1}), respectively, and λ is the energy of vaporization (J g^{-1}).

The soil heat flux was measured with the autocalibrating soil heat flux plates (Hukseflux) buried at 8 cm depth. The energy stored in the layer above the heat flux plates was calculated as the specific heat of the soil (Cs) and the change in soil temperature (ΔTs) over the output time interval (t),

$$S = \frac{\Delta T_s C_s d}{t} \qquad (7)$$

Where *d* is the depth of the soil heat flux measurement (8 cm).

The soil heat capacity was calculated as,

$$Cs = \rho_b * C_d + \theta_v * \rho_w * C_w \qquad (8)$$

Where ρ_b is the soil bulk density (1.5 g cm^{-3}), C_d is the heat capacity of the soil (840 J $kg^{-1}K^{-1}$), θ_v is the volumetric soil water content (v/v), ρ_w is the density of water (1 g cm^{-3}), and C_w is the heat capacity of water (4.1796 J cm^{-3} K^{-1}).

Gap filling methods and flux partitioning

Data gaps shorter than two hours were linearly interpolated. Gaps larger than two hours in flux data were filled with the Marginal Distribution Sampling algorithm (MDS) (Reichstein et al., 2005), which is an enhancement of the method used by Falge et al. (2001). The MDS method is a combination of the Mean Diurnal Variation and the "Look-Up" Table methods, but takes into account the covariation of fluxes with meteorological variables and the temporal autocorrelation of fluxes. It consists in building tables of average NEE values under similar conditions of global radiation (Rg, ±50 Wm^{-2}), air temperature (±2.5°C), andvapor pressure deficit (VPD, ±5.0 hPa) for data windows of ±7, ±14, ±28 and ±56 days. The online MPI Jena tool http://www.bgc-jena.mpg.de/REddyProc/brew/REddyProc.rhtmlbased on the ReddyProc R package (The R project, 2014) was used for the gap filling procedure.

Flux partitioning of NEE was done with the same online MPI Jena tool. Nighttime NEE data is fitted to the Loyd and Taylor (1994) respiration model to estimate the ER component. Then, ER is modeled for observed air temperature along the day and is extracted from daytime NEE data and the residual is the GEE.

Environmental drivers

Daytime and nighttime NEE was modeled with a rectangular hyperbolic response function to PPFD (Ruimy et al. 1995) modified with the exponential model of respiration (Gilmanov et al. 2010)

$$NEE = \frac{\alpha * PPFD * A_{\max}}{\alpha * PPFD + A_{\max}} + R_b * Q_{10}^{(\frac{T-Tref}{10})} \quad (9)$$

Where α is the apparent quantum yield (µmol CO_2 m^{-2} s^{-1}/µmol PPFD m^{-2} s^{-1}), *Amax* is maximum photosynthetic capacity (µmol CO_2 m^{-2} s^{-1}), R_b is basal respiration at reference temperature (15 °C, µmol CO_2 m^{-2} s^{-1}), Q_{10} is the temperature sensitivity coefficient, depicting the increase of respiration rate with a 10 °C of temperature increment (calculated parameter, unitless), and T is air temperature (°C). Similar to the procedure employed by Gilmanov et al. (2010), daytime and nighttime NEE were used to fit the model. This approach accounts for the hysteresis effect observed commonly in grasslands where NEE declines afternoon even at similar PPFD values than at the morning. The model assumes that the hysteresis effect is due to the enhancement of ER as soil temperature is dephased forward from PPFD; however, other factors like vapor pressure deficit (VPD) or plant internal hydraulic constraints could be implicated on NEE reductions (Reichsteinet al., 2005). Implications on parameter estimation will be discussed.

Vapor pressure deficit was estimated as

$$VPD = ((1 - RH)/100) * e_s \quad (10)$$

Where *VPD* is the vapor pressure deficit (hPa), *RH* is the relative humidity (%), and e_s is the saturation vapor pressure (hPa), and

$$e_s = 6.1121 * \exp\left(\frac{17.502 * T}{T + 240.97}\right) \quad (11)$$

Where *T* is the air temperature.

Only gap filled values were used for nonlinear regressions between NEE and environmental drivers. Data were fitted by 1-week time window with the PROC NLIN of SAS (The SAS system, Logan, Utah, USA) using the Marquardt method. A bootstrapping procedure with replacement (Efron and Tibshirani, 1993, 1000 resamples) was used to estimate the 95% bias corrected confidence intervals of

hyperbolic response function parameters. Overlap of confidence intervals were used to detect significant differences of physiological parameters among weeks and years.

Linear models were used to test the relationship between NEE, GEE, ER and precipitation. Carbon fluxes and precipitation were integrated at different time-windows from one week to one year, and residuals of observed and calculated C fluxes of the temporal linear model were used to proof the influence of precipitation legacy effects at different time-scales.

$$Legacy = NEE_{modeled} - NEE_{observed} \qquad (12)$$

This differs from analysis in other studies (e.g., Sala et al. 2011, Reichmann et al. 2013) where legacies (residuals) are calculated from a modeled ANPP of a global trend or a long-term record of ANPP in the site. We adopted this approach because of the lack of long-term data in our site, and because we wish to advance this approach considering the overall lack of long-term NEE data around the world..

Enhanced vegetation index (EVI) data

Enhanced vegetation indices (EVI) from NASA's MODIS (Moderate Resolution Imaging Spectro radiometer) instruments were obtained for the site throughout the study period to estimate growing season length (GSL) as an estimation of green biomass. Enhanced vegetation index data of 250 m spatial resolution and 16 day time-resolution was used. A smoothing procedure with the Savitsky-Golay (Savitsky and Golay, 1964) filter was used to eliminate outliers of EVI derived from adverse atmospheric conditions (e.g. clouds and dust). Then, EVI data were linearly interpolated to coincide with daily or weekly time scales of NEE data used in the other analysis.

A similar analysis to Zhang et al. (2003) was performed to determine phenological aspects of the EVI data like the start and the end of the growing season. Each growing and senescence cycle was fitted with a pair of sigmoidal functions on smoothed EVI data, the first describing the passage of dormant vegetation to the

beginning of the growing season until a maximum of vegetation, and the last describing the senescence process from the peak of vegetation.

$$EVI_t = \frac{A_0 - A_1}{1 + e^{\frac{t - t_0}{dt}}} + A_1 \qquad (13)$$

where, A_0 is the initial background EVI value (basal EVI), A_1 is the maximum EVI value, t is the time (days), t_0 is the center of the curve, and dt is related to the slope of the curve with larger slopes indicating shallower curves.

The rate of change in the curvature of EVI_t function was used to identify phenological transition dates (Eq. A1, A2). Maximum and minimum change rates were related to transitions from approximately stable linear stages to another (e.g., the starting and the end of the growing season).

Ecosystem water use efficiency

The ecosystem *water* use efficiency was calculated as the inherent water use efficiency (IWUE) after Beer et al. (2009), which is equivalent to the leaf level intrinsic water use efficiency (WUE_i), as a proxy of carbon uptake-surface conductance relationship. This parameter has shown better coupling between C and water fluxes as an insight of being a more ecologically meaningful parameter (Kuglitsch et al., 2008).

$$IWUE = GEE_i * VPD_i / ET_i \qquad (14)$$

Where i denotes an integration time period, one day for this study. VPD_i is the vapor pressure deficit average at daylight, and ET_i is the integrated evapotranspiration (mm d^{-1}). Gross ecosystem exchange was preferred to NEE for calculating EWUE due to ER is not tightly coupled to water fluxes (Kuglitsch et al., 2009). Moreover, in the logic of deriving an analogous parameter to WUE_i, carbon assimilation is approximated by GPP from NEE partitioning (and GEE≈GPP, Beer et al., 2009).

To avoid an over representation of evaporation from the bare soil in ET measurements, data of rainy days and up to two days following the event were excluded from the analysis (Beer et al. 2009). Only days with complete half-hourly data or gap-filled with high confidence were used (Reichstein et al. 2005). Weekly IWUE estimates were obtained by averaging daily integrated IWUE. The linear relationship between weakly averaged GEE*VPD and ET was used to compare IWUE among years, being the slope the IWUE of the whole year. A homogeneity of slopes test ($\alpha = 0.05$) was used to compare IWUE conditions.

Hydroecological years

Since biological activity in semiarid grasslands is controlled by precipitation and soil water availability, in addition to the precipitation seasonality, we decided to use the concept of hydroecological year (HEY, Thomas et al. 2009) instead of calendar year, to evaluate interannual variability of C fluxes and their environmental drivers. This approach is based on the premise that there are environmental signals such as, mean air temperature or the beginning of summer precipitation that triggers changes in phenology (Thomas et al. 2009). At the study site, the first freeze in the year generally occurs in November with average minimum temperatures < 0 ºC, concomitantly with a significant precipitation decrease. Thus, we decided to consider this month as the end of the growing season and to start the HEY calendar in December. Precipitation events at the end of December can stimulate C uptake at the beginning of the following year, as was the case for 2014. Even though environmental clues that triggered the beginning and ending of the growing season are not observed at the same time each year. Displacing the beginning of the year by one month was enough to account for the winter rains at the end of 2012 and 2013, keeping years of similar length, and keeping the time-step of the analysis. Since EC measurements started in January 2011, this year only had 11 months of data; however, the absence of precipitation since August 2010 until April 2011 kept the ecosystem dormant in cold months, thus we believe that there was no significant bias in comparing 2011 as a whole year discounting the contribution of December 2010.

Seasonal time-scales separation was done dividing HEY in dry and humid seasons. The dry season comprises from December to May and the humid season from June to November. Hereafter, these time periods will be referred as winter (dry) and summer (humid) seasons. Carbon fluxes and environmental variables at each season were considered separately for legacy effects analysis.

Results

Energy balance

Closure of energy balance was > 70% for all years, with exception of the period before October, 2011, where storage and soil heat flux were not included in the balance (first slope of Fig. 2a, slope = 0.46) because soil heat flux sensors were not installed at that time. The addition of storage and soil heat flux data improved the energy closure by 10 – 46% and was better in humid than in dry conditions (data not shown). Observed slopes lower than 1 indicated that eddy covariance measurements underestimated sensible and/or latent heat fluxes.

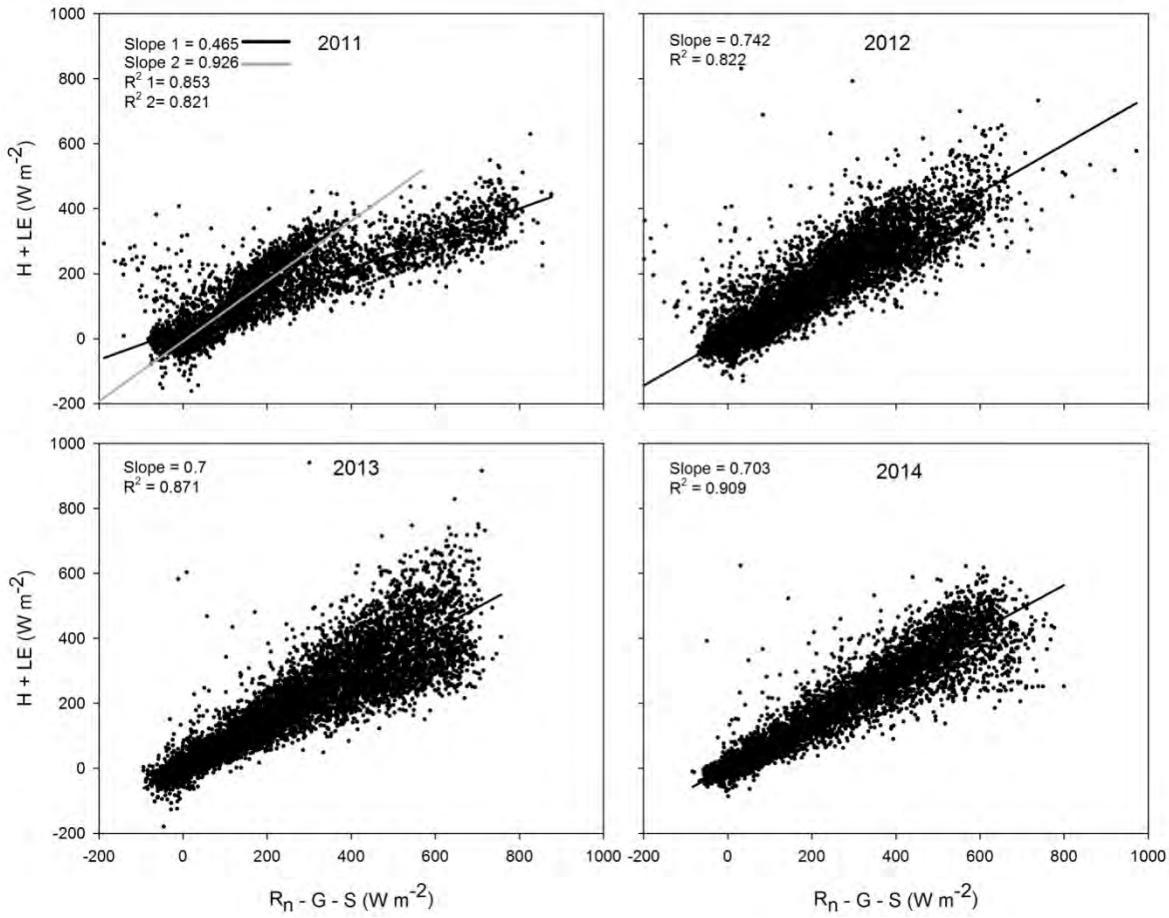

Figure 2.Energy balance for each year during the study period, including all available data. Points represent half hour energy flux data. The line represents the linear fitting between available energy and sensible and latent energy fluxes. The two lines for 2011 describe the energy balance without the addition of storage and soil heat flux (slope 1), and with the inclusion of both terms (slope 2).

Environmental variables

Daily and seasonal patterns of environmental variables were similar among years. The peak of maximum PPFD was reached at midday, whereas air temperature and VPD where dephased by 4 hours (Figure 3). Maximum daily averaged PPFD values were reached in summer (780 µmol m^{-2} d^{-1}) and the minimum was observed in winter. Mean air temperature was 16.1 ± 0.04, 15.9 ± 0.04, 16.3 ± 0.04 °C, and 15.9 ± 0.04 for 2011, 2012, 2013, and 2014, respectively (annual average ± 1 S.E.), agreeing with the historical average. The first year showed both the lowest

and the highest air temperature (-4.4 and 31.2 °C, respectively), and the largest VPD values where observed during the hottest and driest months of the year.

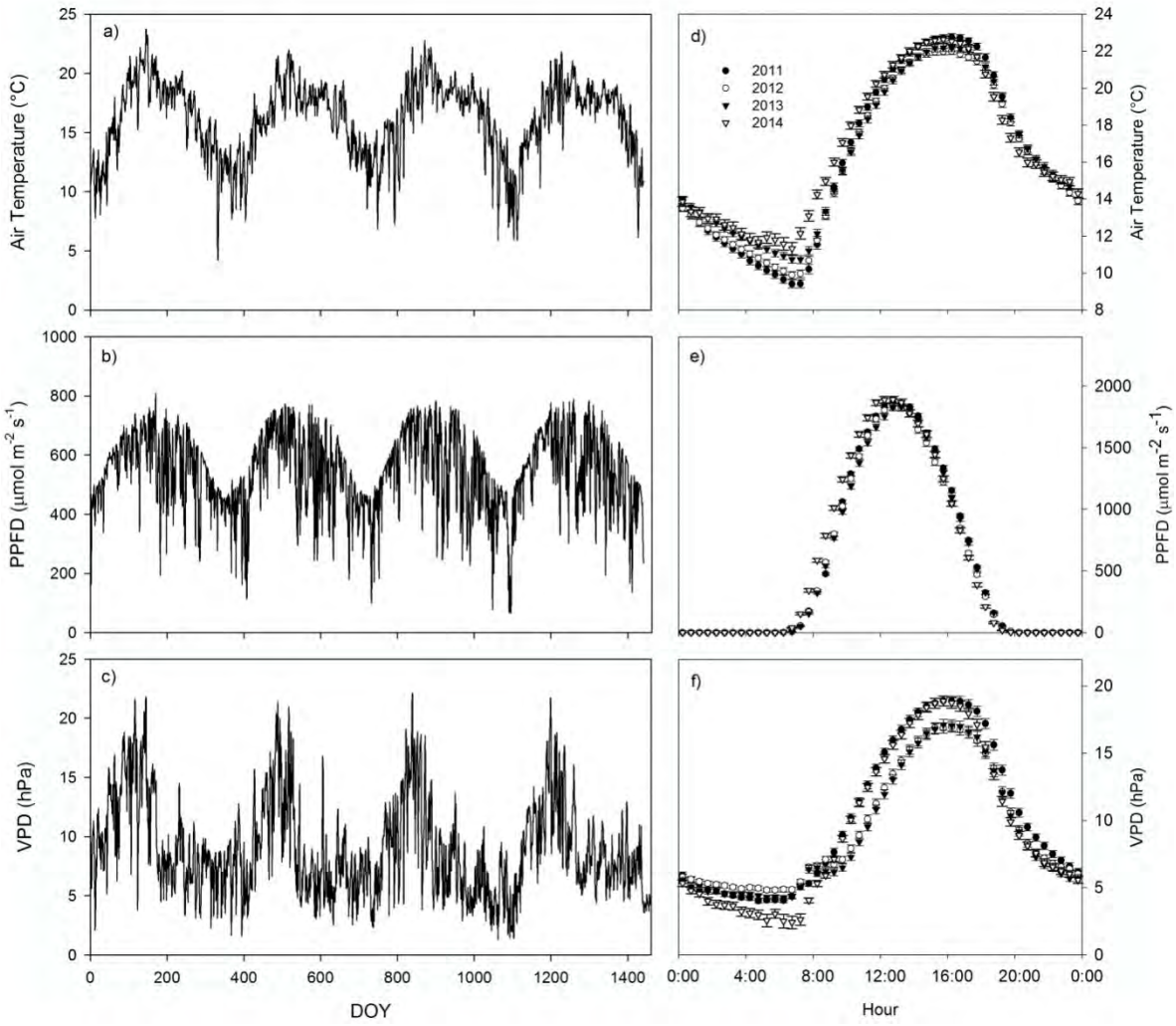

Figure 3 Interannual variation of air temperature (°C), photosynthetic photon flux density (PPFD), and vapor pressure deficit (VPD) for the study period (values are daily means). Lines represent daily mean values (a – c) and points are the average daily cycle (annual means by hour ± 1 S.E.).

The summer rain regime resulted in 95% of the rain fell during the July-September period with characteristic low fraction (~5%) during winter. However in this study, 2012 and 2014 where an exception to this historical winter precipitation pattern because winter rain accounted for 20% of total annual precipitation (Figure 4a). Cumulative precipitation for 2011 (288.5 mm) was below the 30-years average for

the site (420 mm), while 2012 was a slightly dry year (355.2 mm), 2014 was the wetter year (528.5 mm) compared to the MAP, and 2013 was the wettest year from all with 601 mm, just 100 mm below the highest historical record (700 mm in 1978). The frequency of precipitation differed across the 4 y of this study, but they were similar in the magnitude of individual rain events with more than 60% of precipitation events <5 mm (Fig. 5a); however, precipitation events > 10 mm accounted for most of the annual precipitation. The largest number and magnitude of precipitation events were observed during 2013. Volumetric soil water content at both 2.5 and 15 cm depth varied with precipitation. Maximum soil VWC (0.3, Fig. 5b) was reached several times in the 4 years within summer and at the end of winter season in 2012, but maximum VWC was maintained for short time periods. More variation in VWC was observed at shallow depths (2.5-5.0 cm), where moist-dry cycles were faster than those at 15 cm (Figure 4b).

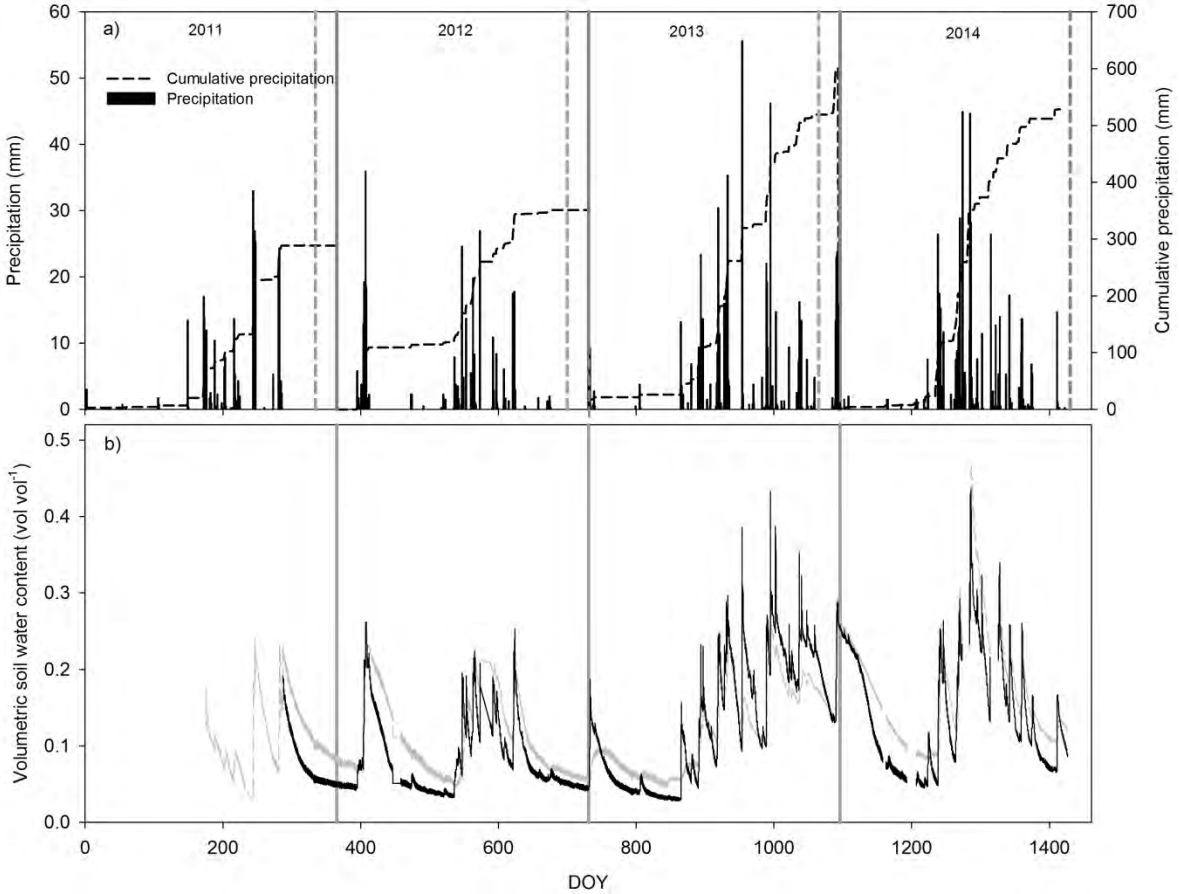

Figure 4.Seasonal and interannual variation of daily precipitation and cummulative precipitation (a), and volumetric soil water content at 2.5 cm and 15 cm depth (gray and black line, respectively, b).

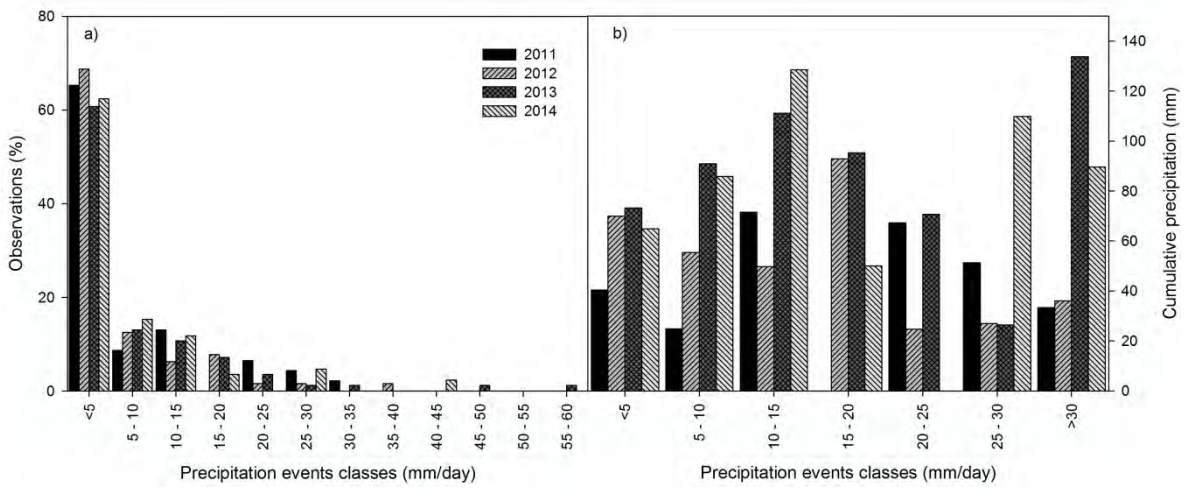

Figure 5.Distribution of precipitation events (a) and cumulative precipitation by precipitation events classes (b).

Diurnal and seasonal patterns of NEE

Diurnal patterns of NEE were characterized by a net carbon release during the night and a net carbon uptake during the day, with maximum C uptake before midday (10:00 – 11:00 h), which coincided with colder temperatures and lower vapor pressure deficit (Figure 6). During the dry months net carbon release occurred at midday.

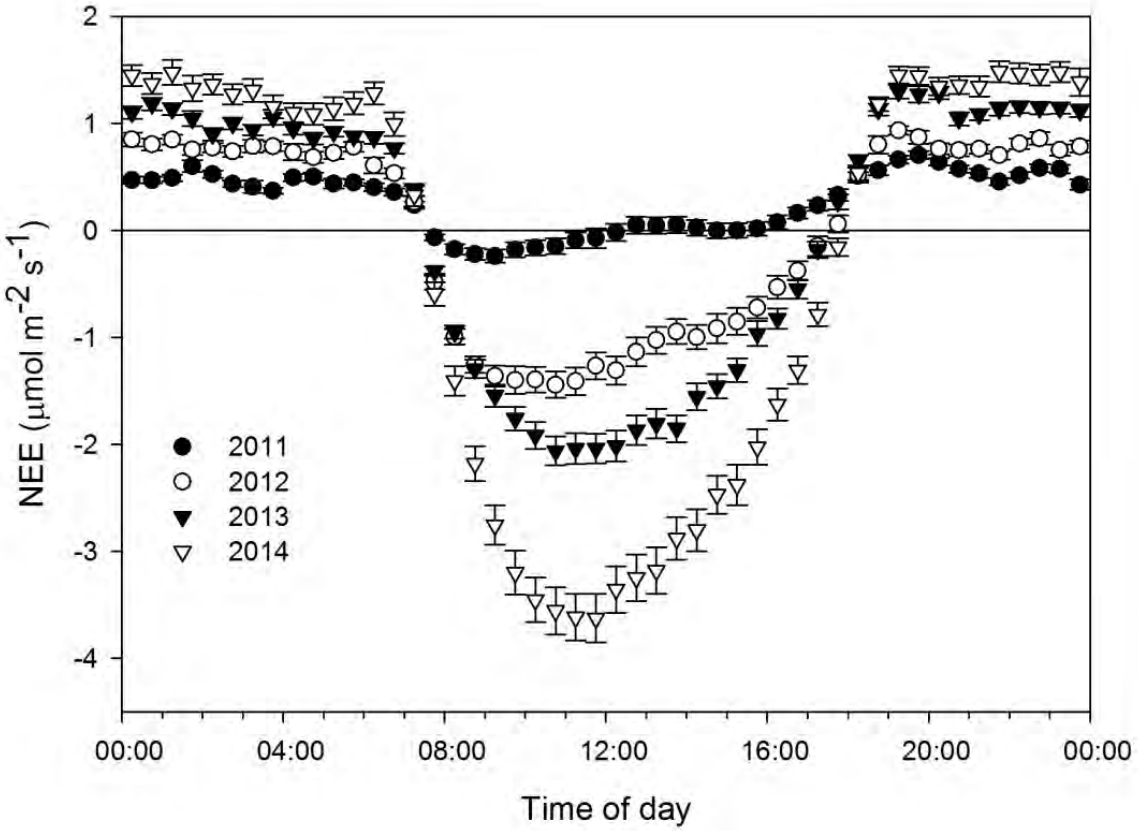

Figure 6.Whole year averaged daily course of net ecosystem exchange among years (NEE, µmol m^{-2} s^{-1}, mean ± 1 S.E.).

A marked seasonal pattern of NEE was observed for the four years. Null or net C release was observed in winter and spring where dry and hot conditions were prevalent. Some rains in May produced a net C release but not C uptake. However, a large precipitation event at the end of winter in both 2012 and 2014 triggered an important CO_2 efflux to the atmosphere, but this was followed by a net C uptake following the reactivation of grasses. In contrast, a short precipitation pulse at the start of 2013 did not trigger plant activity; instead, a large pulse of C release was observed (Figure 7).

Using hydroecological years instead of calendar years

The use of hydroecological years (HEY) as a more biologically—and synoptically meaningful division of time showing a slightly different result than the calendar year. Annual C balances in calendar years remained approximately similar among years, however annual precipitation differed significantly among years. Thus, while 2011 was the driest year it was the largest C source, whereas 2013 the wettest year (600 mm), it still was a net C source of 32.8 g C m^{-2} y^{-1}. This balance was far (-400%) from the C uptake estimated for 2014 that received 50 mm less PPT. The largest differences in the study comparing temporal schemes (calendar vs. HEY) were observed in the C balance-annual precipitation relationship. Thus, under a calendar year schema, NEE was poorly explained by precipitation (R^2 = 0.26, Fig. A1), whereas GEE and ER exhibited a close relationship (0.65 and 0.85 for GEE and ER, respectively, Figure A1). With the HEY scheme all these relationships resulted in more explained the variance (R^2 = 0.62, 0.92, 0.90 respectively, Fig. 8). However, analysis of residuals in both schemes did not show relationship with previous-year precipitation (Figs. 9, A2).

CO2 balance and precipitation legacy effects

A high precipitation variability throughout the years caused contrasting annual balances. The driest year (2011 hydroecological year, 288.5 mm) exhibited the largest C emissions with 93.82 g C m^{-2} y^{-1}. A slight net C uptake was observed in 2012 with -15.85 g C m^{-2} $y^{-1}$of C uptake, with a precipitation 50 mm below the historic MAP. Surprisingly, a very wet year (2013, 523.4 mm) showed a net C release of 16.37 g C m^{-2} y^{-1}, even though the site received 70 mm above MAP, and 120 mm more than 2012, whereas the wettest year (2014, 610.4 mm) coincided with the largest C uptake of about -121.02 g C m^{-2} y^{-1} (Fig. 7). Annual precipitation was linearly correlated to annual C balance, explaining 63% of NEE variability, but the individual NEE components displayed better correlation. Annual precipitation explained more than 90% variability of GEE and ER (Fig. 8).The response of GEE to precipitation was 50% greater than the one observed for ER (slope = 1.539 g C m^{-2} y^{-1} $mm^{-1}$and 1.084 g C m^{-2} y^{-1} mm^{-1} for GEE and ER, respectively).

The relationship between NEE residuals (legacies) and previous year precipitation was not significant (R^2 = 0.041, P > 0.05. Fig. 9). A similar scenario was found for GEE and ER legacies, where relationship between GEE and ER residuals were also not correlated with previous-year precipitation (R^2 = 0.016 and 0.031, for ER and GEE, respectively P >0.05). In contrast, when data was at the seasonal-HEY time-scale (Dec-May and Jun-Nov) current PPT explained only 34% of NEE variability (Fig. 10a), and 95% and 85% for ER and GEE, respectively (Fig. 11a), which were similar to annually-integrated C fluxes-PPT relationships. Residuals of NEE, ER and GEE during the summer season were strongly correlated with the dry season PPT that corresponds to winter PPT (First slope of Fig. 10b and 11b). Precipitation of the winter season strongly controlled the C balance of the following summer season. Hence, a wet winter enhanced C uptake (negative NEE) of the 2012 and 2014 summers, while dry winters decreased C uptake (from expected precipitation) in 2011 and 2013. This occurred even though summer 2013 was the wettest period of the four years (466.3 mm). In contrast, residuals of winter NEE were not correlated with precipitation of the previous summer season, but C-fluxes were more related to current PPT (Fig. 10a and second slope of Fig. 10b and 11b). Slopes for ER and GEE for half HEY followed the same pattern than for whole years. Ecosystem respiration responded slower than GEE to PPT, but the pattern was most linear than hyperbolic as was hypothesized (Figure 11a). The difference between slopes was more evident for residuals, where summer GEE rose faster to winter PPT than ER (Fig. 11b).

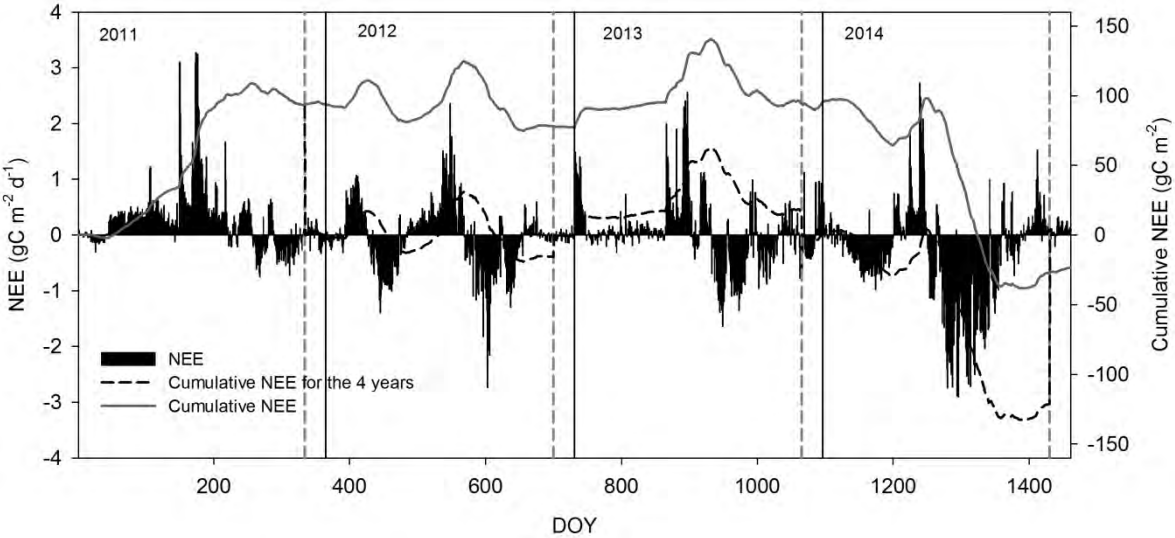

Figure 7.Seasonal and interannual variation of integrated NEE (black bars, g C m^{-2} d^{-1}), and cumulative NEE for each hydroecological year (HEY, dashed lines) and across the calendar year (solid lines). Vertical solid lines represent the division between calendar years, whereas dashed vertical lines stand for HEY divisions.

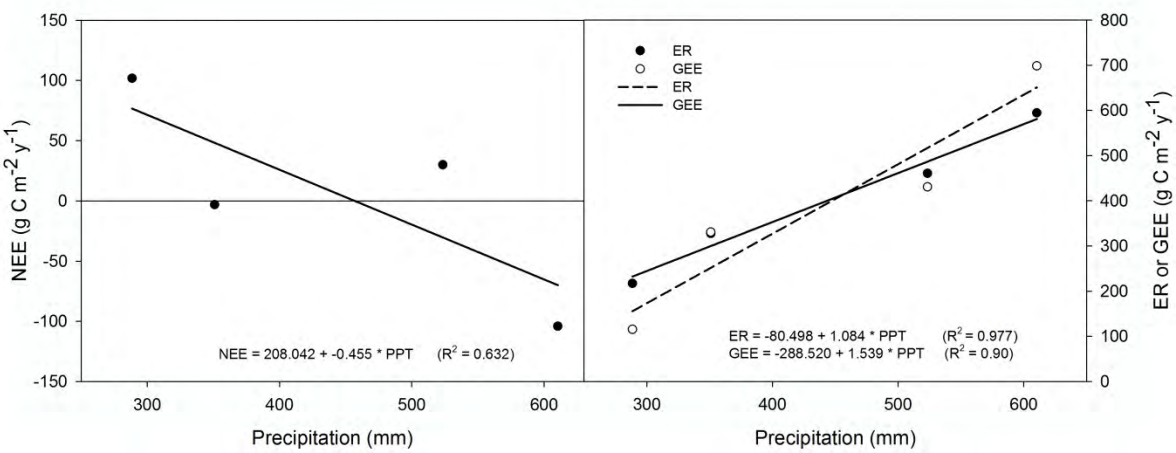

Figure 8.Linear relationship between annual precipitation and annually integrated NEE (a) and NEE partitioned fluxes (GEE and ER) (b).

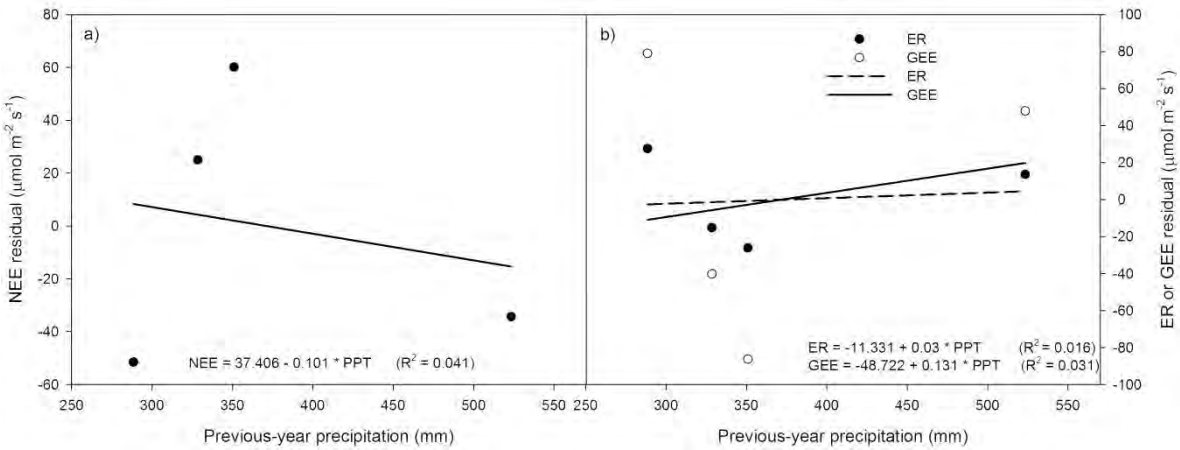

Figure 9.Legacy effects of previous precipitation year. Points represent legacies calculated with Eq. 9, and lines show the linear fitting between legacies and previous-year precipitation.

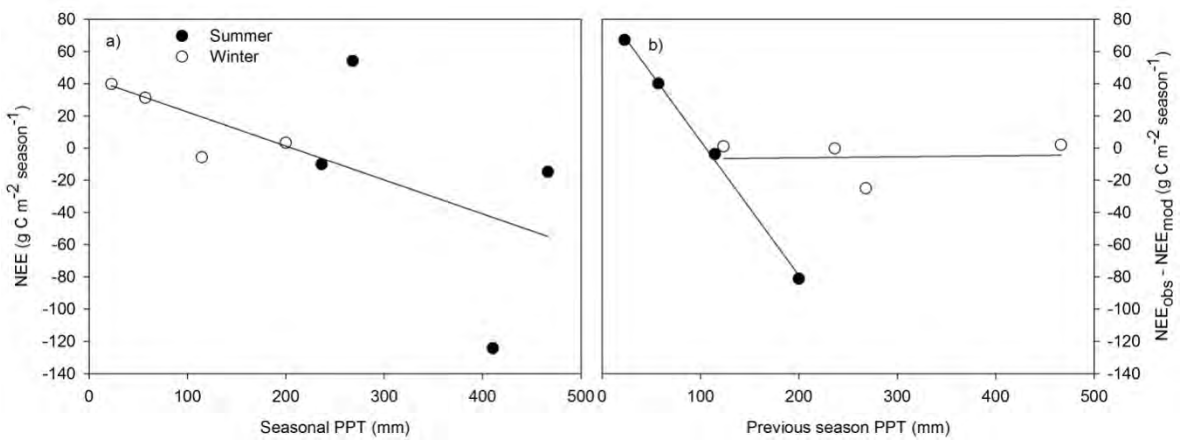

Figure 10.a**)** Relationship between NEE and current PPT for half hydroecological years (Dec – May, and Jun – Nov), and b) relationship between residuals of NEE-current PPT model and previous half-HEY period PPT. White dots stand for December-May period (winter-spring), and black dots stand for June-November periods (summer-fall).

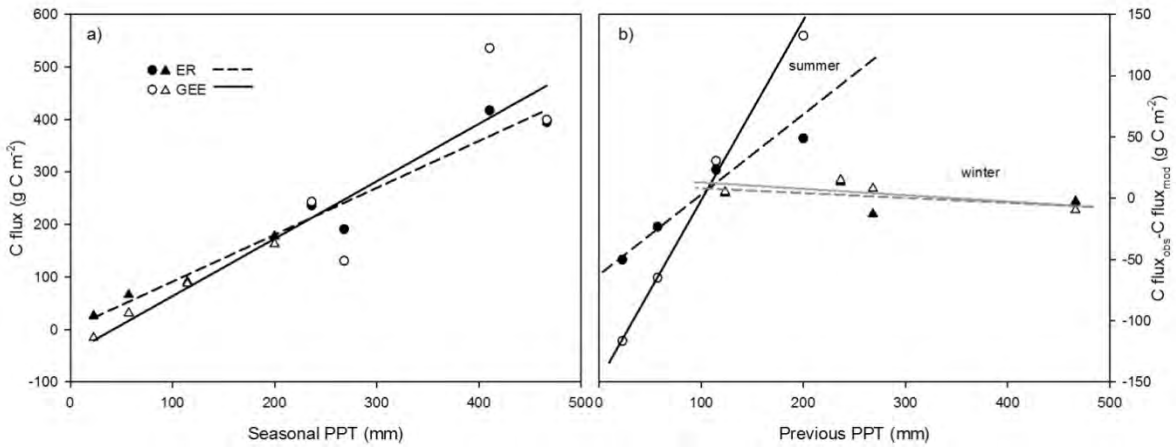

Figure 11. a) Relationship between Ecosystem respiration (ER), gross ecosystem exchange (GEE) and current half-hydroecological year PPT, and b) relationships of residuals of ER and GEE and previous half-HEY period PPT. White dots refer to winter-spring and black dots refer to summer-fall periods.

Environmental drivers

The modified light response curve (Eq. 8) at week time-step intervals explained > 60% of NEE variability for all years. The lowest correlation was observed in 2011 with a R^2= 0.67 increasing along the years until reaching a value of 0.9 in 2014 (Fig. 12). Slopes < 1 for all years indicated underestimation of photosynthesis and respiration, dampening the peaks of both fluxes.

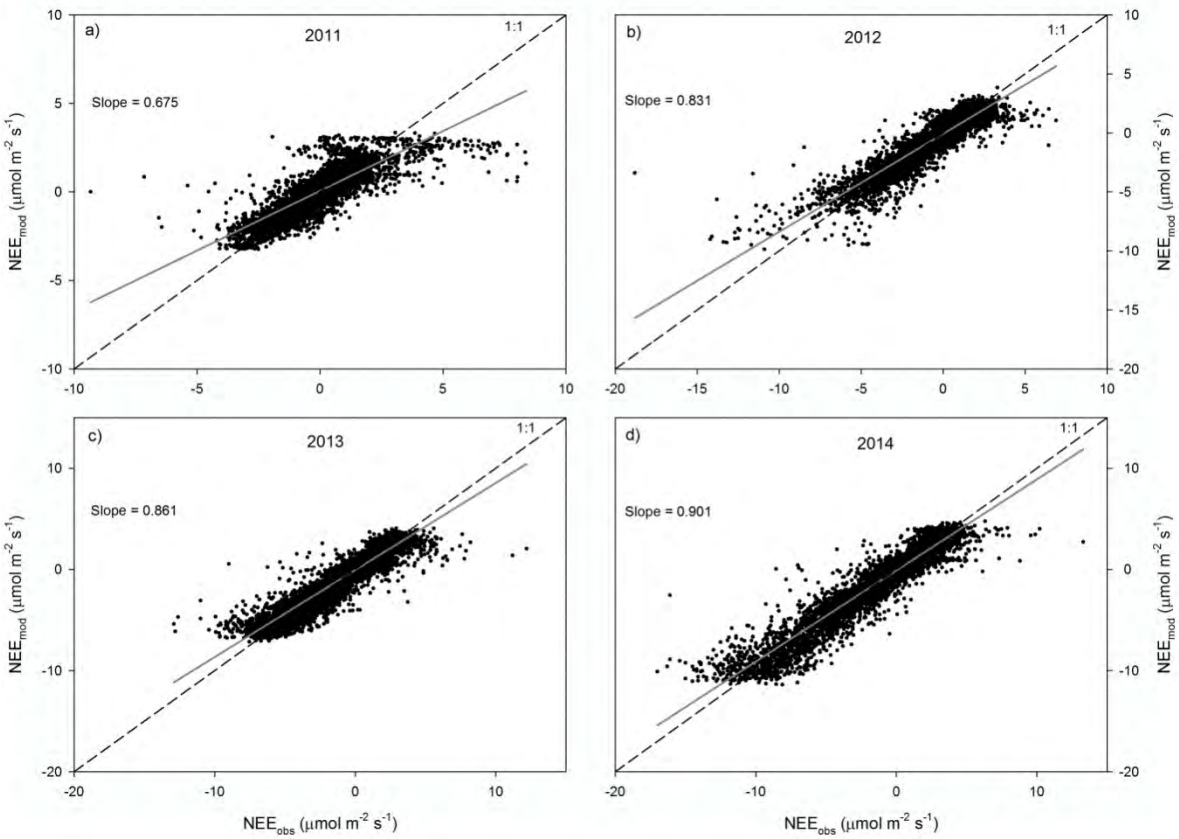

Figure 12.Observed and modeled NEE fluxes for each year. Solid gray lines represent the linear fit between observed and modeled NEE whereas the dashed lines stand for the 1:1 relationship.

Apparent quantum yield (α) followed a similar course through time for all 4 years (Fig. 13a). Maximum α values were observed at the peak of the growing season at week 33 for 2011 – 2013 and week 27 for 2014 ($-0.0426^{-0.0199}_{-0.0953}$, $-0.0266^{-0.0196}_{-0.0330}$, $-0.0216^{-0.0168}_{-0.0265}$, and $-0.0247^{-0.0208}_{-0.0289}$, for 2011, 2012, 2013, and 2014, respectively. Mean values with BICs). All these values were lower than the mean alpha (α = 0.06 mol mol^{-1}; Ehleringer and Pearcy, 1983) measured in C4 grasses at leaf level at 30 °C. Notwithstanding the wet winter periods of 2012 and 2014, α did not increase, in contrast with maximum photosynthetic capacity (Fig. 13b) and basal respiration (R_b, Fig. 13d). Overall, 2014 showed an earlier increase of the parameter response starting at week 20 with the largest Amax and R_b of the four years. .. Lower respiration rates were recorded in 2011 and 2012, however, they

exhibited some similarity, e.g., stimulated by precipitation pulses as the ones observed at the start of 2014.. The sensitivity of respiration to temperature (Q_{10}) remained almost invariable around a value of 2 across time and did not differ among years (Fig. 13c). Some peaks of $Q_{10} > 4$ were likely a result of enhanced respiration rates that followed precipitation pulses. Since these respiration pulses are transient, lasting only for a couple of days, the time step of one week of the analysis produced very large confidence intervals suggesting no significant difference respect to the mean trend.

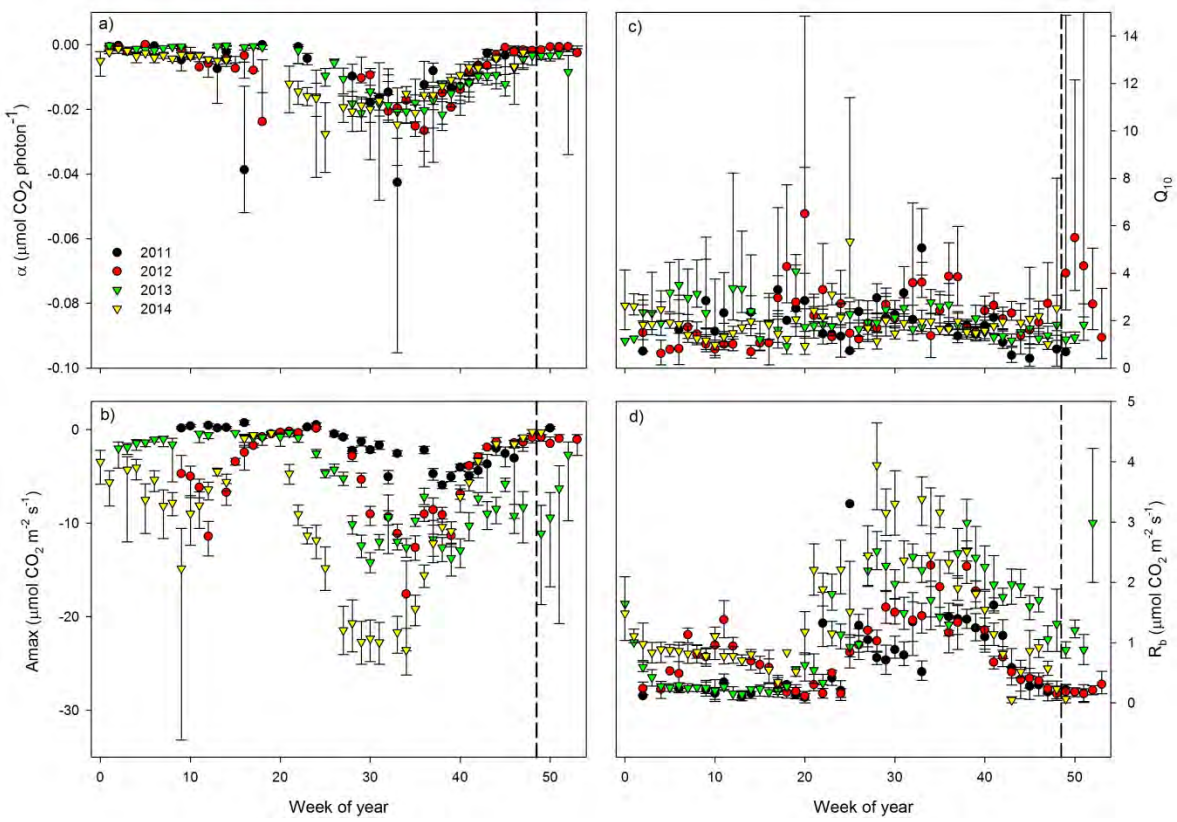

Figure 13.Seasonal and interannual variation of physiological parameters obtained from the modified light response curve (Eq. 8). Points are weekly mean values ± 1 S.E. of apparent quantum yield (α, a), maximum photosynthetic capacity (Amax, b), respiration sensitivity to temperature (Q_{10}, c), and basal respiration at 15 °C (R_b, d). Vertical dashed lines stand for the end of the hydroecological year (HEY, at week 48) and the beginning of the next year.

Enhanced vegetation index (EVI)

The enhanced vegetation index showed a positive linear correlation with GEE, explaining more than 70% of GEE variability ($P < 0.05$, Fig. 14). The HOS test showed differences in the response of GEE to EVI with the largest rate of change observed in 2014 (19.83 ± 0.92 g C m^{-2} d^{-1} EVI^{-1}), which was larger than 2012 and 2013, and similar to 2011 (15.3 ± 1.38, 16.29 ± 0.79, and 19.70 ± 1.83 g C m^{-2} d^{-1} EVI^{-1}, respectively). Years presenting winter precipitation showed a clear initial larger slope during this wet period that stands out for the rest of the year (Fig. 14). Ecosystem respiration also showed a positive linear relationship with EVI ($p<0.05$, $R^2>0.70$, data not presented), but the rate of change did not differ among years. Even though NEE was significantly correlated with EVI ($p<0.05$, except for 2011), correlation coefficients were overall low 0.58, 0.18, and 0.17, for 2014, 2013 and 2012, respectively. Whereas, length of the growing season was negative-linearly correlated with annual NEE ($p<0.05$, $R^2=0.81$), with a rate of change of -1.6 g m^{-2} y^{-1} of C uptake per additional day of growing season (Fig. 15).

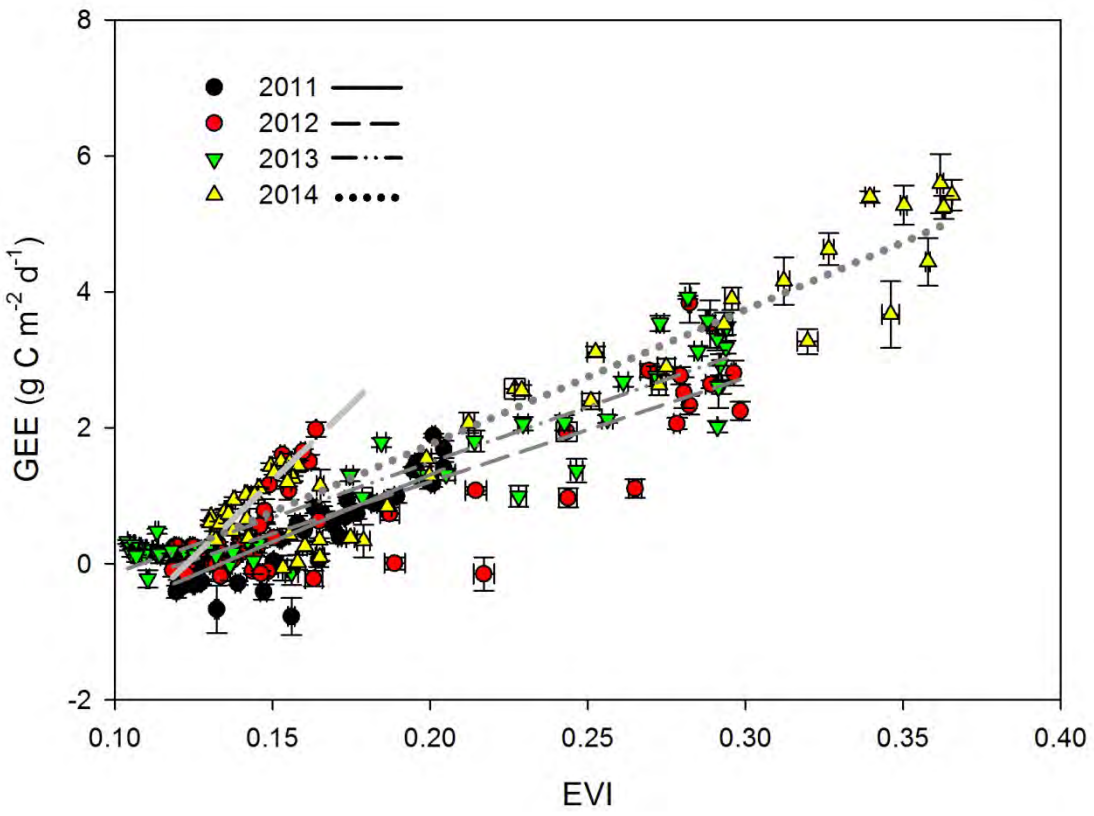

Figure 14.Relationship between Enhanced Vegetation Index (EVI) and gross ecosystem exchange (GEE, g C m^{-2} d^{-1}) for eachr year. Points indicate weekly means (±1 S.E.), and lines are the lineal fittings. The shortest line with steeper slope in light gray colour that stands out from the rest, describes the trend of the relationship observed during the winter growing season of 2012 and 2014.

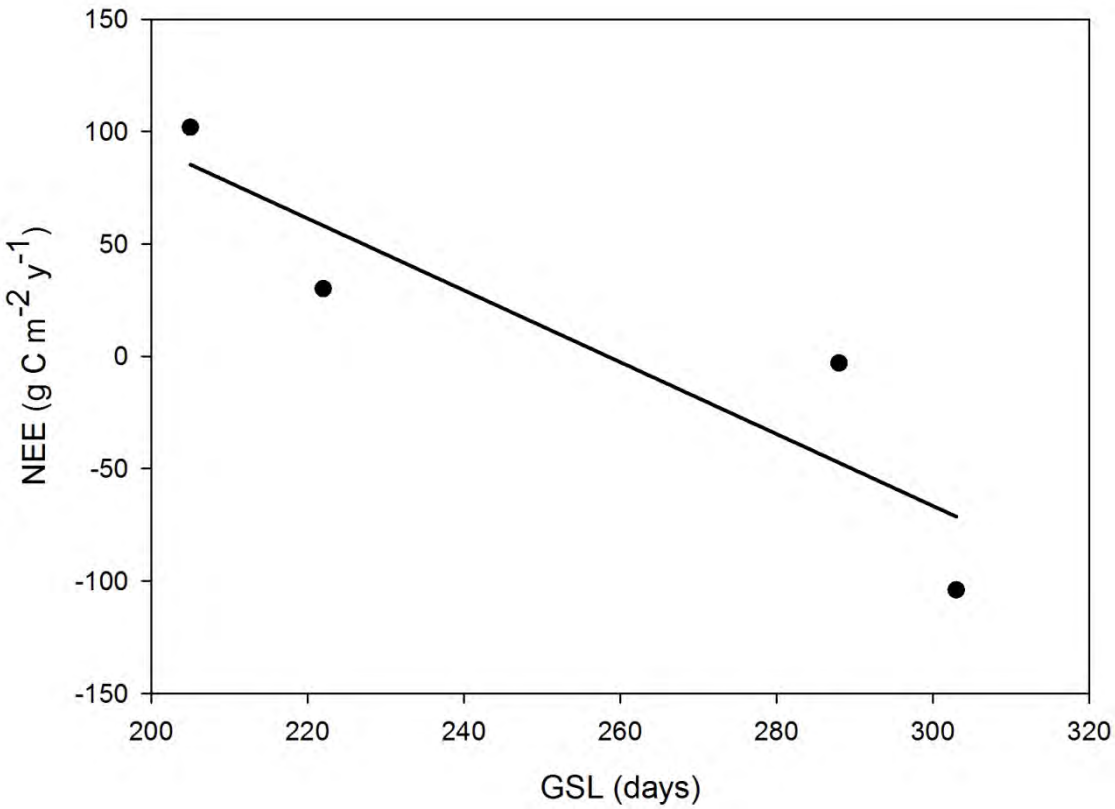

Figure 15.Relationship between the growing season length (GSL, days) and the annual net ecosystem exchange (NEE, g C m^{-2} y^{-1}).

Inherent water use efficiency

The semiarid grassland was more efficient for water use in 2012 (IWUE = 21.6 ± 0.74 g C hPa / kg H_2O) and 2014 (19.5 ± 0.83 g C hPa / kg H_2O) during winter and spring, however IWUE was similar in summer among all years, except 2014 that showed the largest IWUE values (maximum IWUE = 22.44 ± 0.83g C hPa / kg H_2O, Fig 16a). The grassland ecosystem reached highest efficiency at the middle of the growing periods regardless of whether it was winter or summer (Fig. 16a). The homogeneity of slopes analysis revealed that 2014 exhibited more water use efficiency compared to the other years ($F=97.04$, $p<0.05$, Figure 16b).

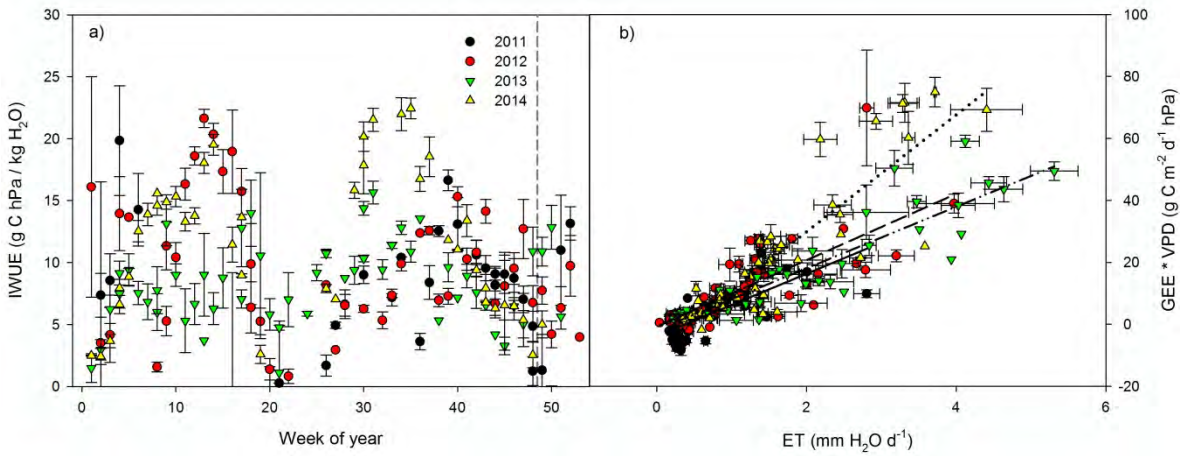

Figure 16.Seasonal and interannual variation of inherent water use efficiency (IWUE, g C hPa / kg H_2O, means by week ± 1 S.E.). Vertical dashed line in plot represents the division of hydroecological years (a). Relationship between the weekly averaged GEE * VPD (g C m^{-2} d^{-1}hPa ± S.E.) and ET (mm H_2O d^{-1} ± S.E.) for 2011 ___, 2012 _ _ _, 2013_._._, and 2014 .... (b). Only IWUE values for growing periods are shown.

Discussion

Energy balance

The energy balance in the site underestimated the amount of total available energy during the four years of the study; however, the energy closure was just slightly below the mean reported by FLUXNET sites (0.79 ± 0.01, Wilson et al. 2002; 0.84 ± 0.2, Stoy et al. 2013) with estimates ranging from 0.53 to 0.99 (Wilson et al. 2002). Lack of closure is a common problem in eddy covariance systems and it has been recognized as some combination of; i) different footprints measured by EC and radiation sensors, ii) low frequency transport (Malhi et al. 2005), iii) heat storage above the heat flux plates, iv) convection and coherent structures effects on coordinate rotation of anemometer (Foken et al. 2005), v) wave phase differences between soil surface heat flux, net radiation, and turbulent heat fluxes (Gao et al. 2010), vi) different eddy diffusivities for water, temperature and other scalars, i.e., CO2 (Shaw 1985), and vii) all the error terms in the sonic vector calculations are included into the vertical velocity (w) component (Frank et al

2013). In this study, closure of energy fluxes improved as years became wetter (higher fraction of LE) and with the addition of soil heat flux and storage, therefore it is likely that the largest bias was caused by soil heat fluxes. Heat flux measurements using soil heat flux plates just below the soil surface (buried ~1 mm depth) increased the energy balance closure by 20% in a sandy desert (Heusinkveld, 2004).

Environmental drivers

Solar radiation, measured as photosynthetic photon flux density, and air temperature explained in the short time the largest proportion (>70%) of NEE variability for the semiarid grassland (half hourly fluxes in a weekly scale). Both climatic factorshave shown to largely contribute toNEE variabilityat the short-temporal scalein a diversity of ecosystems from drylands to humid forests (Lal et al., 2002; Gilmanov et al. 2010; Yi et al., 2010). Interestingly, diurnal peaks in NEE were observed before the largest PPFD incidence (around midday), with larger C uptake during the morning than after midday even when similar PPFD conditions occurs, suggesting more water limitations in the afternoon (stomatal closure). This hysteresis effect has been observed elsewhere and is owed to; 1) high air temperature and VPD, and lack of available surface water produces stomata closure and subsequent photosynthesis dampening, or 2) the stimulation of soil respiration due to increased soil temperature that is out-of-phased from PPFD driven rates of photosynthesis (Lasslop et al. 2012, Phillips et al. 2011). Some reports indicate that grasslands around the world experience diurnal hysteresis (Gilmanov et al. 2010). Also Delgado-Balbuena et al. (2013) reported the same effect, however it was argued to be a consequence of the large abundance of herbaceous plants, with C_3-metabolism and a trend for photorespiration at high temperatures (~35 °C, as observed in summer) (Lambers et al. 2008). In this study for 2012 and 2014, we also observed a massive germination and growth of herbaceous C_3 plants during the growing season; however, there was no evidence of decreased apparent quantum yield and maximum photosynthetic capacity (Figure 13), implying that additional growth in C_3 plants did not contribute to the

observed hysteresis. The use of the modified light-response model (Eq. 8) incorporated the hysteresis effect.

Large uncertainty of ER estimation has been a common problem of different modeling approaches and several ecosystems (Moffat et al. 2007, Yan et al. 2015). Low correlation coefficients between ER and temperature, particularly in the dry season, suggest that soil water content was the main ER driver, leaving temperature as a secondary control when the ecosystem is not water limited. For instance, Delgado-Balbuena et al. (2013) showed that both soil volumetric water content (VWC) and air temperature acted as main controls for ER at monthly scales. The inclusion of VWC as additional factor for the light response curve of this study did not improve ER estimates. Soil water content was correlated with nighttime NEE (=ER) at larger time-scales (e.g. weakly) as used for light-response curves (Fig. A5) and the relationshipwas strongest in humid conditions. EVI however, as a proxy of plant biomass, was more correlated to ER than the one observed to VWC (Table A2), and both variables explained more than 80% of nighttime NEE variability for all years (Fig. A5). This implies that in this semiarid ecosystem during the growing season, either; 1) autotrophic ER component was dominant, or 2) root exudates stimulated the heterotrophic ER component. In this way, soil moisture exerted an indirect control that stimulated soil microorganisms activity at short-time scales making nutrients available and also triggering delayed plant (Vargas et al. 2010). The paradigm of temperature as main driver of soil respiration has been recently challenged in several studies, suggesting that nutrients (Huang et al. 2015), soil organic matter quality (Billings and Ballantyne, 2013), and plant biomass (Chen et al. 2014) are the key controls of soil respiration rates (biotic factors). This notion was supported when the light-response curve was fitted to monthly time steps using EVI as an additional variable. The model explained >60% of NEE variability, which was slightly lower than the model using weekly timesteps (data not shown).

Implications for the use of whole day data in light-response curve models

Several modifications to the light response model have been carried out since Ruimy et al. (1995) first proposed it. Including the addition of temperature into the respiration model considers the diurnal variability of ecosystem respiration as a function of the diurnal cycle of air or soil temperature. This is an improvement to the model because respiration is not constant throughout the whole night but varies with temperature. However, the model does not address the differences in daytime and nighttime respiration rates when 1) ER is overestimated at daytime because of light inhibition of leaf mitochondrial respiration (Kok effect, Heskel et al. 2013), 2) high VPD reduces photosynthesis, however it is interpreted by the model as an increase of respiration, overestimating ER at the time when it is extrapolated to night time, and 3) photosynthates allocation from shoots to roots is a delayed process that positively impacts ER at the end of the day (Vargas et al. 2011), further stimulating ER, but results in a potential bias during the night. These phenomena were likely observed at the site for all four years as a slight peak of positive NEE (efflux) just before falling the night (18:00-19:00 h, Fig. 6). By using the whole day NEE to fit the light-response curve we likely adjusted for differences between daytime and nighttime ER; nevertheless, ER was underestimated in all years (Figure 12).

NEE responses to PPT

The semiarid grassland showed a large range in interannual NEE. The ecosystem behaved as C source (1017.3and 299.7 kg C ha^{-1} y^{-1}, for 2011 and 2013, respectively), sink (-1040 Kg C ha^{-1} y^{-1}, 2014) and almost neutral (-31.5 kg C ha^{-1} y^{-1}, 2012) during the study period. These annual C flux rates are low but are in the range of values reported for other grassland ecosystems including from the short grass to tall grass (+400 to -800 g C m^{-2} y^{-1}, Novick et al., 2004), and just in the range of other semiarid grasslands (-164 to 210 g C m-2 y-1, Emmerich, 2003, Mielnick et al., 2005, Archibald et al. 2009, Rajan et al., 2013). Annual carbon balance differences among years resulted from the large differences in both annual total precipitation as well as precipitation distribution (Figs. 4, 5). In examining the

role of precipitation closer, we had a precipitation gradient going from the lowest (2011) to almost the wettest in modern records (2013 and 2014). In addition, we also observed distinctive precipitation distributions with two years exhibiting dry winters (2011 and 2013) and two years with wet winters (2012, 2014). In synthesis, highest C emissions were recorded during the drought year (2011); however, the other year with a dry winter (2013) also contributed with 300 Kg C ha^{-1} y^{-1} to the atmosphere despite of having the highest precipitation record during the study (Fig. 4). While years with wet winters behaved as either a neutral (2012) or as C sink (2014), in this last case capturing around 1 ton C ha y^{-1}. Thus, in a broad temporal view balancing wet and dry years, this semiarid grassland comply more to a neutral system agreeing with global trends for grasslands (Novick et al., 2004).

Precipitation legacies

Since we argue that precipitation is the main driver of interannual productivity, then it should also control C fluxes in dryland ecosystems. In our site, NEE was negatively related to annual precipitation with highest C capture occurring in the wettest years (Fig. 8), while GPP and ER were positively related to annual PPT displaying highest rates in wettest conditions. Still, examination of annual C balances in relation to previous years precipitation showed that two drought years (2010 and 2011, the last being the most severe drought in the past 70 years) did not appear to negatively affect C uptake for 2012 (Fig. 7). In fact, these previous dry years apparently stimulated C uptake by the grassland, contrary to expectations from our H_2 (Fig. 9a). In opposition, the C balance for 2013, the wettest year, that was preceded by an average precipitation year turned out to be a small C source (30 g C m^{-2} y^{-1}, Fig. 7). Whereas, a wet to wet transition from 2013 to 2014 contributed to enhance C uptake in 2014, which is more in agreement with the positive PPT – C balance effect (H2, Sala et al., 2015). Discrepancies that have been reported between spatial and temporal scales of the productivity-PPT relationship have being attributed to legacy effects. Precipitation legacy hypotheses proposed carry over effects of precipitation from one year to the next either reducing or enhancing current year relative to expected productivity

estimated with current year precipitation. In this study, when analyzing residuals (legacy effects) of C balance (NEE, GEE and RE) - annual PPT relationship, resulted in non-linearly correlated when using previous year PPT as it should be expected from legacy effects hypothesis 1 suggested by Sala et al. (2012) (Fig. 9).

However, when PPT legacy effects were considered at seasonal scale, winter PPT showed a negative relationship with summer C balances as was hypothesized (H1); in contrast, winter C balances were not responsive to the preceding summer PPT (Figure 10). Similar close relationships were observed on NEE components, as GPP and ER maintained a close relationship to preceding winter PPT (Fig. 11).Winter precipitation in these predominantly summer-rain ecosystems turned out to be more important than thought, based on the average 6% of winter rain contribution to the total annual precipitation.

According to these results, wet winters promote C uptake in the following summer as postulated by the wet to dry transition (H2, Sala et al., 2013). For instance, the very wet winters of 2012 and 2014 promoted net C uptake in the following dry and wet summers, whereas the small winter precipitation of 2011 and 2013 diminished C uptake for the following summers (2011 and 2013). This response corresponds to the hypothesized (H3) switch from dry to wet conditions (Sala et al., 2013). The effects of these legacies are likely related to changes in green biomass and plant cover. For instance, the enhanced vegetation index (a surrogate of green biomass) showed a quasi-continuum period of growing vegetation, all the way from the occurrence of winter rain to the beginning of summer PPT (Fig. A4). Also, basal EVI values (A_0 parameter of summer curves of Eq. 4, Table A1) were higher when they were preceded by a winter growing period, indicative of remnant green/active vegetation. The lowest A_0 observed between the summers of 2012 and 2013 (as no winter growing season was observed) can be interpreted as the full senescent vegetation state. During this period, the basal EVI was lower than that observed in 2011, likely as a consequence that senescent leaf biomass reflecting more radiation than bare soil as was observed in spring 2011 as a result of plant cover lost. These results agree with Sala et al. (2012) and others (Reichmann and Sala

2013, Reichmann et al., 2012) that suggest the legacy precipitation effects are a consequence of structural and community composition changes. Larger shoot and root biomass as well as plant recruitment after a wet year persists and then assist for a better exploitation of resources on the next year, in contrast to dry years that cause biomass lost due to plant mortality and slower plant growth. Another evidence for precipitation legacies comes from previous studies at this site showing slight correlation of plant cover with winter PPT, but null relationship with annual or summer PPT (Aguado-Santacruz, 1993). Reports on other semiarid grassland sites, have showed strong correlation between winter PPT and productivity (Robertson et al., 2008), while Robertson et al. (2010) also exhibited control of winter PPT on grass cover density in the same ecosystem.

What are the possible mechanisms that explain this clear effect on productivity due to this small amount of rain that is received when the vegetation is dormant? The strong seasonal characteristics of native grasses from semiarid grasslands, contributed to the evolution of mechanisms of carbohydrates translocation from shoots to crown and roots before entering dormancy of the aboveground biomass at the end of summer and early fall at the end of November, used as criteria to set the hydroecological years; Sarath et al. 2014). First, this mechanism prevents dehydration that could lead to grasses death in a prolonged drought. The amount of reserves will depend on the amount of humidity from the preceding winter-spring period since that would greatly determine productivity the next growing season because these reserves are used for refoliation (Volaire and Norton, 2006). *Bouteloua gracilis*, the dominant species of the semiarid grassland, withstands seasonal drought through an incomplete dormancy or partial senescence (Arredondo, personal communication) leaving active green tissue at the tussock base. This characteristic also observed in other grass species (Volaire and Norton, 2006) allows rapid plant responses following a rain pulse. Thus, it is likely that winter rains acts as a mechanism to “ameliorate the decaying of physiological conditions” permitting grasses to maintain their meristems alive for up to 6-7 months of drought. At the same time, it allows grasses a rapid refoliation response after summer precipitation starts.

These differences in the refoliation response to the start of PPT were evident with the parameters of Eq. 4 that describe the rate of change of EVI (interpreted here as refoliation rates), in the transition from senescence to the peak of the growing season (*dt*, and the slope of the curve at t_0, Table A1). Here, refoliation rates for the 2011drought period and for the two wet winter periods in 2012 and 2014, showed 5-fold lower rates than the ones observed for the summer-growing seasons of 2012 – 2014. Rates of change for winter EVI likely were also limited by temperature or other environmental factors (e.g. amount of PPT, temperature) since summer EVI slope in 2013 was large, similar to summer 2012 and 2014 even when winter rains were almost absent.

Dynamics of soil water content at 15 cm depth are another factor that may be implicated in differences of C balances among years. Winter precipitation in 2012 and 2014 was large enough to recharge deep soil layers, to the point that it was available for plants at depths were grasses have their largest root biomass (between 10 and 30 cm; Medina-Roldán, 2007; Delgado-Balbuena et al., 2013). In addition to promote plant growth in winter-spring seasons, winter PPT contribute to maintain VWC at lower stresslevels for plants (e.g. above 10%), likely helping to the large refoliation rates as discussed above.

Soil biogeochemical changes between dry-wet or wet-dry transitions are other plausible causes of precipitation legacies in this ecosystem. Soil nutrients particularly nitrogen are scarce in semiarid grasslands (Lauenroth and Burke, 2008) and their availability is also controlled by soil water (directly related to precipitation). The dynamics of soil nitrate (NO_3^-) content in our site shows an increase at the end of the summer growing season, whereas ammonium (NH_4^+) decreases (Muñoz-Flores et al., 2014). Nitrogen mineralization is not dependent on soil moisture but its mobilization, thus NO_3^- accumulates in the soil during drought. No evidence for this legacy mechanism was found for winter – summer seasons (or is negligible respect to structural changes), but a slight effect is likely to occur from summer to winter seasons (Fig. 10ab). Accumulation of nitrate in soil during droughts and between summer-winter periods serves to increase efficiency of

green biomass to fix C as was observed in the 2-fold larger slopes of EVI-GEE relationship in winter 2012 and 2014 (largest slopes of Fig. 14). This higher C uptake per EVI unit was due to the maximum photosynthetic capacity (A_{max}) of winter that was similar to the one achieved in summer 2011 – 2013 (Fig. 13b) even when winter EVI peaks are half and a third of summer peaks .

Moreover, a high inherent water use efficiency (IWUE, Fig. 16a) in winter appears to be related to a larger N availability, as a consequence of major plant investment in their photosynthetic apparatus rather than in reductions of water loss as was evidenced by the high Amax (Ripullone et al., 2004). Thus, since maximum photosynthetic capacity and IWUE are plant traits linearly related to leaf nitrogen content (Lambers et al., 2008; Livingston et al., 1999), these results suggest a nutrient mediated slight negative legacy precipitation effect of wet summers to winters that is in agreement with linear negative hypothesis of Sala et al. (2012). The opposite trend for the slopes (no statistically significant) between summer season PPT – winter C fluxes (positive for NEE and negative for GEE and ER, Fig. 10b and 11b) describe this legacy effect. Also, the fast revegetation rates reported for summer 2013 were likely influenced by nitrogen accumulation in soil after six months of drought. We can conclude that is likely that biogeochemical legacies operate in this ecosystem, but structural vegetation changes (in leaf area) are dominant and mainly determine the dynamics of PPT – C balance response in the semiarid grassland.

Shorter than one year precipitation legacies observed in this study are in agreement with other studies; for instance, Craine et al. (2012) reported short-lasting effects of drought and heat waves on productivity of a humid grassland (<4 months for the former and 25 days for the last) with no clear effects at the end of the growing season. In another study in the mixed-praire, precipitation has the strongest effects on NDVI just after 40 days (Li and Guo, 2012). Jobbágy et al. (2002) on the other hand, showed two months delay of PPT legacies on above ground net primary productivity (ANPP) on a semiarid steppe. Robertson et al. (2010) also observed PPT legacies from previous winter season on density and

species richness on a semiarid grassland of the Chihuahuan Dessert. Considering species characteristics, *B. gracilis* can recover photosynthetic capacity within 24h from a prolonged interpulse PPT period (Thomey et al., 2014) and it is also able to initiate new root growth just 48h after PPT occurrence (Medina-Roldán et al., 2013). Thus, the dominant species at our site has the capacity of a fast recovery to long lasting droughts.

Precipitation legacies: NEE components

Even when annual balances of GEE and ER were strongly correlated with APPT, similar to NEE balance, they were better explained at seasonal rather than annual time-scale. Thus, winter precipitation controlled GEE and ER balance of summer (agreeing with our H4), suggesting the capability of the ecosystem to response to rapid (seasonal) changes in the environmental drivers. We attribute to similar mechanisms of structural changes and soil nutrient accumulation for the effect of PPT legacies on GEE and ER, with larger effects on the autotrophic component of ER. This is inferred from the stronger correlation observed between ER, basal respiration (R_b) and EVI than the relationship with soil volumetric water content (data not shown), suggesting a strong control of ER variability by root biomass, and photosynthates allocation from shoots to roots (Vargas et al., 2011). Gross ecosystem exchange was more sensitive to current PPT than ER as was hypothesized (H5), and this difference was even larger for the PPT legacy effect (three-fold larger, Fig. 11b). Both GEE and ER were more linearly related to seasonal PPT and previous-seasonal PPT contrary to the asymptotic response that was expected for GEE as suggested by other studies (e.g. Shi et al., 2014). Differences in sensitivity to PPT are consequence of asymmetric control of environmental drivers on fluxes. Even though ER is controlled by soil water availability, this process is less sensitive to a precipitation reduction due to the strongest control (i.e. the heterotrophic component) of C from recalcitrant soil organic matter that changes very slowly (Medina-Roldán et al 2008, Schmidt et al. 2011). For example, Shi et al. (2014) showed that ER is less sensitive to a precipitation decrease because it only responds to long-term controls. Thus, a

significant heterotrophic ER reduction would occur only after a multi-year drought that could reduce soil carbon (a source limiting effect). In this semiarid grassland, only slight soil C reduction has been observed after decades of plant cover change (Medina-Roldán et al. 2008).

Several studies have repoted the role of winter precipitation in productivity and ER in arid ecosystems with summer season PPT. For instance, Chimner and Welker (2005) ina mixed grass prairie with *B. gracilis* as the dominant summer (C4) grass, obtained larger summer ER rates followingaddition of PPT or snow in winter. More recently, Verduzco et al. (2015) found high relationship between the amount of winter precipitation and ER, whereas ecosystem productivity was more related with summer PPT in a tropical dry forest in the North of Mexico.In addition, Li et al. (2015) showed a high dependence of growing season NDVI of previous year fall/winter PPT in a arid-semiarid desert. These studies coincide with our general findings,however our results clearly demonstratedand quantitatively determinedthe contribution of winter PPT to summer net ecosystem productivity (as NEE≈NEP). We showed that both ER and GEE are largely controlled by winter PPT. On the other hand, using the approach of Sala et al. (2012) with Eq. 9, we confirmed the PPT legacy hypothesis but with the legacy mechanisms operating at seasonal scales, in contrast with the annual scales as have been proposed (Reichmann et al., 2013).

Conclusions

Carbon fluxes in the semiarid grassland showed high diurnal, seasonal and interannual variability. Changes in C flux rates were controlled by environmental variables (solar radiation and temperature) at short time scales, whereas were driven by changes in biomass at longer time-rates. We demonstrated that there is a legacy between the summer C balance and the previous winter precipitation; however, there is not a significant precipitation legacy of summer to the next winter. Also, we argued that these legacy effects are driven by changes in the structure of the ecosystem as an indirect response of soil water availability, such as an increase of biomass and leaf area from EVI data was observed after large

winter precipitation, with biogeochemical changes as secondary drivers (e.g. soil nitrogen accumulation after drought). The strong relationship between winter precipitation and the C balance found in this study is highly relevant for the tropical semiarid grasslands under climate change scenarios. Global circulation models for this ecosystem forecast 10% and 20% reduction for summer and winter precipitation, respectively, and 3.0 - 3.5 °C increase of mean air temperature for the end of the 21st Century (Christensen et al. 2007). Notwithstanding aboveground productivity between 100 - 800 g DM m^{-2} reported for semiarid grasslands is low compared to mesic and humid ecosystems, still these ecosystems allocate 75-90% of their total productivity belowground in the form of root biomass (250-1000 g DM / m2; Gibson, 2009, Medina-Roldán et al., 2007), contributing to the formation of large organic and inorganic C pools in soils (15 to 110 Tha^{-1}, Schlesinger, 1985). Mobilization of this C could be increased due to precipitation patterns. In regard to results presented here, we can expect more C release under summer PPT reduction scenario that will be potentiated by the larger reduction of winter precipitation.

Appendix

Phenological phases calculations with EVI

$$K = \frac{d\alpha}{ds} = \frac{f''_{(t)}}{\left(1+\left[f'_{(t)}\right]^2\right)^{3/2}} = \frac{2((A_0 z^2 - A_1 z^2)(z+1) - A_0 z - A_1 z)(dt^2(z+1)^2)^{-1}}{\left[1+\left(\frac{-(A_0 - A_1)z}{dt(z+1)^2}\right)^2\right]^{3/2}} \quad \text{(Eq. A1)}$$

$z = e^{(t-t0)/dt}$

Where K is the curvature of the function (Eq. 10).

$$K' = \frac{-\frac{(A_0 - A_1)z}{dt^3(z+1)^2} + \frac{6z^2(A_0 - A_1)}{dt^3(z+1)^3} - \frac{6z^3(A_0 - A_1)}{dt^3(z+1)^4}}{\left(\frac{z^2(A_0 - A_1)^2}{dt^2(z+1)^4} + 1\right)^{3/2}}$$

$$-\frac{3\left(\frac{2z^2(A_0-A_1)}{dt^3(z+1)^4}-\frac{4z^3(A_0-A_1)^2}{dt^3(z+1)^5}\right)\left(\frac{2z^2(A_0-A_1)}{dt^2(z+1)^3}-\frac{z(A_0-A_1)}{dt^2(z+1)^2}\right)}{2\left(\frac{z^2(A_0-A_1)^2}{dt^2(z+1)^4}+1\right)^{5/2}} \quad \text{(Eq. A2)}$$

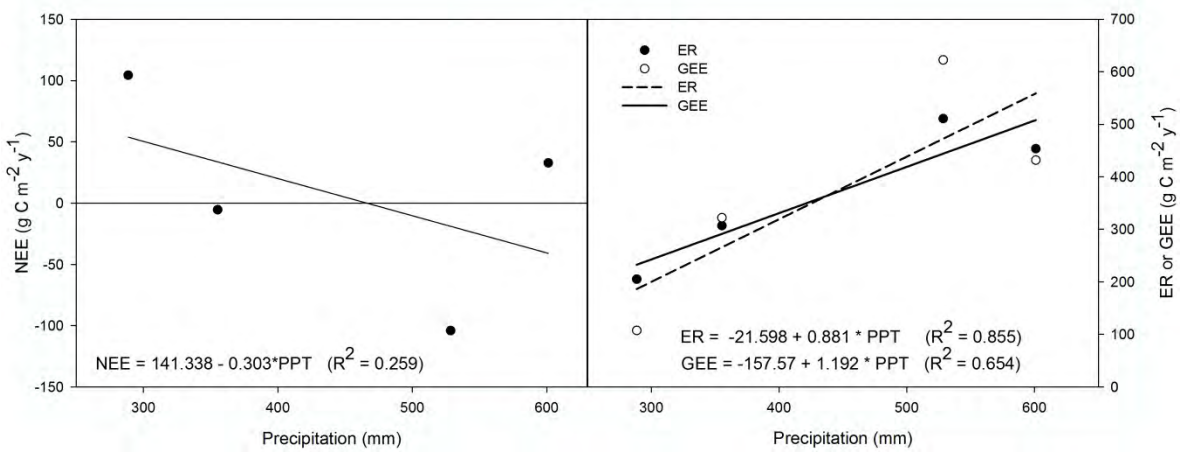

Figure A 1. Linear relationship between annual precipitation and annually integrated NEE (a) and their partitioned fluxes (GEE and ER, b) by calendar years.

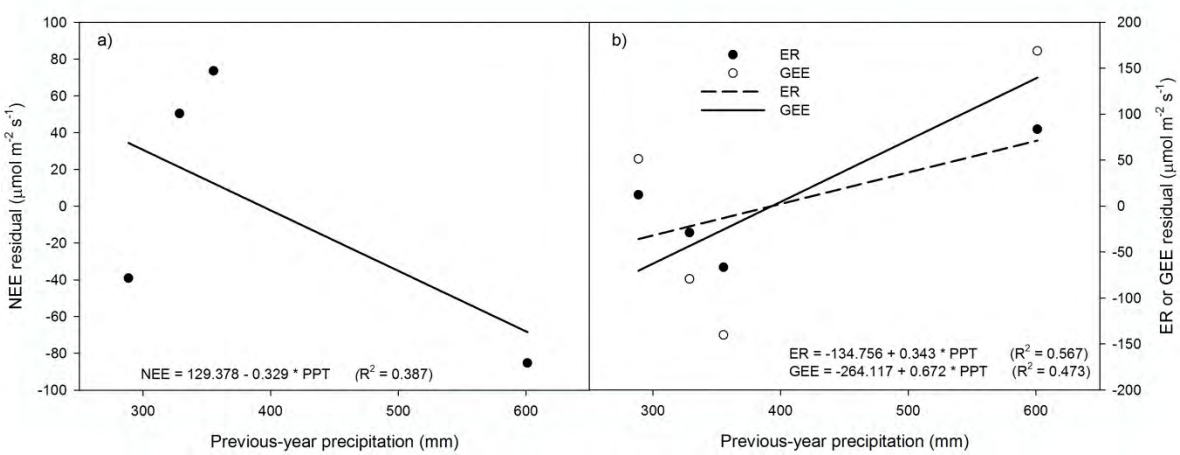

Figure A 2. Linear relationship between previous-year precipitation and residuals of current-year PPT - integrated NEE relationship (a) and their partitioned fluxes (GEE and ER, b) by calendar years.

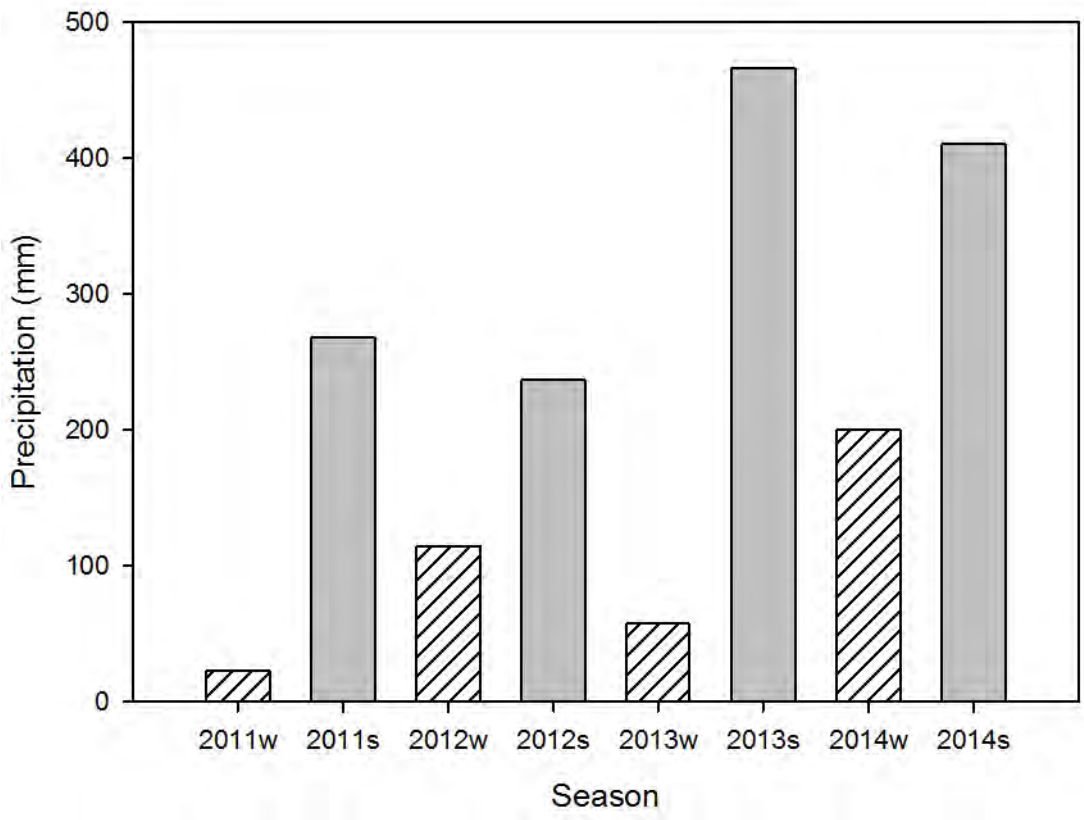

Figure A 3. Cumulative seasonal precipitation, where *w* stands for winter and *s* for summer season.

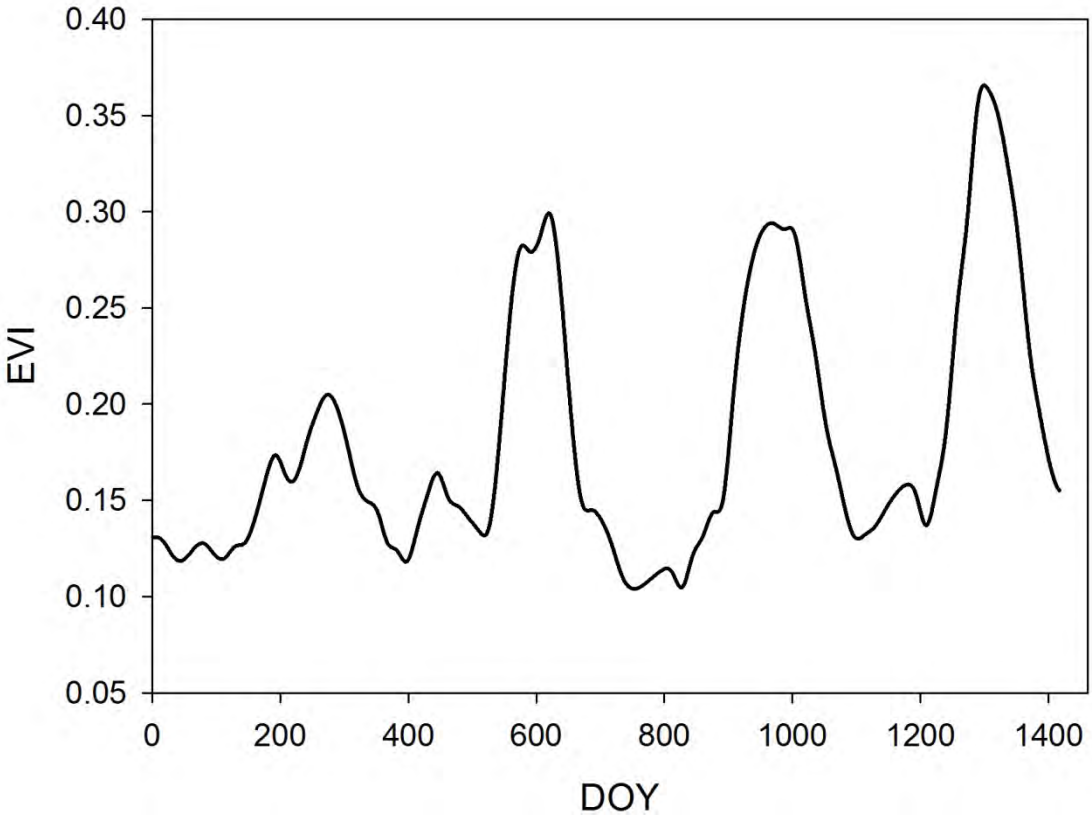

Figure A 4. Enhanced vegetation index (EVI, uniteless) values for the entire measurement period. DOY stands for day of year since 01/01/2011.

Table A 1**.** Calculated parameters for EVI curves from Eq. 10. A0 stands for basal EVI, A1 is the maximum EVI, t0 is the center of the curve (date), dt is related to the slope of the curve with larger slopes indicating shallower curves, and slope at t0 is the calculated slope at the center of the curve (EVI/day). Values are means ± 1 S.E. Uppercase acronyms after year mean S for summer and W for winter seasons, and lowercase *s* and *e* stand for the start and the end of the growing seasons, respectively.

Year	A_0	A_1	t_0	*dt*	Slope t_0
2011-Ss	0.117 ± 2.99E-03	0.199 ± 4.15E-03	08/07/11 ± 4.75	34.00 ± 5.17	6.00E-04
2011-Se	0.125 ± 2.10E-03	0.195 ± 2.20E-03	22/11/11 ± 2.15	-15.03 ± 2.05	-1.16E-03
2012-Ws	0.126 ± 9.48E-04	0.155 ± 1.23E-03	23/02/12 ± 1.87	10.74 ± 1.78	6.72E-04
2012-We	0.134 ± 3.14E-03	0.154 ± 8.72E-03	22/04/12	-0.29	-1.64E-02

2012-Ss	0.123	± 7.50E-03	0.312	± 9.09E-03	06/07/12	± 2.48	18.84	± 2.85	2.50E-03
2012-Se	0.107	± 2.17E-03	0.310	± 5.15E-03	15/10/12	± 1.68	-21.69	± 1.48	-2.34E-03
2013-Ss	0.110	± 2.42E-03	0.288	± 2.78E-03	21/06/13	± 1.22	18.41	± 1.24	2.41E-03
2013-Se	0.130	± 2.67E-03	0.301	± 5.18E-03	06/11/13	± 1.67	-18.81	± 1.59	-2.27E-03
2014-Ws	0.132		0.152		17/02/14		8.52		5.72E-04
2014-Ss	0.143	± 2.05E-03	0.360	± 2.71E-03	10/06/14	± 0.78	14.96	± 0.73	3.62E-03
2014-Se	0.088	± 1.31E-01	0.361	± 4.29E-02	11/10/14	± 20.77	-25.36	± 18.2	-2.68E-03

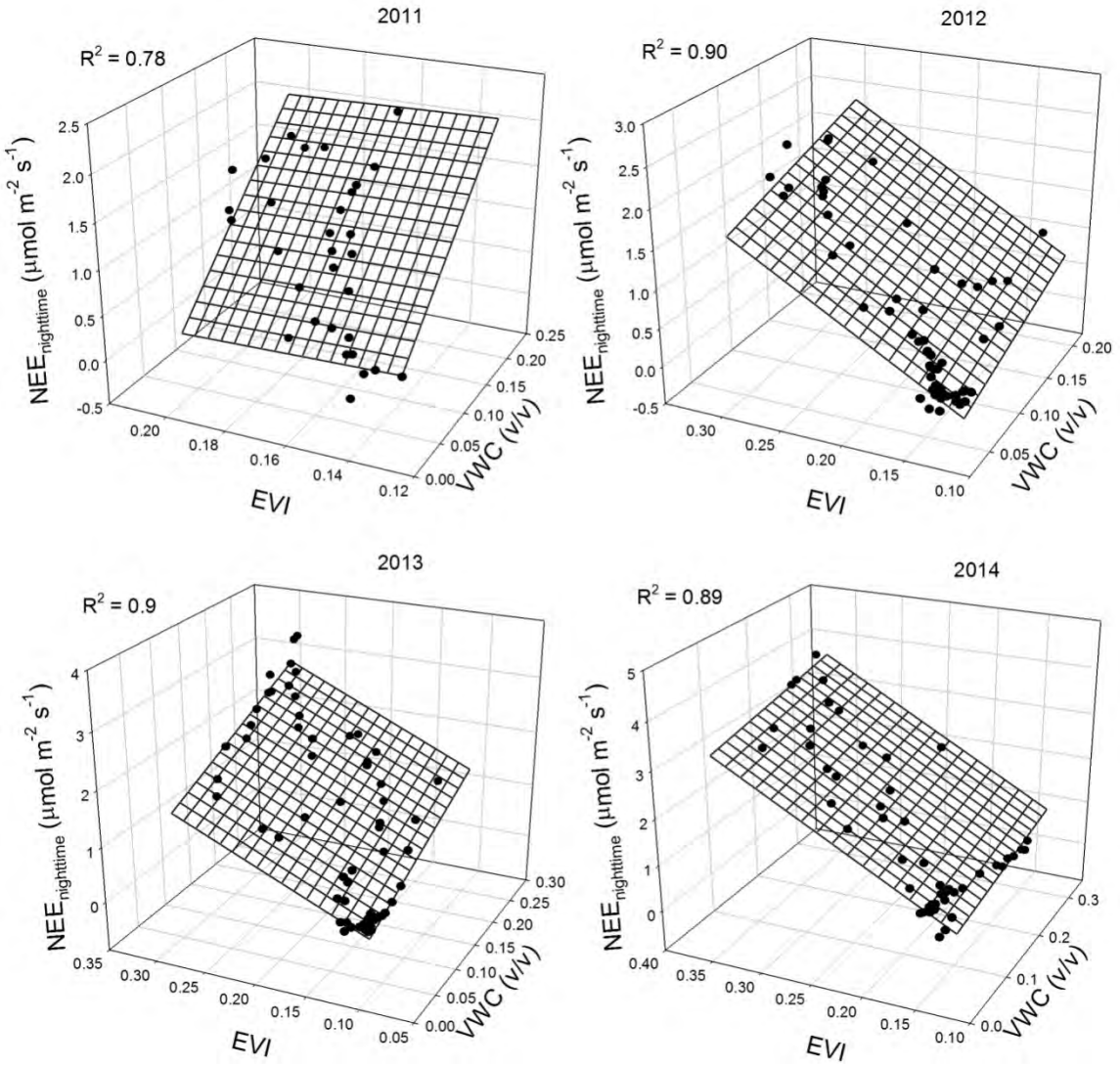

Figure A 5. Bivariate relationship among weakly means of soil volumetric water content (VWC, v/v) at 2.5 cm depth, enhanced vegetation index (EVI), and

nighttime NEE (g C m-2 s-1). The plane describes the fitting of the model NEEnighttime = y0 + a*VWC + b*EVI. Parameters of models in Table A2.

Table A 2. Calculated parameters for bivariate curves among soil volumetric water content (VWC, v/v) at 2.5 cm depth, enhanced vegetation index (EVI), and nighttime NEE (g C m^{-2} s^{-1}) in the form, $NEE_{nighttime} = y_0 + a*VWC + b*EVI$. All regressions were significant at α = 0.05.

Year	Parameter	Mean	± S.E.	t	P	R^2
	y_0	-0.215	0.503	-0.427	0.6724	0.78
2011	a	9.878	1.329	7.433	<0.0001	
	b	-0.728	3.491	-0.209	0.8364	
	y_0	-1.093	0.087	-12.617	<0.0001	0.9
2012	a	3.919	0.825	4.749	<0.0001	
	b	8.929	0.561	15.903	<0.0001	
	y_0	-0.904	0.110	-8.197	<0.0001	0.9
2013	a	5.276	0.722	7.307	<0.0001	
	b	7.964	0.802	9.925	<0.0001	
	y_0	-1.226	0.152	-8.049	<0.0001	0.89
2014	a	2.274	0.859	2.647	0.0110	
	b	11.615	0.750	15.484	<0.0001	

References

Aguado-Santacruz, G.A., 1993. Efecto de factores ambientales sobre la dinámica vegetacional en pastizales de los Llanos de Ojuelos, Jalisco: un enfoque multivariable (MSc). Colegio de Postgraduados, Chapingo, México.

Archibald, S.A., Kirton, A., Merwe, M.R., Scholes, R.J., Williams, C.A., Hanan, N., 2009.Drivers of inter-annual variability in Net Ecosystem Exchange in a semi-arid savanna ecosystem, South Africa.Biogeosciences 6, 251–266.

Bahn, M., Rodeghiero, M., Anderson-Dunn, M., Dore, S., Gimeno, C., Drosler, M., Williams, M., Ammann, C., Berninger, F., Flechard, C., Jones, S., Balzarolo, M., Kumar, S., Newesely, C., Priwitzer, T., Raschi, A., Siegwolf, R., Susiluoto, S., Tenhunen, J., Wohlfahrt, G., Cernusca, A., 2008. Soil

Respiration in European Grasslands in Relation to Climate and Assimilate Supply. Ecosyst. N. Y. N 11, 1352–67. doi:10.1007/s10021-008-9198-0

Beer, C., Ciais, P., Reichstein, M., Baldocchi, D., Law, B.E., Papale, D., Soussana, J.-F., Ammann, C., Buchmann, N., Frank, D., Gianelle, D., Janssens, I.A., Knohl, A., Köstner, B., Moors, E., Roupsard, O., Verbeeck, H., Vesala, T., Williams, C.A., Wohlfahrt, G., 2009. Temporal and among-site variability of inherent water use efficiency at the ecosystem level. Glob.Biogeochem. Cycles 23, GB2018.doi:10.1029/2008GB003233

Billings, S.A., Ballantyne, F., 2013. How interactions between microbial resource demands, soil organic matter stoichiometry, and substrate reactivity determine the direction and magnitude of soil respiratory responses to warming. Glob. Change Biol. 19, 90–102. doi:10.1111/gcb.12029

Briggs, J.M., Knapp, A.K., 1995. Interannual variability in primary production in tallgrass prairie: Climate, soil moisture, topographic position, and fire as determinants of aboveground biomass. Am. J. Bot. 82, 1024 – 1030.

Chen, G., Yang, Y., Robinson, D., 2014. Allometric constraints on, and trade-offs in, belowground carbon allocation and their control of soil respiration across global forest ecosystems. Glob. Change Biol. 20, 1674–1684. doi:10.1111/gcb.12494

Chimner, R.A., Welker, J.M., 2005. Ecosystem respiration responses to experimental manipulations of winter and summer precipitation in a Mixedgrass Prairie, WY, USA. Biogeochemistry 73, 257–270. doi:10.1007/s10533-004-1989-6

Christensen, J.H., B. Hewitson, A. Busuioc, A. Chen, X. Gao, I. Held, R. Jones, R.K. Kolli, W.-T. Kwon, R. Laprise, V. Magaña Rueda, L. Mearns, C.G. Menéndez, J. Räisänen, A. Rinke, A. Sarr and P. Whetton, 2007: Regional Climate Projections. In: Climate Change 2007: The Physical Science Basis. Contribution of Working Group I to the Fourth Assessment Report of the Intergovernmental Panel on Climate Change [Solomon, S., D. Qin, M. Manning, Z. Chen, M. Marquis, K.B. Averyt, M. Tignor and H.L. Miller

(eds.)]. Cambridge University Press, Cambridge, United Kingdom and New York, NY, USA.

COTECOCA, (Comisión Técnico Consultiva para la Determinación de Coeficientes de Agostadero), 1979. Coeficientes de agostadero de la República Mexicana. Estado de Jalisco. SARH-Subsecretaría de Ganadería, México, D. F.

Craine, J.M., Nippert, J.B., Elmore, A.J., Skibbe, A.M., Hutchinson, S.L., Brunsell, N.A., 2012. Timing of climate variability and grassland productivity.Proc.Natl. Acad. Sci. 109, 3401–3405. doi:10.1073/pnas.1118438109

Delgado-Balbuena, J., Arrendondo J.T., Loescher, H.W., Huber-Sannwald, E., Chavez-Aguilar, G., Luna-Luna, M., Barretero-Hernandez, R., 2013. Differences in plant cover and species composition of semiarid grassland communities of central Mexico and its effects on net ecosystem exchange. Biogeosciences 10, 4673–4690.doi:10.5194/bg-10-4673-2013

Efron, B., Tibshirani, R., 1993. An introduction to the bootstrap, Monographs on statistics and applied probability. Chapman & Hall, New York.

Ehleringer, J., Pearcy, R.W., 1983. Variation in Quantum Yield for CO2 Uptake among C3 and C4 Plants. Plant Physiol. 73, 555–559. doi:10.1104/pp.73.3.555

Emmerich, W.E., 2003. Carbon dioxide fluxes in a semiarid environment with high carbonate soils. Agric. For. Meteorol. 116, 91–102.

Falge, E., Baldocchi, D., Olson, R., Anthoni, P., Aubinet, M., Bernhofer, C., Burba, G., Ceulemans, R., Clement, R., Dolman, H., others, 2001.Gap filling strategies for long term energy flux data sets. Agric. For. Meteorol. 107, 71–77.

Foken, T., Göockede, M., Mauder, M., Mahrt, L., Amiro, B., Munger, W., 2004. Post-Field Data Quality Control, in: Lee, X., Massman, W., Law, B. (Eds.), Handbook of Micrometeorology, Atmospheric and Oceanographic Sciences Library. Springer Netherlands, pp. 181–208.

Frank, J.M., Masman, W.J., Ewers, B.E. 2013. Underestimates of sensible heat flux due to vertical velocity measurement errors in non-orthogonal sonic anemometers. Agricultural and Forest Meteorology, 171-172, 72-81.

Friedlingstein, P., Houghton, R.A., Marland, G., Hackler, J., Boden, T.A., Conway, T.J., Canadell, J.G., Raupach, M.R., Ciais, P., Le Quéré, C., 2010. Update on CO2 emissions. Nature Geosci 3, 811–812. doi:10.1038/ngeo1022

Gao, Z., Horton, R., Liu, H.P., 2010. Impact of wave phase difference between soil surface heat flux and soil surface temperature on soil surface energy balance closure.J.Geophys.Res.Atmospheres 115, D16112.doi:10.1029/2009JD013278

García, E., 2003. Distribución de la precipitación en la República Mexicana. Bol. Inst. Geogr. UNAM, InvestigacionesGeográficas 50, 67–76.

Gibson, D.J., 2009. Grasses and grassland ecology. Oxford University Press, New York.

Gilmanov, T.G., Aires, L., Barcza, Z., Baron, V.S., Belelli, L., Beringer, J., Billesbach, D., Bonal, D., Bradford, J., Ceschia, E., Cook, D., Corradi, C., Frank, A., Gianelle, D., Gimeno, C., Gruenwald, T., Guo, H., Hanan, N., Haszpra, L., Heilman, J., Jacobs, A., Jones, M.B., Johnson, D.A., Kiely, G., Li, S., Magliulo, V., Moors, E., Nagy, Z., Nasyrov, M., Owensby, C., Pinter, K., Pio, C., Reichstein, M., Sanz, M.J., Scott, R., Soussana, J.F., Stoy, P.C., Svejcar, T., Tuba, Z., Zhou, G., 2010. Productivity, Respiration, and Light-Response Parameters of World Grassland and Agroecosystems Derived From Flux-Tower Measurements. Rangel. Ecol. Manag. 63, 16–39. doi:10.2111/REM-D-09-00072.1

Heskel, M.A., Atkin, O.K., Turnbull, M.H., Griffin, K.L., 2013. Bringing the Kok effect to light: a review on the integration of daytime respiration and net ecosystem exchange.Ecosphere 4, art98.

Heusinkveld, B.., Jacobs, A.F.., Holtslag, A.A.., Berkowicz, S.., 2004. Surface energy balance closure in an arid region: role of soil heat flux. Agric. For. Meteorol. 122, 21–37. doi:10.1016/j.agrformet.2003.09.005

Houghton, R.A., Woodwell, G.M., 1989. Global Climatic Change. Sci. Am.; (United States) 260:4.

Hsu, J.S., Adler, P.B., 2014. Anticipating changes in variability of grassland production due to increases in interannual precipitation variability.Ecosphere 5, art58. doi:10.1890/ES13-00210.1

Huang, G., Li, Y., Padilla, F.M., 2015. Ephemeral plants mediate responses of ecosystem carbon exchange to increased precipitation in a temperate desert. Agric. For. Meteorol. 201, 141–152. doi:10.1016/j.agrformet.2014.11.011

Jobbágy, E.G., Sala, O.E., 2000.Controls of grass and shrub aboveground production in the patagonian steppe. Ecol. Appl. 10, 541–549. doi:10.1890/1051-0761(2000)010[0541:COGASA]2.0.CO;2

Kormann, R., Meixner, F., 2001. An Analytical Footprint Model For Non-Neutral Stratification. Bound.-Layer Meteorol. 99, 207–224. doi:10.1023/A:1018991015119

Kuglitsch, F.G., Reichstein, M., Beer, C., Carrara, A., Ceulemans, R., Granier, A., Janssens, I.A., Koestner, B., Lindroth, A., Loustau, D., Matteucci, G., Montagnani, L., Moors, E.J., Papale, D., Pilegaard, K., Rambal, S., Rebmann, C., Schulze, E.D., Seufert, G., Verbeeck, H., Vesala, T., Aubinet, M., Bernhofer, C., Foken, T., Grünwald, T., Heinesch, B., Kutsch, W., Laurila, T., Longdoz, B., Miglietta, F., Sanz, M.J., Valentini, R., 2008. Characterisation of ecosystem water-use efficiency of european forests from eddy covariance measurements. Biogeosciences Discuss. 5, 4481–4519. doi:10.5194/bgd-5-4481-2008

Lambers, H., Chapin, F.S., Pons, T.L., 2008a.Plant physiological Ecology, 2nd ed. Springer New York, New York.

Lambers, H., Chapin, F.S., Pons, T.L., Lambers, H., Chapin, F.S., Pons, T.L., 2008b.Respiration. Springer New York, pp. 101–150.

Lasslop, G., Migliavacca, M., Bohrer, G., Reichstein, M., Bahn, M., Ibrom, A., Jacobs, C., Kolari, P., Papale, D., Vesala, T., Wohlfahrt, G., Cescatti, A., 2012.On the choice of the driving temperature for eddy-covariance carbon

dioxide flux partitioning.Biogeosciences 9, 5243–5259.doi:10.5194/bg-9-5243-2012

Lauenroth, W.K., Burke, I.C. (Eds.), 2008. Ecology of the shortgrass steppe: a long-term perspective. Oxford University Press, Oxford ; New York.

Lauenroth, W.K., Sala, O.E., 1992. Long-Term Forage Production of North American Shortgrass Steppe. Ecol. Appl. 2, 397–403. doi:10.2307/1941874

Loescher, H. W., B. E. Law, L. Mahrt, D. Y. Hollinger, J. L. Campbell, S. C. Wofsy, 2006.Uncertainties in- and interpretation of carbon flux estimates using the eddy covariance technique.*J. Geophys. Res.-Atmos,* 111, D21S90, doi:10.1029/2005JD006932.

Li, Z., Guo, X., 2012. Detecting Climate Effects on Vegetation in Northern Mixed Prairie Using NOAA AVHRR 1-km Time-Series NDVI Data. Remote Sens. 4, 120–134. doi:10.3390/rs4010120

Li, F., Zhao, W., Liu, H., 2015.Productivity responses of desert vegetation to precipitation patterns across a rainfall gradient. J Plant Res 128, 283–294. doi:10.1007/s10265-014-0685-4

Livingston, N.J., Guy, R.D., Sun, Z.J., Ethier, G.J., 1999. The effects of nitrogen stress on the stable carbon isotope composition, productivity and water use efficiency of white spruce (Piceaglauca (Moench) Voss) seedlings. Plant Cell Environ. 22, 281–289. doi:10.1046/j.1365-3040.1999.00400.x

Malhi, Y., McNaughton, K., Randow, C.V., 2005. Low Frequency Atmospheric Transport and Surface Flux Measurements, in: Lee, X., Massman, W., Law, B. (Eds.), Handbook of Micrometeorology, Atmospheric and Oceanographic Sciences Library. Springer Netherlands, pp. 101–118.

Medina-Roldán, E., Arredondo Moreno, J.T., García Moya, E., Huerta Martínez, F.M., 2007. Soil Water Content Dynamics Along a Range Condition

Gradient in a Shortgrass Steppe. Rangel. Ecol. Manag. 60, 79–87. doi:doi: 10.2111/05-219R2.1

Medina-Roldán, E., Arredondo, J.T., Huber-Sannwald, E., Chapa-Vargas, L., Olalde-Portugal, V., 2008.Grazing effects on fungal root symbionts and carbon and nitrogen storage in a shortgrass steppe in Central Mexico. J. Arid Environ. 72, 546–556. doi:10.1016/j.jaridenv.2007.07.005

Medina-Roldán, E., Huber-Sannwald, E., Arredondo, J.T., 2013. Plant phenotypic functional composition effects on soil processes in a semiarid grassland. Soil Biol. Biochem. 66, 1–9. doi:10.1016/j.soilbio.2013.06.011

Mielnick, P., Dugas, W.A., Mitchell, K., Havstad, K., 2005. Long-term measurements of CO2 flux and evapotranspiration in a Chihuahuan desert grassland. J. Arid Environ. 60, 423–436. doi:10.1016/j.jaridenv.2004.06.001

Moffat, A.M., Papale, D., Reichstein, M., Hollinger, D.Y., Richardson, A.D., Barr, A.G., Beckstein, C., Braswell, B.H., Churkina, G., Desai, A.R., Falge, E., Gove, J.H., Heimann, M., Hui, D., Jarvis, A.J., Kattge, J., Noormets, A., Stauch, V.J., 2007. Comprehensive comparison of gap-filling techniques for eddy covariance net carbon fluxes. Agric. For. Meteorol. 147, 209–232. doi:10.1016/j.agrformet.2007.08.011

Muñoz-Flores, L., Riego-Ruiz, LR., Arredondo-Moreno, JT., Luna-Luna, M., Argüello-Astorga, GR. and Huber-Sannwald, E. 2014. How grazing and fire regime influence soil biogeochemical cycling in a native grassland in central Mexico. The first global soil biodiversity conference: assessing soil biodiversity and its role for ecosystem services, Dijon, France, 2 – 5 December, 2014

Oesterheld, M., Loreti, J., Semmartin, M., Sala, O.E., Oesterheld, M., Semmartin, M., 2001. Inter-Annual Variation in Primary Production of a Semi-Arid Grassland Related to Previous-Year Production. J. Veg. Sci. 12, 137.doi:10.2307/3236681

Phillips, C.L., Nickerson, N., Risk, D., Bond, B.J., 2011. Interpreting diel hysteresis between soil respiration and temperature.Glob. Change Biol. 17, 515–527. doi:10.1111/j.1365-2486.2010.02250.x

Propastin, P., Kappas, M., 2009.Modeling Net Ecosystem Exchange for Grassland in Central Kazakhstan by Combining Remote Sensing and Field Data. Remote Sens. 1, 159–183.

Raich, J.W., Schlesinger, W.H., 1992. The global carbon dioxide flux in soil respiration and its relationship to vegetation and climate.Tellus B 44, 81–99.

Rajan, N., Maas, S.J., Cui, S., 2013. Extreme Drought Effects on Carbon Dynamics of a Semiarid Pasture.Agron. J. 105, 1749. doi:10.2134/agronj2013.0112

Reichmann, L.G., Sala, O.E., 2014. Differential sensitivities of grassland structural components to changes in precipitation mediate productivity response in a desert ecosystem. Funct. Ecol. 28, 1292–1298. doi:10.1111/1365-2435.12265

Reichmann, L.G., Sala, O.E., Peters, D.P.C., 2012. Precipitation legacies in desert-grassland primary production occur through previous-year tiller density. Ecology. doi:10.1890/12-1237.1

Reichmann, L.G., Sala, O.E., Peters, D.P.C., 2013. Water controls on nitrogen transformations and stocks in an arid ecosystem. Ecosphere 4, art11. doi:10.1890/ES12-00263.1

Reichstein, M., Falge, E., Baldocchi, D., Papale, D., Aubinet, M., Berbigier, P., Bernhofer, C., Buchmann, N., Gilmanov, T., Granier, A., Grünwald, T., Havránková, K., Ilvesniemi, H., Janous, D., Knohl, A., Laurila, T., Lohila, A., Loustau, D., Matteucci, G., Meyers, T., Miglietta, F., Ourcival, J.-M., Pumpanen, J., Rambal, S., Rotenberg, E., Sanz, M., Tenhunen, J., Seufert, G., Vaccari, F., Vesala, T., Yakir, D., Valentini, R., 2005. On the separation of net ecosystem exchange into assimilation and ecosystem respiration: review and improved algorithm. Glob. Change Biol. 11, 1424–1439. doi:10.1111/j.1365-2486.2005.001002.x

Robertson, T., Zak, J., Tissue, D., 2010. Precipitation magnitude and timing differentially affect species richness and plant density in the sotol grassland of the Chihuahuan Desert. Oecologia 162, 185–197. doi:10.1007/s00442-009-1449-z

Robertson, T.R., Bell, C.W., Zak, J.C., Tissue, D.T., 2009. Precipitation timing and magnitude differentially affect aboveground annual net primary productivity in three perennial species in a Chihuahuan Desert grassland. New Phytol. 181, 230–242. doi:10.1111/j.1469-8137.2008.02643.x

Ruimy, A., Jarvis, P.G., Baldocchi, D.D., Saugier, B., 1995. CO2 Fluxes over Plant Canopies and Solar Radiation: A Review. Academic Press, pp. 1–68.

Running, S.W., 2008.Ecosystem Disturbance, Carbon, and Climate.Science 321, 652 –653. doi:10.1126/science.1159607

Sala, O.E., Gherardi, L.A., Reichmann, L., Jobbagy, E., Peters, D., 2012. Legacies of precipitation fluctuations on primary production: theory and data synthesis. Philos. Trans. R. Soc. B Biol. Sci. 367, 3135–3144. doi:10.1098/rstb.2011.0347

Sala, O.E., Lauenroth, W.K., 1982. Small rainfall events: An ecological role in semiarid regions. Oecologia 53, 301–304. doi:10.1007/BF00389004

Sala, O.E., Parton, W.J., Joyce, L.A., Lauenroth, W.K., 1988. Primary Production of the Central Grassland Region of the United States. Ecology 69, 40–45.

Sarath, G., Baird, L.M., Mitchell, R.B., 2014. Senescence, dormancy and tillering in perennial C4 grasses. Plant Sci. 217-218, 140–151. doi:10.1016/j.plantsci.2013.12.012

Savitzky, A., Golay, M.J.E., 1964. Smoothing and Differentiation of Data by Simplified Least Squares Procedures. Anal. Chem. 36, 1627–1639. doi:10.1021/ac60214a047

Schlesinger, W.H., 1985. The formation of caliche in soils of the Mojave Desert, California.Geochim.Cosmochim. Acta 49, 57–66. doi:10.1016/0016-7037(85)90191-7

Schmidt, M.W.I., Torn, M.S., Abiven, S., Dittmar, T., Guggenberger, G., Janssens, I.A., Kleber, M., Kögel-Knabner, I., Lehmann, J., Manning, D.A.C., Nannipieri, P., Rasse, D.P., Weiner, S., Trumbore, S.E., 2011.Persistence of soil organic matter as an ecosystem property. Nature 478, 49–56. doi:10.1038/nature10386

Shaw, R. 1985. On diffusive and dispersive fluxes in forest canopies. In B.A. Hutchinson and B.B. Hicks (eds) *The Forest Atmosphere Interaction.* D. Reider Pub., Dorecht, 407- 419 pp.

Sherry, R.A., Weng, E., Arnone Iii, J.A., Johnson, D.W., Schimel, D.S., Verburg, P.S., Wallace, L.L., Luo, Y., 2008. Lagged effects of experimental warming and doubled precipitation on annual and seasonal aboveground biomass production in a tallgrass prairie. Glob. Change Biol. 14, 2923–2936. doi:10.1111/j.1365-2486.2008.01703.x

Sierra, C. A., H. W. Loescher, M. E. Harmon, A. D. Richardson, D. Y. Hollinger, and S. S. Perakis, 2009. Interannual variation of carbon fluxes from a tropical, a temperate, and a boreal evergreen forest: the role of forest dynamics and climate. *Ecology,* 90, 2711-2723.

Shi, Z., Thomey, M.L., Mowll, W., Litvak, M., Brunsell, N.A., Collins, S.L., Pockman, W.T., Smith, M.D., Knapp, A.K., Luo, Y., 2014. Differential effects of extreme drought on production and respiration: synthesis and modeling analysis. Biogeosciences 11, 621–633. doi:10.5194/bg-11-621-2014

Stoy, P.C., 2013. A data-driven analysis of energy balance closure across FLUXNET research sites: The role of landscape-scale heterogeneity. Agric. For. Meteorol. 171-172, 137–152. doi:10.1016/j.agrformet.2012.11.004

Stoy, P.C., Katul, G.G., Siqueira, M.B.S., Juang, J.-Y., Novick, K.A., Uebelherr, J.M., Oren, R., 2006.An evaluation of models for partitioning eddy covariance-measured net ecosystem exchange into photosynthesis and respiration. Agric. For. Meteorol. 141, 2–18. doi:10.1016/j.agrformet.2006.09.001

Taylor, J., and H.W. Loescher, 2013.Automated Quality Control Methods for Sensor Data: A Novel Observatory Approach.*Biogeosciences,* 10, 4957-4971. doi:10.5194/bg-10-4957-2013.

Thomas, C.K., Law, B.E., Irvine, J., Martin, J.G., Pettijohn, J.C., Davis, K.J., 2009. Seasonal hydrology explains interannual and seasonal variation in carbon and water exchange in a semiarid mature ponderosa pine forest in central Oregon. J Geophys Res 114, G04006.

Thomey, M.L., Collins, S.L., Friggens, M.T., Brown, R.F., Pockman, W.T., 2014. Effects of monsoon precipitation variability on the physiological response of two dominant C4 grasses across a semiarid ecotone. Oecologia 176, 751–762. doi:10.1007/s00442-014-3052-1

Vargas, R., Baldocchi, D.D., Bahn, M., Hanson, P.J., Hosman, K.P., Kulmala, L., Pumpanen, J., Yang, B., 2011. On the multi-temporal correlation between photosynthesis and soil CO2 efflux: reconciling lags and observations. New Phytol. 191, 1006–1017. doi:10.1111/j.1469-8137.2011.03771.x

Vargas, R., Detto, M., Baldocchi, D.D., Allen, M.F., 2010.Multiscale analysis of temporal variability of soil CO2 production as influenced by weather and vegetation.Glob. Change Biol. 16, 1589–1605. doi:10.1111/j.1365-2486.2009.02111.x

Verduzco, V.S., Garatuza-Payán, J., Yépez, E.A., Watts, C.J., Rodríguez, J.C., Robles-Morua, A., Vivoni, E.R., 2015. Variations of net ecosystem production due to seasonal precipitation differences in a tropical dry forest of northwest Mexico: Carbon exchange at a tropical dry forest. Journal of Geophysical Research: Biogeosciences 120, 2081–2094. doi:10.1002/2015JG003119

Volaire, F., Norton, M., 2006.Summer Dormancy in Perennial Temperate Grasses. Ann. Bot. 98, 927–933. doi:10.1093/aob/mcl195

Wilson, K., Goldstein, A., Falge, E., Aubinet, M., Baldocchi, D., Berbigier, P., Bernhofer, C., Ceulemans, R., Dolman, H., Field, C., others, 2002. Energy balance closure at FLUXNET sites. Agric. For. Meteorol. 113, 223–243.

Wu, Z., Dijkstra, P., Koch, G.W., PeñUelas, J., Hungate, B.A., 2011. Responses of terrestrial ecosystems to temperature and precipitation change: a meta-analysis of experimental manipulation. Glob. Change Biol. 17, 927–942. doi:10.1111/j.1365-2486.2010.02302.x

Yahdjian, L., Sala, O.E., 2006. Vegetation structure constrains primary production response to water availability in the Patagonian steppe. Ecology 87, 952–962.

Yan, W., Hu, Z., Zhao, Y., Zhang, X., Fan, Y., Shi, P., He, Y., Yu, G., Li, Y., 2015.Modeling Net Ecosystem Carbon Exchange of Alpine Grasslands with a Satellite-Driven Model. PLoS ONE 10, e0122486. doi:10.1371/journal.pone.0122486

Yang, F., Zhou, G., 2013.Sensitivity of temperate desert steppe carbon exchange to seasonal droughts and precipitation variations in Inner Mongolia, China. PloS One 8, e55418. doi:10.1371/journal.pone.0055418

Yi, C., Ricciuto, D., Li, R., Wolbeck, J., Xu, X., Nilsson, M., Aires, L., Albertson, J.D., Ammann, C., Arain, M.A., 2010.Climate control of terrestrial carbon exchange across biomes and continents.Environmental Research Letters 5, 034007.

Zhang, X., Friedl, M.A., Schaaf, C.B., Strahler, A.H., Hodges, J.C., Gao, F., Reed, B.C., Huete, A., 2003. Monitoring vegetation phenology using MODIS. Remote Sens. Environ. 84, 471–475.

Chapter 2

Drivers and dynamics of CO_2 fluxes following precipitation events in the semiarid grassland

Keywords: Priming effect, Birch effect, net ecosystem exchange, ecosystem respiration, gross ecosystem exchange, eddy covariance.

Introduction

Arid lands comprise a wide range of ecosystem types covering more than 30% of terrestrial land (Lal, 2004). These ecosystems share a main characteristic; annual potential evapotranspiration is greater than annual precipitation due to atmospheric high pressure zones (Hadley cells), continental winds, cold ocean winds and orographic effects (rain shadow effect) that reduce the rainfall amount (Maliva and Missimer, 2012). Precipitation (PPT) usually occurs as infrequent, discrete and largely unpredictable events (Noy-Meir, 1973; Loik et al, 2004). This results in water-limited ecosystems where biological activity is restricted to periods of water availability (Lauenroth and Sala, 1992). In consequence, the productivity and stability of these ecosystems are more likely prone to changes in climate, in particular, changes to the historic amount and periodicity (frequency) of mean annual precipitation (MAP).

Precipitation patterns are defined by the characteristics of individual PPT events in terms of its magnitude (size of PPT event) and its frequency (inter-event time period) (Loik et al., 2004). Dry ecosystems share PPT patterns that are characterized by small PPT events < 5 mm d^{-1} with short inter-event periods (<10 days) (Loik et al., 2004). The quantity of PPT fundamentally influences grassland ecosystem productivity (Hao et al., 2010). An increase in the amount of precipitation above the mean annual precipitation (MAP) on wet years enhances both ecosystem productivity and respiration, favoring carbon (C) sequestration. In contrast, reduced PPT suppresses both of these fluxes resulting in a net C loss (Knapp and Smith, 2001; Wu et al., 2011). Changes of precipitation patterns (*i.e.* timing) on the other hand, act differentially on C uptake and respiration processes, which are dependent on vegetation type and soil characteristics (Bates et al., 2006, Robertson et al., 2009). For instance, larger and more infrequent PPT events reduce both productivity (<10%) and soil respiration (<16%, in both autotrophic and heterotrophic fractions) in a mesic grassland (Knapp et al., 2002). In contrast, more frequent but smaller PPT events with short inter-event periods favored C uptake in a semiarid grassland within the Chihuahuan Desert (Robertson et al.,

2009).

For short-term responses, carbon and nitrogen mineralization rates increase following a PPT event, as a result of soil microorganisms becoming active with the increase of soil water content (Turner and Haygarth, 2001). This “priming effect” (Borken and Matzner, 2009) also called the Birch effect (Birch, 1964), describes the soil carbon released mainly from heterotrophic sources to the atmosphere following soil rewetting, as a result (and possible combination) of several processes that include; 1) deterioration of soil aggregates caused by drying and rewetting cycles that expose organic substrates not previously available for biogeochemical activity (Huxman et al., 2004), 2) decomposition and releasing of nutrients from death soil microorganism due to the effects of drought (Jarvis et al., 2007), and 3) releasing of intracellular osmolytes that were accumulated by soil microorganisms under drying conditions for osmotic protection (Killham and Firestone, 1984), but that are released after wetting up to avoid cellular lysis (Halverson et al., 2000). All these processes make available a large amount of labile C and nutrients that stimulate immediate microbial and fungal hyphae biomass growth after soil wet up. In addition, replacement of CO_2 enriched soil pore spaces by infiltrated water also enhances soil C efflux following a PPT event (Huxman et al., 2004a).

Size and timing of PPT events also have shown to modify the magnitude and duration of the Birch effect by modulating soil wet-dry cycles. The size of a precipitation event may determine the temporal duration and the biota components that is stimulated (Huxman et al., 2004a), and thus, defines the magnitude and direction of CO_2 efflux (Chen et al., 2009). It is not clear however, how different size PPT events influence CO_2 flux responses. Overall, small precipitation events (*e.g.*, 2 mm) that induce changes in soil humidity at the soil surface do not induce plant growth but activate soil microorganisms, *i.e.*, the biological soil crust (BSC; Collins et al., 2008). For instance, PPT events <10 mm d^{-1} on a short-grass steppe promoted only net loss of C by soil respiration. It is unclear however if the ‘lower’ threshold is biological meaningful, or if becomes just a detection limit. In contrast,

larger events resulted in C gain because plant photosynthesis was activated (Parton et al., 2012). On the other hand, the preceding soil condition (i.e. the soil respiration rate and soil moisture before the PPT event) in the ecosystem also controls the magnitude and duration of C flux. Carbon mineralization rates are sequentially reduced with successive rewetting cycles as the amount of available organic labile carbon declines due to plant and microorganisms uptake on favorable soil water conditions (Jarvis *et al*., 2007). Thus, precipitation events after long drought periods (several months in seasonal ecosystems) may trigger large soil respiration episodes compared to consecutive PPT events (e.g. inter event-periods <10 days), because long lasting droughts allow accumulation of labile C and nutrients in soils, as plants and microorganisms do not have access to them because of limited water availability (Reichmann et al., 2013).

At the ecosystem scale, ecosystem respiration (ER) that includes soil respiration (autotrophic and heterotrophic) and above ground plant respiration, both maintenance and growth respiration (Randerson et al., 2002) is also affected by the processes described above. In general, deserts and grasslands have shown larger CO_2 efflux rates after rewetting compared to other temperate ecosystems and croplands (Kim et al., 2012). Thus, ecosystems can turn into net C sources after rain events, because ER is stimulated immediately (Huxman et al., 2004a). Field observations in an oak and C_3 grass savanna reported between 60 and 80-fold increase of the basal respiration rate (Xu *et al.,* 2004) after PPT events. However, there was only 0.5-fold increase reported for a controlled experiment in semiarid C_4 grassland (Thomey*et al*., 2011). The dynamics of the net ecosystem exchange, the balance between ER and the gross ecosystem exchange (GEE) depend also in the amount of the rainfall event. For instance, a small PPT event only stimulate ER derived from microorganisms located directly on or beneath the soil surface, resulting in a net C loss. In contrast, large precipitation events trigger plant responses (increase GEE) turning the ecosystem up in a net C sink (Huxman et al., 2004a). This suggests that daily precipitation size and distribution are key factors that modify the C balance of arid and semiarid ecosystems (Kim et al., 2010) that on the other hand, are not considered in current modelling approaches.

The characteristics and dynamics of short-term C fluxes induced by PPT events were addressed by Ogle and Reynolds (2004) into their “Threshold-Delay” model (T-D model) where they argue for a low and upper threshold based on PPT event size corresponding to stimulation of biota responses (the threshold component of the model). Precipitation events smaller in size than a PPT threshold does not promote any respiration or plant photosynthesis response (low level). In contrast, PPT events larger than the upper threshold saturate the respiration or photosynthesis response; however this will be a function of the physiological characteristics of plant-microorganisms functional types or soil structural constraints. The T-D model also suggests that plant-microorganisms functional types respond differently in magnitude, and their responses are separated in time (a delay component in the model). Moreover, the model also includes the effects of previous conditions of the response variable (C flux, Fig. 1a).

The T-D model may be used to describe short-term ecosystem scale processes such as net ecosystem C exchange (NEE) at diel timescales, when it is affected by a PPT event. Huxman et al., (2004a) related in a conceptual framework the dynamics of the NEE and its components with characteristics that can be described with parameters of the T-D model (Fig. 1b). According to Huxman et al. (2004a), the affect of the precipitation on ecosystem C fluxes is based on the relationship among PPT amount, depth of PPT infiltration, spatial separation of roots and microorganism across the soil profile, and lag times between the soil microorganism and plant mediated processes. Similar to the T-D model, GEE and ER also have different PPT event size thresholds, with ER responding to smaller PPT events; and again it is unclear if these thresholds are biologically meaningful or whether they are just a detection limit. In addition, both GEE and ER have asymptotic responses to large PPT events (the upper PPT thresholds), being the upper ER threshold lower that in GEE.

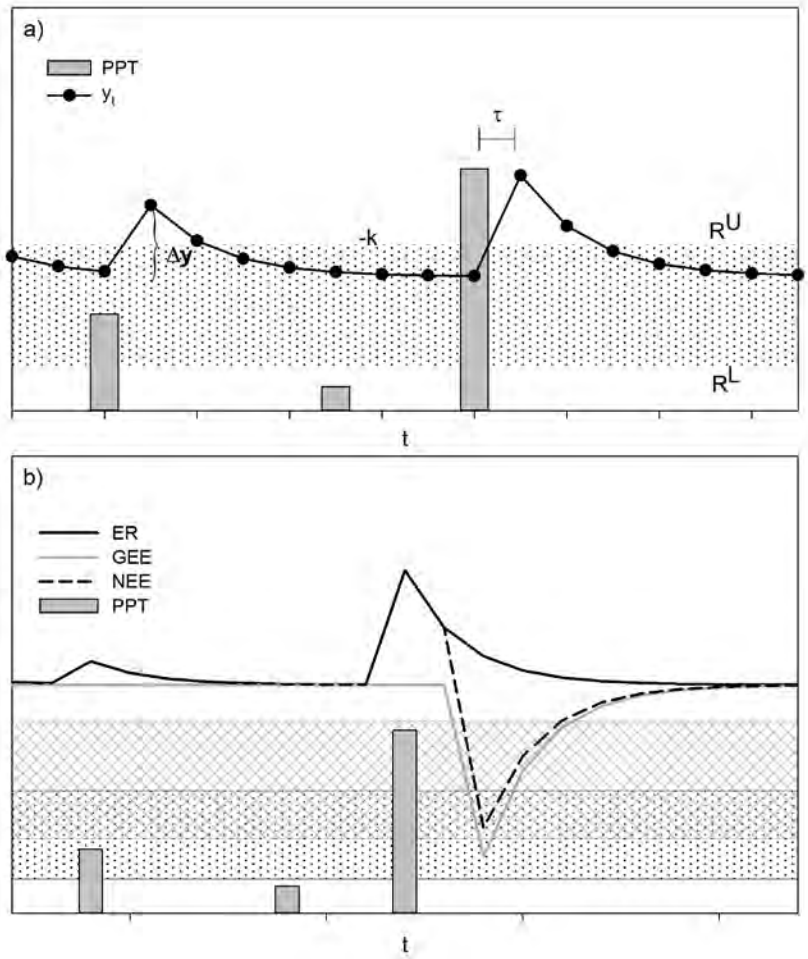

Figure 1. The Threshold-Delay model (Ogle and Reynolds, 2004). a) The magnitude of the increase in the response variable (Δt, e.g. carbon flux, y_t) is determined by the size of PPT event and by the previous state of the response variable. The decreasing rate of the response following the stimulus is denoted by –k. The low PPT threshold (R^L) indicates the minimum size PPT event to stimulate a response, and the upper PPT threshold (R^U) indicatesPPT events that do not cause additional increment in the response variable. The time interval between the stimulus and the response is described by τ. b) The response of the net ecosystem exchange (NEE), that is the balance between the gross ecosystem exchange (GEE) and ecosystem respiration (ER), vary in response to changes of GEE and ER. According to the T-D model, GEE and ER have different PPT thresholds (doted band and mesh stand for effective PPT events size for ER and GEE,

respectively), with ER responding to smaller size PPT events than GEE, therefore, small PPT events favor C release whereas large PPT events stimulate net C uptake by the ecosystem. Differences of time responses between soil microorganisms and plants to soil wet up led GEE and ER to differ in time delays (τ), with shorter time delays for ER than GEE (Huxman et al., 2004a). The hypothetical curve for NEE and its components was calculated introducing arbitrary parameters in the T-D model equations of Ogle and Reynolds (2004) (Eq. A1-A3).

The semiarid grassland in Mexico is characterized by small PPT events with > 60% of the annual PPT events being < 5 mm d^{-1} (Unpublished data). In addition, precipitation is characterized by short inter-event dry periods (inter-event periods < 10 days), but also include long dry periods lasting from six to nine months. These long dry periods may allow for nutrients and C resources to accumulate in soils, becoming available with the first summer rains. Thus, small size PPT events are likely to activate BSC on the soil surface covering up to 60% of plant interspaces (Concostrina-Zubiri et al., 2014), stimulate ER instead of C uptake, particularly after long dry periods (between wet-dry seasons). *Bouteloua gracilis* the keystone species in the semiarid grassland of Mexico (Medina-Roldán et al., 2007, 2013) may contribute however, to C uptake considering its adaptations to small PPT (Sala and Lauenroth, 1982). This is specially important since global circulation models forecast a 10% and 20% reduction of summer and winter precipitation, respectively at the end of the 21st Century (Christensen et al., 2007). Moreover, while these forecasts a predict fewer PPTs events, they also predict these events depositing more precipitation per storm (Solomon et al., 2007, Easterling et al., 2000).

The objective of this study was to evaluate the effect of PPT patterns (periodicity) and magnitude of individual PPT events on daily ecosystem C balance (NEE) for the semiarid grassland in Mexico. Over a four year study period, we examined event-based PPT amount, the period between PPT events, *a priori* daytime NEE rate and *a priori* soil moisture content as the main drivers of daily mean NEE change rate. Because we were interested on short-term NEE change and its

components, only short-term NEE change within days following a PPT event were evaluated. Effects on daily mean GEE (GEE = -NEE + ER) was also evaluated at the beginning of the growing season. Based on the T-D model (Ogle and Reynolds, 2004), we expected that; 1) semiarid grassland should exhibit a quick response (short time-delay) to PPT events through positive NEE fluxes (C release, H1), 2) even small PPT events (<5 mm) should positively enhance the daily mean NEE rates (Low PPT threshold, H2). However, ER and GEE should differ in their time response and PPT thresholds, with shorter time-delays and lower PPT thresholds for ER than GEE (H3). This response is based on the fact that small PPT events should enhance ER mainly through heterotrophic respiration of soil surface microorganisms that are activated within one hour after wet up (Placella et al., 2012), whereas larger PPT events are required to reach roots at deeper soil profiles and plants require longer times for growing. Finally, we expected that, 4) the daily NEE rate change should be determined by the size of the PPT event, but the response should be modified by the previous soil moisture condition or previous NEE rates of the ecosystem as predicted by the T-D model (H4).

Materials and methods

Site description

The study site is located on a shortgrass steppe, within the Llanos de Ojuelos subprovince NE of Jalisco state, Mexico. The shortgrass biome in Mexico extends from the North American Midwest along a strip that follows the *Sierra Madre Occidental* through the *Chihuahuan* Desert into the sub-province *Llanos de Ojuelos*. Vegetation is dominated by grasses, with *Bouteloua gracilis* H.B.K. Lag ex Steud (blue grama) as the key grass species, forming under well preserved conditions near mono-specific stands. The region has a semiarid climate with mean annual precipitation of 424 mm ± 11 mm (last 30 years, unpublished data) distributed mainly between June and September and exhibiting 6 to 9 months of no rain. Winter rain accounts for < 5% of the total annual precipitation (Aguado-Santacruz, 1993, García, 2004). Mean annual temperature varies between 17.5 ± 0.5 °C, with mean temperature extremes ranging from 2.2°C for the coldest to 26.8

°C for the warmest month, respectively. The topography is characterized by valleys and gentle rolling hills with soils classified as haplic xerosols (associated with lithosols and eutric planosols), and haplic phaeozems (associated with lithosols) (Aguado-Santacruz, 1993). Soils are shallow with average depth of 0.3-0.4 m containing a cemented layer at ~ 0.5 m deep, with textures dominated by silty clay and sandy loam soils (Aguado-Santacruz, 1993, COTECOCA, 1979).

The study site is a fenced area of ~64 ha of semiarid grassland divided into 16 paddocks of ~4 ha that are subjected to different grazing regimes and fire management. A 6 m high tower was placed at the center of the area of interest to support carbon-energy flux measurements and meteorological instruments as well. That location allowed an ever-changing and integrated measurement footprint of 320 m, 410 m, 580 m, and 260 m from the tower according to the N, E, S, and W orientations, respectively. Eddy covariance instruments were placed at 3 m high to cover a fetch of 300 m.

Meteorological and soil measurements

Meteorological data was collected continuously at a rate of 1 s and averaged at 30 min intervals using a datalogger (CR3000, Campbell Scientific Inc., Logan, Utah). Variables measured included; air temperature and relative humidity (1000 Ω PRT, HMP45C, Vaisala, Helsinki, Finland) housed into a radiation shield (R.M. Young Company Inc., Traverse City, MI), incident and reflected shortwave and longwave solar radiation (NR01, Hukseflux, Netherlands), photosynthetic photon flux density (PARLITE, Kipp and Zonen, Delft, the Netherlands) where measured at 2 m.a.g.l. Soil variables were measured at a 5 min frequency and averaged at 30 min intervals. These included volumetric soil water content (CS616, Campbell Sci., Logan, UT) positioned horizontally to 2.5 cm and 15 cm deep, average soil temperature of the top 8 cm soil profile, and soil temperature at 5 cm deep (T108 temperature probes, Campbell Scientific Inc., Logan, UT). Soil temperature variables were acquired by another datalogger (CR510, Campbell Scientific Inc., Logan, UT). Precipitation was measured with a bucket rain gauge installed 5 m away from the tower (FTS, Victoria, British Columbia, Canada) at 1 m.a.g.l.

Net ecosystem CO_2 exchange measurements

An open path eddy covariance system was used to measure NEE over the semiarid grassland. The system consisted of a three-dimensional sonic anemometer (CSAT-3D, Campbell Sci., Logan, UT) for measuring wind velocity on each polar coordinate (u, v, w) and sonic temperature (θs), and an open-path infrared gas analyzer (IRGA, Li-7500, LI-COR Inc., Lincoln, NE) to measure CO_2 and water vapor concentrations. Instruments were mounted in a tower at 3 m above soil surface oriented towards the prevailing winds. Because prevailing winds change along the year, EC was oriented SW in winter and turned East during summer on the last two years. The IRGA sensor was mounted next to—and 10 cm offset from the anemometer transducers, the center of the IRGA optical path was centered with the distance between the vertically oriented sonic transducers, and tilted 45° to avoid dust and water accumulation in the IRGA optical path. Digital signal of both sensors were recorded at a sampling rate of 10 Hz in a datalogger (CR3000, Campbell Scientific Inc., Logan, UT). Instruments were installed in December 2010 and were continuously operating during four years (2011-2014). Few power failures throughout the study period and a lighting in 2012 were the main causes of gaps in the data time series, but on ~ 60% of half-hour data periods per year were available (and 42247 30-min averaging periods after quality filtering was used).

NEE was estimated as:

$$NEE = \overline{w'CO_2'} \qquad (1)$$

overbar denotes time averaging and primes are the deviations of instantaneous values (at 10 Hz) from a block-averaged mean (30 min) of vertical windspeed (*w*, m s^{-1}) and molar fraction of CO_2 (μmol CO_2 mol^{-1}), respectively. Micrometeorological convention was used, where negative NEE values stand for ecosystem C uptake. We did not estimate a storage flux because of the low vegetation stature and well mixed conditions, therefore we assumed it would be 0 over a 24-h period (Loescher et al. 2006).

Data processing

Raw eddy covariance data were processed in EdiRe (v1.5.0.10, The University of Edinburgh). Wind velocities, sonic temperature, [CO_2], and [H_2O] signals were despiked, considering outliers those values with a deviation larger than 8 standard deviations. A 2-D coordinate rotation was applied to sonic anemometer wind velocities to obtain turbulence statistics perpendicular to the local stream line. Lags among horizontal wind velocity and scalars were removed with a cross-correlation procedure to maximize the covariance among signals. Carbon and water vapor fluxes were estimated as molar fluxes (mol m^{-2} s^{-1}) at 30 min block averages, and then they were corrected for air density fluctuations (WPL correction, Webb et al. 1980). To account for frequency loss on NEE, frequency response correction was done considering the cospectra of $w'\theta'$ as ideal, and then comparing the summed cospectral density in the inertial subrange to that of the total spectra of $w'\theta'$ and $w'CO_2'$ (Baldocchi and Meyers, 1989). Sensible heat flux was estimated from the covariance between fluctuations of horizontal wind velocity (w') and sonic temperature (θ'_s). This buoyancy flux was corrected for humidity effects (Schotanus et al. 1983, Foken et al., 2012) and momentum fluctuations (cross wind correction, Schotanus et al. 1983).

Fluxes were submitted to quality control procedures, i) stationarity (<50%), ii) integral turbulence characteristics (<50%), iii) flags of IRGA and sonic anemometer (AGC value<75, Max CSAT diagnostic flag = 63) which are strongly related with advices of problem measurement due to rain events, iv) screening of flux values into a logical magnitudes (±20 µmol CO_2 m^{-2} s^{-1}), and v) a threshold u*= 0.1 m s^{-1} was used to filter nighttime NEE under poorly developed turbulence. This threshold was defined through the 99% threshold criterion after Reichstein et al. (2005), where data are split into six temperature classes of equal sample size, and then each temperature class is split into 20 u*-classes. The threshold is defined when the u* class average reaches the 99% of the night-time flux average of the higher u*-classes. The mean of u* thresholds of at least 6 temperature classes is defined as the final threshold. The procedure is done for subsets of three months

per year (J-M, A-J, J-S, and O-D) to account for seasonal variation of vegetation structure.

Ecosystem measures of productivity were derived such that,

$$NEP \approx -NEE \quad (2)$$

$$GPP \approx GEE = -NEE + ER \quad (3)$$

where, NEP is net ecosystem productivity (μmol CO_2 m^{-2} s^{-1}), GPP is gross primary productivity (μmol CO_2 m^{-2} s^{-1}), GEE is gross ecosystem exchange (μmol CO_2 m^{-2} s^{-1}), and ER is ecosystem respiration (μmol CO_2 m^{-2} s^{-1}). Temporally integrated estimates are noted throughout this Chapter. Because of GEE cannot be measured directly, it is estimated from the right hand of Eq. 3. The ER was estimated in two ways, 1) it was estimated from light-response curves (see below), and 2) it was determined from nighttime NEE data (under PPFD < 10 μmol m^{-2} s^{-1} light conditions). Different ER estimation method is indicated throughout the Chapter. Micrometeorological convention is used, thus, negative fluxes stand for C uptake by the ecosystem, whereas positive fluxes indicate C losses to the atmosphere.

For identifying changes induced by PPT events on GEE and ER, daytime and nighttime NEE data on a one day-window was adjusted with a rectangular hyperbolic response function to PPFD (Ruimy et al. 1995) modified with the exponential model of respiration (Gilmanov et al. 2010),

$$NEE = \frac{\alpha * PPFD * A_{\max}}{\alpha * PPFD + A_{\max}} + R_b * Q_{10}^{(\frac{T-Tref}{10})} \quad (4)$$

where, α is the apparent quantum yield (μmol CO_2 m^{-2} s^{-1}/μmol PPFD m^{-2} s^{-1}), A_{max} is maximum photosynthetic capacity (μmol CO_2 m^{-2} s^{-1}), R_b is basal respiration at reference temperature (15 °C, μmol CO_2 m^{-2} s^{-1}), Q_{10} is the temperature sensitivity coefficient, depicting the increase of respiration rate with a 10 °C of temperature increment (calculated parameter, unitless), and T is air temperature (°C). Similar to the procedure employed by Gilmanov et al. (2010), daytime and nighttime NEE were used to fit the model. This approach accounts for the hysteresis effect

observed commonly in grasslands where NEE declines afternoon even at similar PPFD values than at the morning.

In calculating parameters, Amax is obtained at infinite PPFD values that are not realistic, thus, NEE rate was estimated at PPFD=2500 µmol m^{-2} s^{-1}, and 25 °C of air temperature $NEE_{2500,25}$), such that,

$$NEE_{2500,25} = \frac{\alpha * 2500 * A_{\max}}{\alpha * 2500 + A_{\max}} + R_b * Q_{10}^{(\frac{T-Tref}{10})} \quad (5)$$

Changes and transitions from ER dominated NEE fluxes to C-gain processes (GEE) were verified with the form of the light response curve. Linear models were used to identify environmental drivers of C fluxes at one-day intervals.

Gap filling procedures and characterization of PPT events

Data gaps shorter than two hours were linearly interpolated, whereas gaps larger than two hours were left as empty data. Only daytime-NEE data were used for most of the analysis. Even though effects on ecosystem respiration should be better observed in nighttime NEE, this data generally is subjected to quality problems. These include poor developed turbulences causing little data availability and deviation from NEE averages if the whole night cycle is not similarly represented among days. Daily mean ER derived from nighttime NEE data were used for analysis only when more than 50% of the data was available after QA/QC procedures. NEE related PPT events were selected for analysis based on data quality and availability to evenly cover the daytime cycle (on average more than 85% of NEE data) and then averaged through the day. The daytime-scale was selected to avoid confounding diurnal NEE variability and to get better analysis robustness. Even when physical CO_2 displacement and microorganisms activation has been observed to start within less than one hour after a precipitation pulse (Placella et al., 2012; Unger et al., 2010), maximum C efflux was recorded between 9 and 24 h following the PPT. This allowed us to quantify these peaks in our analysis. Precipitation events occurring at night and early morning were considered to affect C fluxes the next immediate day (i.e. the same day for early

morning PPT). The C flux one day before the PPT event was taken as the reference C flux. In the case of a continuous PPT for a whole day, that made that day NEE data useless or unavailable. Precipitation events effect was not evaluated when previous or next-day data after PPT event was not available due to equipment's malfunction, quality problems, previous day-time PPT, etc. Event-response effect ("priming NEE effect") was measured as the difference between mean daytime NEE post-event and mean daytime NEE pre-event, such that;

$$\Delta NEE = NEE_{post\text{-}event} - NEE_{pre\text{-}event}$$

where NEE is the daytime NEE average (μmol m^{-2} s^{-1}).

The micrometeorological convention was followed in this study, thus, negative NEE fluxes stand for ecosystem C uptake, whereas positive NEE fluxes indicate C release to the atmosphere. Similarly, positive ΔNEE indicate reduction of C uptake by the ecosystem following the PPT event.

Intervals between PPT events (hereafter days since last event, DSLE) were counted in days from the last PPT event, regardless its magnitude.

Statistical analysis

Simple and multiple correlation analysis were employed to determine factors controlling C efflux after PPT events; these included PPT event size, inter event-periods (DSLE), *a priori*, current, and change of volumetric water content (VWC) at two depths (2.5 and 15 cm), soil temperature, previous daytime NEE, and enhanced vegetation index (EVI). Quadratic and multiplicative terms of independent variables were included in the analysis after the exploration of univariate relationships if this suggested a type of quadratic curve. The best model was selected based on the highest R^2 and adjusted R^2, and the biological significance of the model. All analyses were performed in SAS V8.0 (The SAS System, Cary Inc., CA, USA) at the $\alpha = 0.05$ chance level.

Results

Precipitation pattern

Precipitation during the four years of the study differed in amount and timing. Cumulative precipitation for 2011 (288.5 mm) was below the 30-years average for the site (420 mm) and was the worst drought of the last 70 years, whereas 2012 was a slightly dry year (355.2 mm), 2014 was a wetter year than the MAP (528.5 mm), and 2013 was the wettest year with 601 mm (Fig. 2). The 4 years differed in precipitation frequency, but they were similar for the proportion of rain event categories, including a 60% of precipitation events fewer than 5 mm (they differed in less than 10%, Fig. 3a). Precipitation events larger than 10 mm however, accounted for most of the annual precipitation at all years (Fig. 3b). Overall, large PPT events were more frequent in the wettest years, with shorter inter-event periods than in dry years. Dry years in contrast were conformed by small PPT events with large inter-event periods (10% inter-event periods < 5 days, Fig. 3a, c). Volumetric soil water content dynamics followed the precipitation pattern, reaching saturation after large or recurrent PPT events. Largely, soil moisture was maintained over a 10% in the wettest years, with the largest peak reaching a 40% in summer 2014 (Fig. 2b). Most VWC variability was observed at 2.5 cm depth rather than 15 cm depth and it was better correlated with precipitation amount per event ($p<0.05$, $R^2 = 0.72$, Fig. 4b), increasing 0.3 % per mm of precipitation. Precipitation events as small as 0.25 mm changed $VWC_{2.5}$ in ~1-2% but this increase lasted for less than one hour (data not shown), whereas VWC_{15} increased only after PPT ~5 mm. For instance, a PPT event of 5 mm immediately increased $VWC_{2.5}$ by 1.6%; in contrast, VWC_{15} increased by 0.5% with the peak delayed 6 days from the PPT event (Fig. A2).

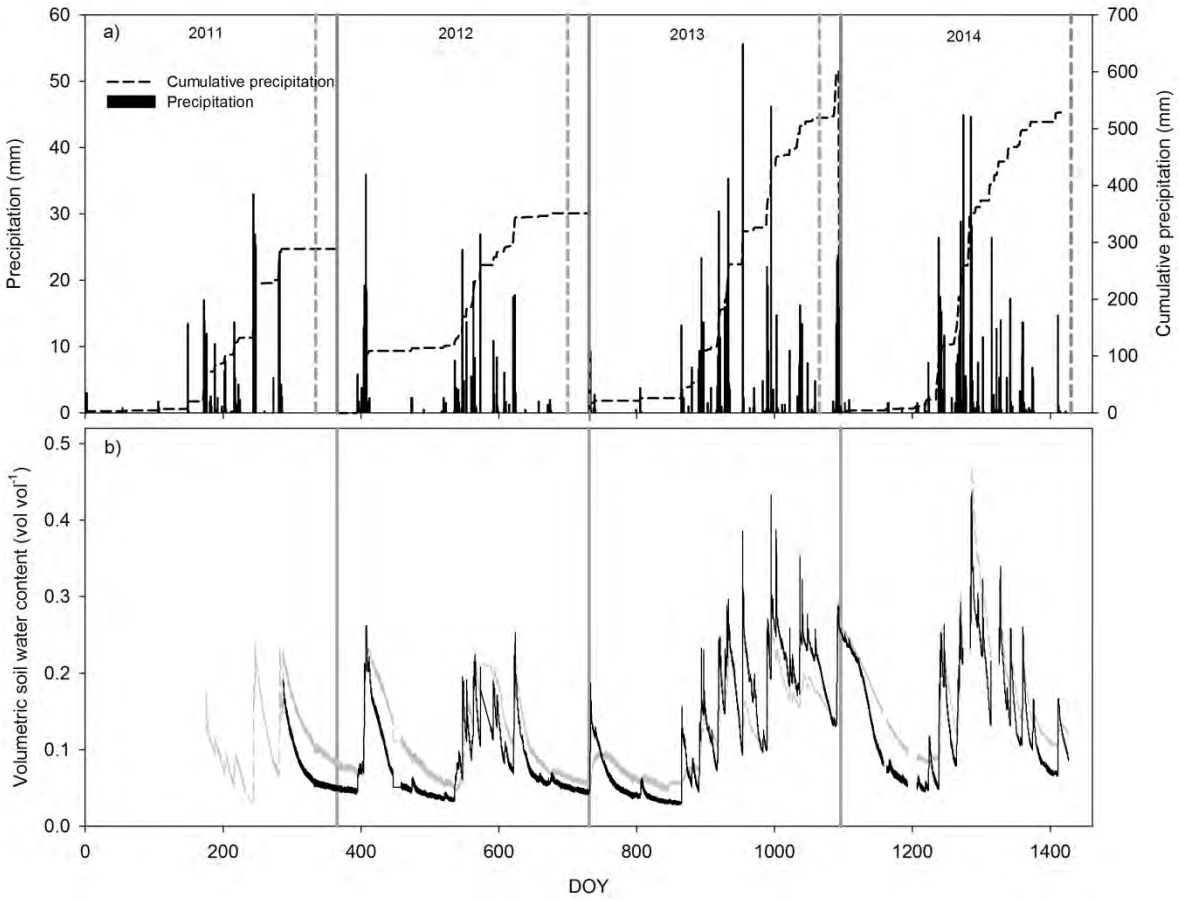

Figure 2. Seasonal and interannual variation of daily precipitation and cummulative precipitation (a), and volumetric soil water content at 2.5 (black line) and 15 cm depth (gray line; b).

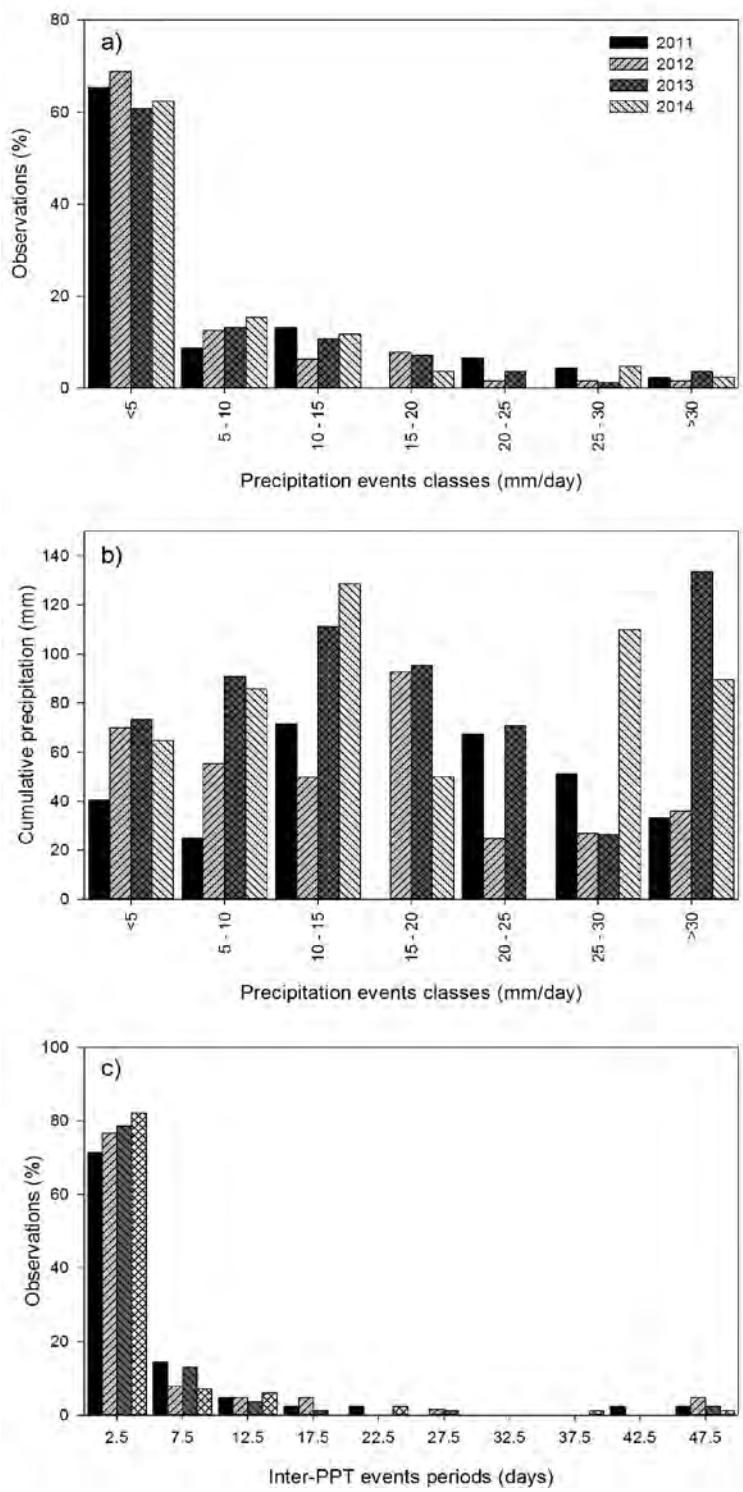
a)
2011
2012
2013
2014
Observations (%)
Precipitation events classes (mm/day)
<5
5 - 10
10 - 15
15 - 20
20 - 25
25 - 30
>30
b)
Cumulative precipitation (mm)
Precipitation events classes (mm/day)
c)
Observations (%)
Inter-PPT events periods (days)
2.5
7.5
12.5
17.5
22.5
27.5
32.5
37.5
42.5
47.5

Figure 3. Distribution of precipitation events (a) and cumulative precipitation by precipitation events classes (b). c) Distribution of inter-event periods (days) for the four years study.

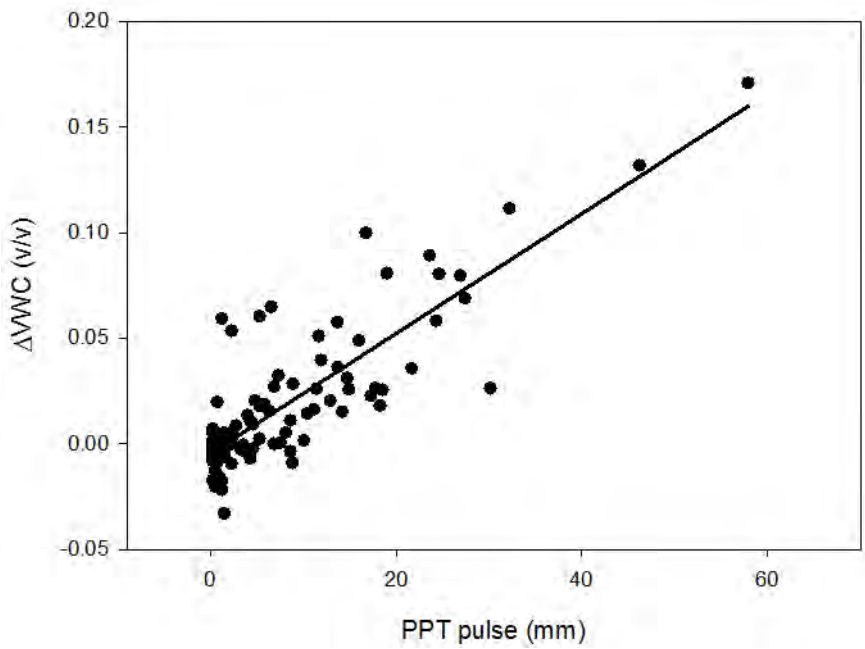

Figure 4. Relationship between size of precipitation event (mm) and the change in soil volumetric water content at 2.5 cm depth (v/v). The line stands for the linear regression such that ΔVWC = -0.0047 + 0.0028 * PPT event (mm), R^2 = 0.72.

Short-term effects of precipitation events on carbon fluxes.

Only the NEE change following the first event (inter-event period > 1 day) was analyzed due to problems of data quality in consecutive PPT events. A total of 72 events including all 4 years were used for statistical analysis, with around 20 PPT events per year. Small precipitation events were dominant in our database, representing the precipitation pattern of the site. The sample was integrated by events in the range from 0.25 to 57.9 mm, and a mean of 7.3 ± 1.3 mm (□□ ±1 SD). Large PPT events occurred after short inter-event periods, and short PPT events were preceded by long inter-event periods. Medium PPT events after long inter-event period were rare, and extreme PPT events after long inter-event periods

were inexistent (Fig. A3). Half-hour NEE data was used to describe dynamics of shorter than one-day responses and to compare with other studies that use data at shorter time-scales. Overall, the analysis of half hour fluxes revealed almost instantaneous positive response of NEE to PPT event that exponentially decreased over time into a half to two hours after the PPT event (Fig. A1). The minimum PPT event to change NEE was as low as 0.25 mm, even lower than the low threshold PPT reported for other arid ecosystems (Hao et al., 2007). At the one-day time scale, NEE positively changed immediately (the next day) after the PPT event, decreasing exponentially over time (Fig. 5). It was not possible to evaluate the short-term effects of PPT events on ER data based on nighttime NEE in the same way than daytime NEE, because of most of ER data following PPT events were rejected due to quality issues.

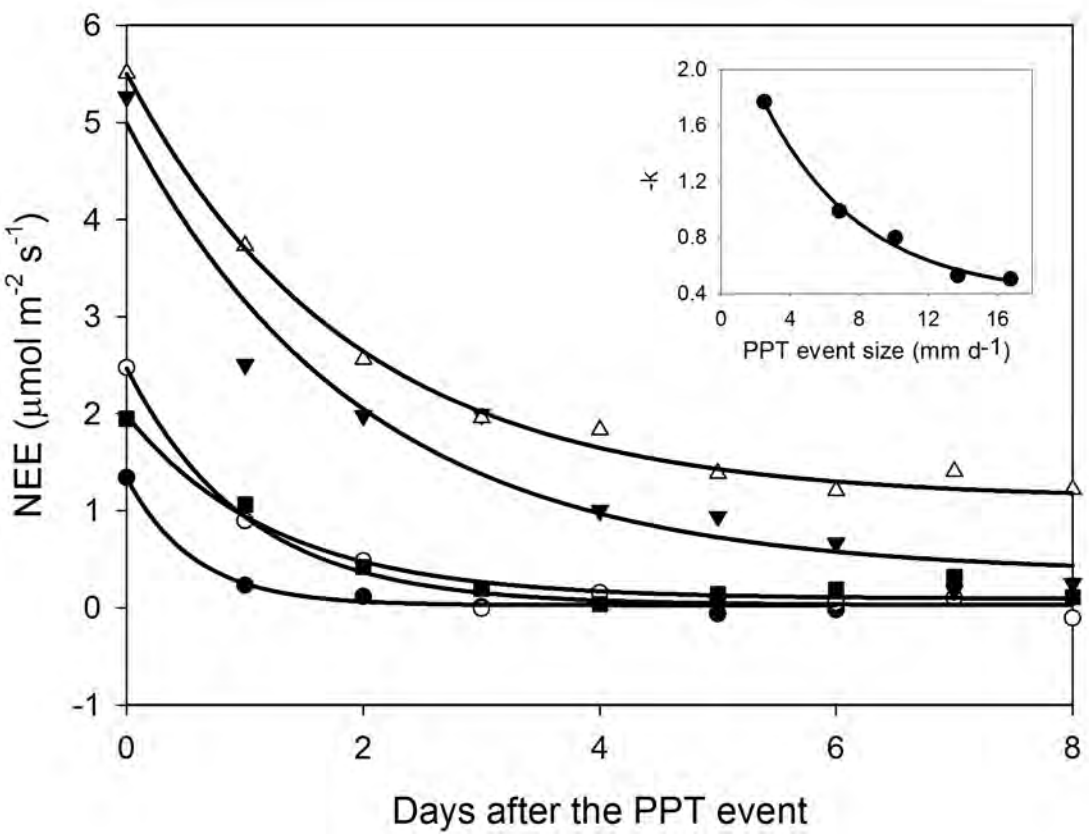

Figure 5. Net ecosystem exchange (NEE) after a precipitation event showing the

decreasing effect through time (days). The decreasing effect rate was adjusted to an exponential negative model NEE = yo + a *exp(-k *t). The insert stands for the relationship between the decaying rate (-k) and the PPT event that originated the NEE change. This relationship was fitted with an exponential model (black line; -k = yo + a *exp(-b*PPT_event). Symbols indicate different PPT event sizes that originated the NEE change, 13.7mm d^{-1} (Δ), 16.74 mm d^{-1} (▼), 6.86 mm d^{-1} (○), 10.08 mm d^{-1} (■), and 2.52 mm d^{-1} (●). Parameters are reported in Table A1.

Flux partitioning through light-response curves at one day-time scale revealed immediate increase of ER after PPT events as low as 0.25 mm. However to promote a change in GEE, it was needed either a larger PPT event or multiple consecutive events (*e.g.,* > 40 mm, Fig. 6a). Thus, dynamics of GEE and ER apparently were more related to changes of soil water content than to PPT event size *per se*. Changes in VWC at 2.5 cm depth stimulated the ER response, whereas the GEE increased only after VWC at 15 cm depth changed of above ~10%. (Fig. 6b). Moreover, in contrast with the almost immediate ER response, the GEE response was delayed about 5 days after the increase in VWC at 15 cm depth at the beginning of the growing season (Fig. 6a, b). These dynamics were confirmed with the available nighttime NEE-derived ER data (data not shown).

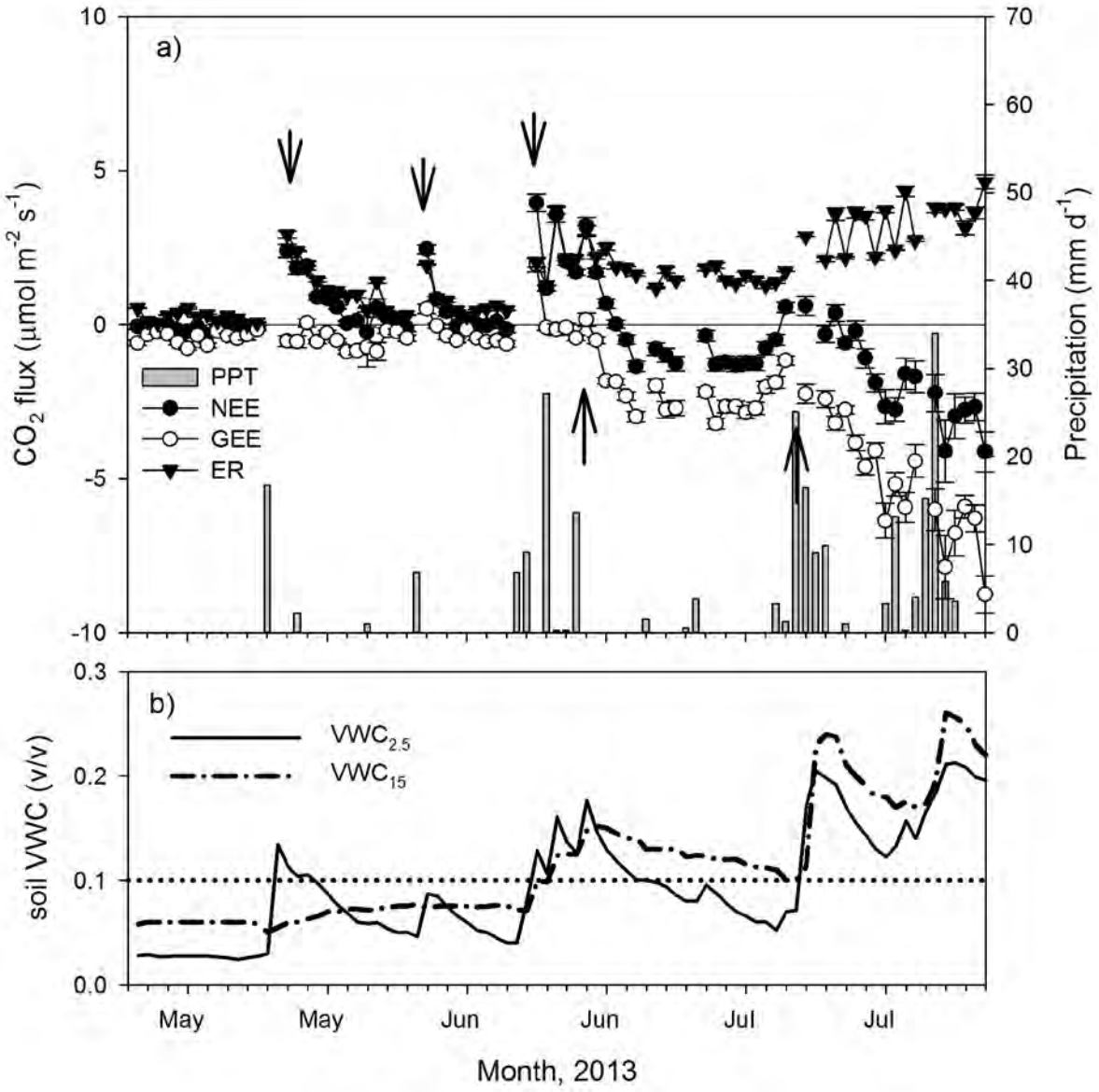

Fig. 6. Dynamics of a) precipitation (mm d^{-1}) and net ecosystem exchange (NEE, µmol m^{-2} s^{-1}, daily means ± 1 SE) and its components, the gross ecosystem exchange (GEE, µmol m^{-2} s^{-1}) and ecosystem respiration (ER, µmol m^{-2} s^{-1}) for the transition from the dry (December – May) to the wet season (June – November) in 2013. b) volumetric soil water content dynamics (VWC, v/v) at two depths (2.5 cm and 15 cm). Arrows indicate apparent changes in GEE and ER trends.

Drivers of the priming NEE effect

Decreasing NEE rates varied depending on the PPT size event, with C efflux pulses lasting longer with initial larger ΔNEE. However, decreasing NEE rates were better explained by PPT event size than the initial ΔNEE (insert Fig. 5). For instance, after a 13.7 mm PPT event and initial daytime NEE = 5.1 μmol m^{-2} s^{-1}, the enhanced C flux exponentially decreased at a rate of ~50% of its earlier value (NEE = 0.8057 + 7.4306 *exp(-0.5274*t), where t is time in days, R^2 = 0.99, Fig. 5) whereas with an initial enhanced NEE ~2.5 μmol m^{-2} s^{-1}, the C flux decreased at a rate of 100%. Finally, the initial enhancement of NEE = 1.3 μmol m^{-2} s^{-1}, was reduced by a rate of 170% (Fig. 5). Different decreasing rates were influenced by the contribution of each particular PPT event in addition to the initial ΔNEE. For instance, cumulative daytime NEE, 8 days after the initial C event indicated a C efflux of 5.4 g C m^{-2} after the PPT event of 13.7 mm, and 0.46 g C m^{-2} with a PPT event of 2.5 mm.

The magnitude of NEE response (ΔNEE) was positively correlated with the PPT event size (Fig. 7a), the inter-event period (Fig. 7b), and the change of VWC at 2.5 cm depth (Fig. 7e,), whereas it was negatively correlated with the previous VWC at 2.5 and 15 cm depth (Fig. 7c, d). No relationship between ΔNEE with previous NEE was found, but larger change in NEE rates were observed when previous NEE ~ 0 (Fig. 7f). Variation in ΔNEE was better explained with a bivariate relationships between PPT event size and inter-event period through a quadratic model ($z=a+bx+cy+dx^2+ey^2+fxy$, $p < 0.05$, R^2 = 0.68, Fig. 8, Table 1 and A2), and with inter-event period and previous VWC ($p < 0.05$, R^2 = 0.66, Table 1 and A2). Both models were equally significant due to the fact that they were related by one variable describing the previous state of the soil (preVWC and DSLE) and the size of the stimulus (PPT_event and ΔVWC). Moreover, both models showed larger C efflux at intermediate independent variable values, and a plateau or lower efflux rates at the highest values. Previous NEE also was related to ΔNEE using the bivariate relationship with ΔVWC at 2.5 cm depth, however the quadratic model explained less variability than the previous relationships (R^2 = 0.54; Fig. A4; Table A2).

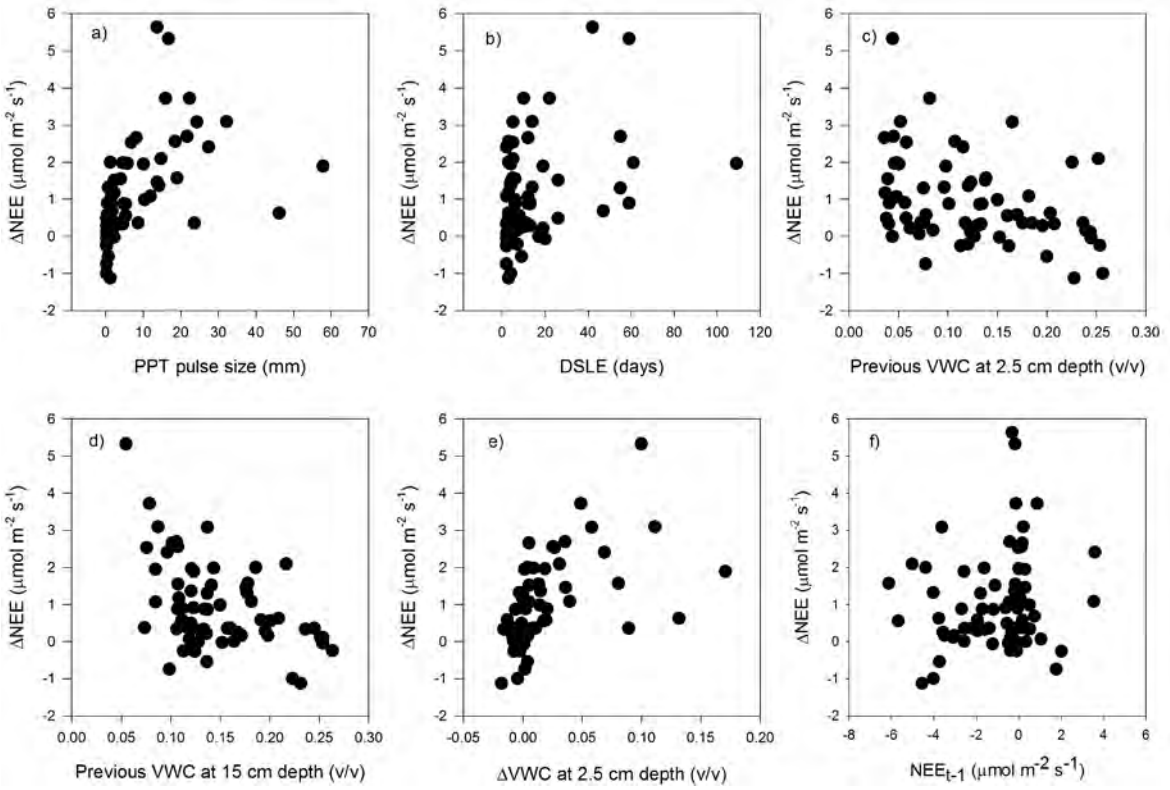

Figure 7. Univariate relationships between change of averaged daytime NEE (ΔNEE, μmol m^{-2} s^{-1}) and, a) PPT event size (mm), b) inter-event period (DSLE, days), c) previous VWC at 2.5 cm depth (v/v), d) previous VWC at 15 cm depth (v/v), e) change in VWC at 2.5 cm depth (v/v), and f) previous NEE (NEE_{t-1}, μmol m^{-2} s^{-1}).

Table 1. Results of bivariate regression analysis among ΔNEE (μmol m^{-2} s^{-1}) and PPT event size (PPT_event, mm), inter-event period (DSLE, days), change of volumetric soil water content (ΔVWC, v/v), and previous volumetric soil water content (prevVWC, v/v). The selected model was $\Delta NEE = a+bx+cy+dx^2+ey^2+fxy$, where a, b, c, d, e, and f are calculated parameters and x and y are any of the independent variables.

Model	Source	Sum of squares	DF	Mean square	F	P>F	R2
DNEE X PPT_event X DSLE	Regr	82.37	5	16.47	28.61	0.000	0.69
	Error	37.43	65	0.58			
	Total	119.80	70				
DNEE X DVWC X PrevVWC	Regr	52.21	5	10.44	21.44	0.000	0.66
	Error	26.78	55	0.49			
	Total	78.99	60				
DNEE X DVWC X NEE_{t-1}	Regr	45.35	5	9.07	12.28	0	0.55
	Error	36.93	50	0.74			
	Total	82.28	55				

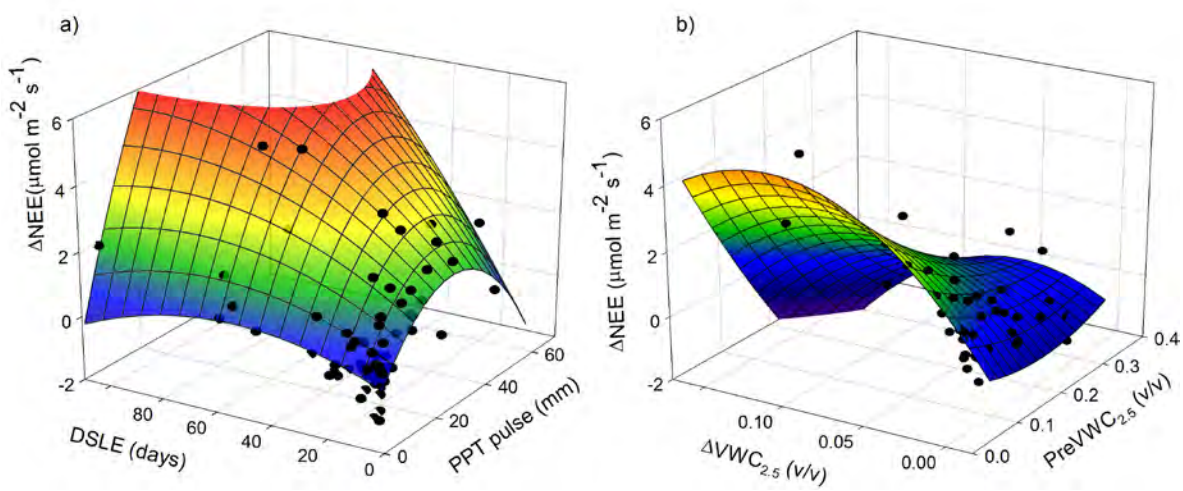

Figure 8. Quadratic relationship among; a) the change of the averaged daytime NEE (ΔNEE, µmol m^{-2} s^{-1}), the size of first PPT event (mm), and the inter-event period (DSLE, days), and b) ΔNEE and change of VWC at 2.5 cm depth ($\Delta VWC_{2.5}$,v/v), and previous VWC at 2.5 cm depth ($PreVWC_{2.5}$, v/v). Parameters presented in Table A2.

Parameters derived from the light-response curves varied after PPT events. Apparent maximum quantum yield (α) showed high variability at daily time-scales without any pattern nor relationship to environmental variables. On the other hand,

net ecosystem exchange at PPFD = 2500 µmol m^{-2} $s^{-1}$and T = 25 °C ($NEE_{2500,25}$) and basal respiration (Rb) showed similar pattern as ΔNEE, with an immediately rise following wet up (Fig. 9a,c), indicating increased ecosystem respiration. The change of $NEE_{2500,25}$ and Rb was related with PPT event size, but the decrease rate of Rb was not dependent on PPT event size in contrast to NEE decreasing rates (Inserts of Fig. 9). Temperature sensitivity of respiration (Q_{10}) was highly variable through the time, but also showed a tendency to increase after large PPT events and eventually decreased as soil dried out.

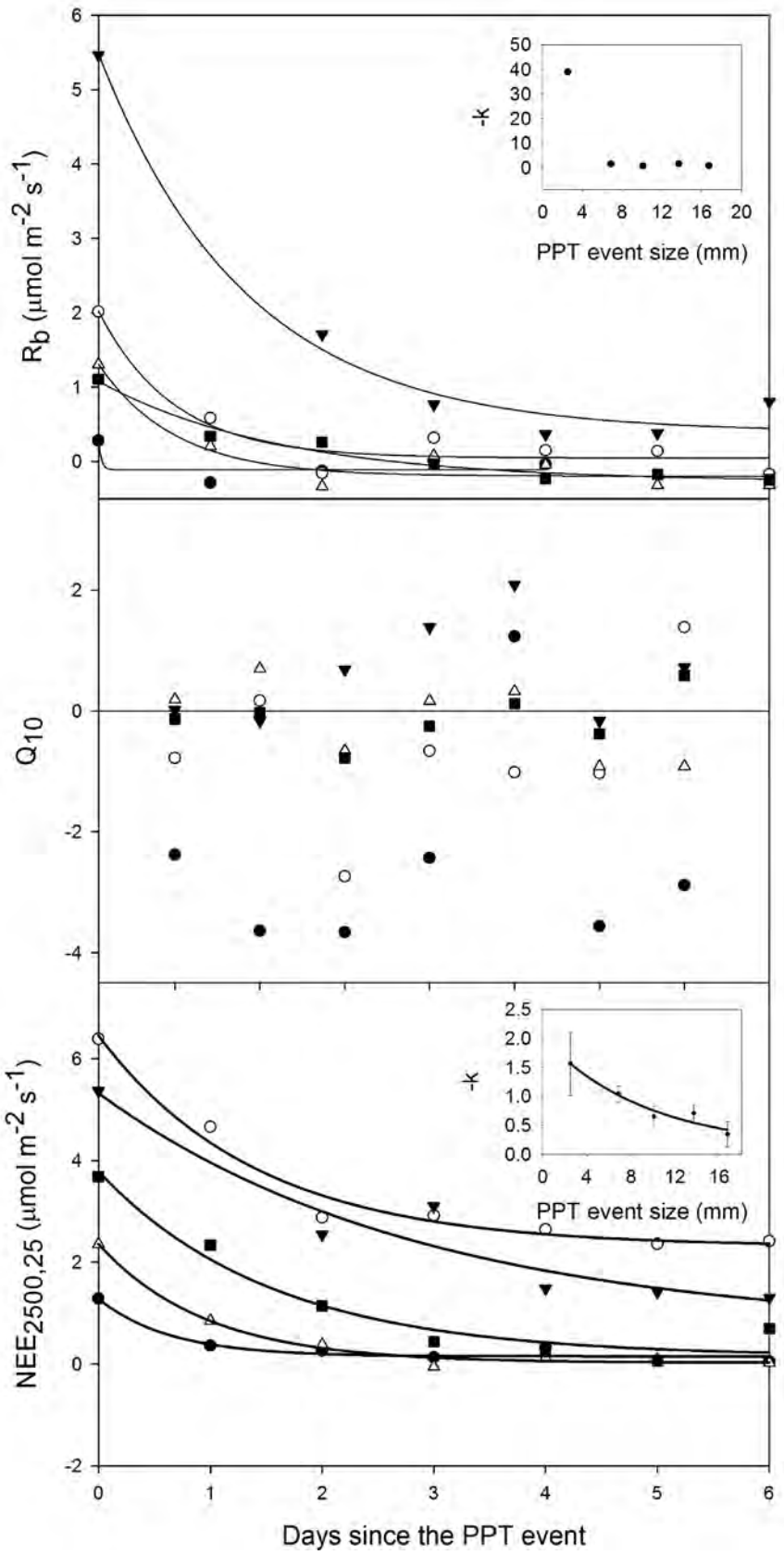
R_b (µmol m^{-2} s^{-1})
-k
PPT event size (mm)
Q_{10}
$NEE_{2500,25}$ (µmol m^{-2} s^{-1})
-k
PPT event size (mm)
Days since the PPT event

Figure 9. Dynamics of, a) basal respiration (Rb), b) temperature sensitivity (Q10), and c) maximum C uptake at PPFD=2500 µmol m^{-2} s^{-1} and 25 °C ($NEE_{2500,25}$) following a PPT event. Insets in Figs. 1 and 3 show the relationship between PPT size event and the exponential decaying rates (-k).

Variable thresholds

No clear thresholds were identified in any of the variables analyzed, with exception of minimum PPT event size to cause a ΔNEE response as was shown above (lower PPT event size threshold = 0.25 mm d^{-1}). Throughout univariate relationships (Fig. 7) however, we could identify upper limits instead. Maximum ΔNEE values were observed at; a previous low VWC in both soil depths (Fig. 7c,d), with medium size PPT events (~20 mm d^{-1}; Fig. 7a), with intermediate inter-event periods (DSLE ~ 40 days; Fig. 7b), and medium changes of soil VWC at 2.5 cm depth (ΔVWC2.5 ~ 0.1; Fig. 7e). Finally, the larger ΔNEE was observed with previously neutral C fluxes (NEE_{t-1} ~ 0; Fig. 7f). The priming NEE effect decreased farther than these limits. For ER and GEE, low PPT event threshold differed. Ecosystem respiration (ER) was the component of NEE that rose after small PPT events ~0.25 mm d^{-1}, whereas a change of GEE was observed only after large PPT events or a sum of consecutive PPT events that changed the VWC at 15 cm depth (Fig 5a,b). Upper limits of ER also were derived from univariate relationships of derived nighttime NEE – ER and environmental variables (Fig. A6). Maximum ER responses were observed at ~12% of $VWC_{2.5}$ and ~20% of VWC_{15}. The upper limit of ER corresponded well to the upper $VWC_{2.5}$ threshold for ΔNEE indicated above.

Discussion

Changes in precipitation timing and frequency are expected to occur in the coming decades with uncertain effects on the C cycle. For this semi-arid ecosystem studies here, carbon fluxes are going to be affected due to the tight relationship and interactions among precipitation, plant functions and microorganisms activity. These ecosystems that are characterized by a high interannual PPT variability, also

exhibit a small sized, individual event, PPT pattern. Several studies have already demonstrated increase in ER rates relative to GEE in response to changing patterns and magnitude of PPT. They attribute this increase to either nutrient accumulation during inter-event periods or cellular lysis after death of soil microorganisms during the course of dry-rewetting cycles (the Birch effect, Birch, 1964), or expulsion of cytoplasmic solutes taken previously up to resist desiccation (Jarvis et al., 1997). While we cannot dismiss any of these hypotheses, and likely all three may contribute towards this overall effect on our system, but we place the most weigh on the priming effect.

"Priming carbon flux effect" of precipitation events

In our study, NEE increased immediately after a PPT event, with half hour delays that last until the following day. This was in accordance to our first hypothesis (H1) proposing that NEE enhancement would follow PPT events with short-term responses (short time delays). Overall, ER had shorter time delays than GEE as was also hypothesized (H3). The increase of ER was observed one day after the PPT event (Fig. 5), whereas GEE increased only 5 days after the PPT event at the beginning of the growing season (Fig. 5). This rapid response have been observed in other studies that examined soil respiration processes, for instance, maximum respiration rates were reported within 10 hours after a PPT pulsed event from a semi-arid oak forest (Unger et al., 2010), while in a Mediterranean pine forest the highest respiration rates were observed within the first two hours after such a pulse (Marañón-Jiménez et al., 2011). At ecosystem level, similar to our study, Huxman et al. (2004b) observed the NEE and ER increase one day after a simulated PPT event, whereas GEE raised three days after the event and achieved the maximum increase, 7 days after the pulse. Causes of larger time-delays of GEE than ER include the delay between the PPT event and the infiltration of water at a given soil layer (*e.g.* 15 cm depth), and the time used by plants for growing of new roots and leaves after the senescence (Ogle and Reynolds, 2004), promoting C losses rather than C uptake in the early growing season (Huxman et al., 2004). In contrast, ER is more related with soil moisture at shallow soil layers that moist immediately after

the PPT event and can get active few hours after soil wet up. Precipitation events and soil moisture dynamics at 15 cm depth were out of phase (up to five days between the PPT event and the SWC_{15} peak, Fig. A2), which is in accordance with the first cause of the larger time-delay.

We suspect that immediate daytime NEE and ER responses were a flux dominated by heterotrophic respiration. Indeed these microbial communities may very well have evolved to take advantage of these short-term availability of water. Short-term responses of less than half an hour have also been reported in studies analyzing soil microorganism activity through molecular and stable isotope techniques (Placella et al., 20012; Unger et al., 2010). Fungi and bacteria on the soil surface have the capability for water-induced re-activation that includes very rapid growth within 1 to 72 hours after a PPT event (Placella et al., 2012). The immediate peak observed (Fig. A1) may have resulted from such rapid activation of bacteria displaying highest activity 1-h after wetting (Placella et al., 2012). Actinobacterias (e.g. actinomycetes) and cyanobacterias identified as rapid responders are common in soil microorganism communities of arid lands, many of these forming the biological soil crusts (BSC, Belnap, 2003). BSC at our site for instance, covers up to 70% of plant interspaces in grazing-excluded conditions and up to 30% in overgrazed sites (Concostrina-Zubiri et al., 2014) with dominance of cyanobacteria BSC. This suggests that NEE peaks might also be attributed to BSC respiration. On the other hand, physical displacement of enriched CO_2 air rom soil pores is another likely source of C flux (Huxman et al., 2004a), but this is expected to be released within the first few minutes after the PPT event as the water infiltrates through the soil profile (rf. Marañón-Jiménez et al. 2011).

Variable thresholds

Due to the relationship of multiple variables was not possible to identify clear thresholds, but maximum limits and trends (Fig 7). The minimum effective PPT event for NEE change response was as low as 0.25 mm d^{-1}, in agreement with our H2 stating that C flux would be stimulated with low PPT events. Also, as indicated in our H3, GEE and ER differed in the lower PPT event size threshold. The

smallest PPT events only stimulated ER as no apparent change was observed in GEE. Even a large PPT event of 20 mm d^{-1} recorded in May (Fig. 5) did not induce GEE increase. Notably the small PPT events inducing changes in VWC at the shallow soil profile (2.5 cm) likely promoted respiration of BSC. In contrast, large or consecutive PPT events that reached deeper soil profiles stimulated GEE (cumulative PPT > 40mm). These results also help to explain why the *a priori* soil moisture and the change of VWC on the soil surface (2.5 cm depth) better explained ΔNEE than moisture dynamics at 15 cm depth (Fig 7b), which confirms our suggestion that immediate CO_2 efflux is derived from soil microorganism respiration.

The low PPT threshold stimulating ER agrees with results from other studies in arid ecosystems or it was even lower. Precipitation events as small as 3 mm induced respiration of BSC (Kurc and Small, 2007), equally PPT events <10 mm d^{-1} on a shortgrass steppe promoted net loss of C (Parton et al., 2012). However, the observed minimum PPT event needed to stimulate the GEE response (the low PPT threshold) was higher than was expected. The dominant species at our site, *B. gracilis*, is reported to respond to PPT events as small as 5 mm (Sala and Lauenroth, 1982). Also, a study by Parton et al. (2012) showed that rain events > 10 mm activated plant photosynthesis in a semiarid grassland, therefore we expected a low PPT threshold between 5 and 10 mm. Instead, in this study large or consecutive PPT events had to occur before an affect on GEE was observed (Fig 5). Nevertheless, is interesting to note that small PPT events in arid ecosystems may not lead to C uptake, but may alleviate stress after severe droughts, rehydrating plant tissues and helping the plant to respond faster after larger PPT events (Sala and Lauenroth, 1982).

Relationships between NEE, GEE, ER, and environmental-soil variables, suggest that both ER and GEE were more related with soil water dynamics than PPT events *per se*. Thus, productivity (GEE) is sensitive to dynamics of soil water content at deeper soil layers (*e.g.,* 15 cm) than ER, and consequently only responds to large or consecutive PPT pulses that increased the soil water content

at this depth. Water infiltration in soil is controlled by soil characteristics like texture and presence of cemented layers that affect the percolation into the soil at the surface (Schlesinger et al., 1989). However, this can be negatively impacted by grazing and plant cover loss that is commonly observed in these semiarid grasslands (Medina-Roldán et al., 2007), which subsequent leads to larger runoff amounts, and less infiltration.

The upper limit of the priming NEE effect was defined at PPT events > 20 mm under previous dry soil. Extrapolation of decaying constants from maximum PPT event size in the site (60 mm; Fig. A6) indicated that the "priming positive NEE effect" last for a similar time for any PPT event greater than 20 mm d^{-1}(lowest –k = 0.38; Fig. A5). This limit is defined by several conditions, including; 1) the largest and most intense events did not completely infiltrate into the soil, forming abundant runoff, hence moistening soil at similar depth than medium-size PPT events, 2) oxygen and CO_2 diffusion limitation at high post event VWC (ΔVWC, large-size PPT event driven) dampened soil respiration, 3) all soil aggregates were disrupted at medium soil VWC (Lado-Monserrat et al., 2014) that likely provided no additional nutrient and C substrates at higher VWC, and 4) a combination of any of these three. Linear relationship between PPT event size and $\Delta VWC_{2.5}$ (Fig. 4) revealed that there was not a strong limitation of water infiltration into the soil, discarding in some way the first condition, whereas reduction of ER derived from nighttime NEE data after $VWC_{2.5}$> 12% supports the second mechanism (Fig A6)

Influence of event size and a priori conditions

The magnitude of NEE enhancement was determined by PPT event size and ΔVWC as well the prior condition of the ecosystem (*i.e.,* length of inter-event period, previous C flux, and previous soil VWC). These results are in agreement with H4 proposing that PPT event size would control the magnitude of the "priming NEE effect", and that previous conditions of the semiarid grassland would modulate the flux. The PPT event and $\Delta VWC_{2.5}$ described the event size since they were highly correlated (Fig. 4). The PPT event size (mm) was better correlated to $\Delta VWC_{2.5}$ (v/v) (Fig. 4) than to ΔVWC_{15} likely as a result of the time required for

water to infiltrate, therefore decoupling PPT event size and ΔVWC at the one-day timescale (Fig. A2).

The quadratic relationships among variables indicated the occurrence of larger C effluxes at medium PPT event size, previous dry soil conditions, and previous NEE~0. Several mechanisms explain these relationships; i) for instance the accumulation of nutrients and labile C in the soil during inter-event periods (Schimel and Bennet, 2004) may explain the rise on C efflux following large inter-event periods or with previous dry soil conditions. In contrast, ii) soil VWC maintained for a long period above a threshold as well as multiple dry-wet cycles favor that labile C sources get depleted (Jarvis et al., 2007; Fierer and Schimel, 2002). Consequently, recalcitrant C sources are left for microorganisms resulting in lower mineralization rates. And iii) repeated dry-wet cycles could over stress microorganisms reducing the populationsize (Van Gestel et al., 1993), hence reducing their initial respiration response.

Variables describing the ecosystem previous condition (DSLE, $preVWC_{2.5}$, and NEE_{t-1}) modified the priming NEE effect. Even though, the previous soil volumetric water condition (preVWC) is biologically more important than the inter-event period (DSLE), because of preVWC offers insight into the potential dry-wet shock, degree of destabilization of soil aggregates, and degree of intracellular osmolyte accumulation (Haynes and Swift, 1990), DSLE explained most variability of ΔNEE than preVWC, it is likely that DSLE in addition to account for these factors, also account for nutrient and labile C accumulation in soil. However, results relating the size of PPT events and the different components of NEE also indicate that the best way to evaluate these responses is through changes of soil water content. Since several factors control water infiltration in soil (e.g. soil porosity, soil type, SOM), the PPT event size per day does not predict accurately the VWC dynamic at deep soil layers. Moreover, characteristics of PPT events such as PPT intensity (mm/t) at shorter time scales than one day also influence water infiltration. For instance, an intense PPT event of 57 mm d^{-1} on August, 2013, with more than 50 mm falling in less than two hours (Fig. 2), did not produce a large change of VWC at 15 cm

depth, however it saturated the soil surface, suggesting that most of water runoff. On average, considering the four years of data, a cumulative PPT above 40 mm on five days were needed for starting the response of GEE and the beginning of the growing season.

No information about nutrient dynamics was available in this study to support the arguments about nutrient accumulation during drought, however earlier studies at the site have shown accumulation of nutrients after PPT events. For instance, Muñoz-Flores et al. (2014) showed N accumulation following precipitation in winter. In another study, Medina-Roldán et al. (2013) obtained an increase of 36% and 34% of extractable NH_4^+ and NO_3^-in a soil column of 15 cm, respectively, after applying a PPT event of 10mm; however, this was observed 2 days after the event. This result is apparently in contradiction with the general knowledge reporting a sudden nutrient availability increase after wet-up, triggering also soil respiration. Instead, this is indicative of N immobilization by nutrient-limited microorganisms (Austin et al., 2004), once microorganisms requirements are met N is released into the soil matrix (Schimel and Bennet, 2004).

Decaying NEE rates

Carbon flux enhancement by rain events was not a steady state phenomenon, but decreased with time. In agreement with the T-D model, NEE exponentially decreased after the PPT pulse (Fig. 6) to almost the original NEE rate. The largest C pulses slowly returned to basal C flux rates and also showed larger NEE remnants than the small pulses (Fig. 6). This suggests that more persistent soil moisture levels achieved with large size PPT events promoted larger and longer lasting C fluxes. If the event is big enough to maintain VWC above a threshold (e.g. above the wilting point for plants) for a long time, NEE is expected to remain higher than pre-event rates until nutrient or labile C is depleted (Jarvis et al., 2007; Xu et al., 2004.. In contrast, when the PPT event is small and the soil remains wet for a short-time, the C flux peak will be small and last less because drying-out and limited microorganisms activity will occur before soil nutrients are even depleted. Thus, net ecosystem exchange (soil respiration dominated) decaying rates (-k, Fig.

6) were more an issue of water availability than nutrient or C source depletion.

About the application of the T-D model to describe the "priming NEE effect"

The analysis of the "priming NEE effect" (Birch effect) under the frame of the T-D model allow us to describe key features of this phenomenon. Environmental variable threshold were low and response time delays were short, similar to other arid ecosystems (Hao et al ., 2010; Placella et al., 2012). Unfortunately we were unable to analyze data at shorter time scales than one day to account for dynamic variability of microorganism functional types and physical CO_2 displacement as Collins et al., (2008) suggested (The TDND model). Bacteria and fungi have different soil moisture thresholds, time-responses and growth dynamics. For instance, Placella et al. (2012) showed that actinobacteria responds faster than bacilli and protobacteria, with time-delays varying from 15 min to 72 h. Different decaying rates shown by Marañón-Jimenez et al. (2011) at shorter than one-hour timescales depicted at least two processes, 1) a shorter and more transient physical CO_2 displacement, and 2) a long lasting microbial respiration process. On this regard, no apparent changes in the dynamic of NEE decaying through time were observed, that could be indicative of different microorganism activity. However, variability of decaying rates, which in this study depended on the PPT event size, should be accounted by the model because cumulative Birch effect can result more important in the annual C balance than the instant C flux (e.g. one day after).

Conclusion

A low PPT threshold for respiration suggest that almost all PPT events occurring in the semiarid grasslands will produce a C efflux, but the magnitude and time that will last this effect will depend on PPT event size and the previous soil conditions. In regard to the characteristics of the PPT pattern at the site, these included; 1) large PPT events with short inter-event periods, and 2) small PPT events preceded of large inter-event periods. Thus, extremely large and long lasting C effluxes developed on large PPT events preceded by long inter-event periods are unlikely

to happen. Knapp et al. (2015) analyzing the predominant PPT pattern across ecosystems concluded that wetter years are better described by large PPT events with short inter-event periods; in contrast, large PPT events in dry years are almost absent. Therefore in dry years, we expecte that small PPT events with large inter-event periods would limit the Birch effect by maintaining the system below threshold conditions. Consecutive PPT events should keep soil water content above a threshold that will promote C uptake by photosynthesis, which in the long term will overcome C loses from the Birch effect. In the case of wet years, the priming NEE flux will be limited by previously high soil moisture and likely previous high NEE (respiration) rates as a consequence of shorter inter-event periods. It is necessary a further analysis of the effect of these PPT events on vegetation since productivity will also depend on PPT event size and will be modulated by previous soil conditions. Additionally, it is likely that productivity will benefit more on accumulated PPT than respiration. Still, more analysis of projected PPT scenarios is required to forecast accurately the PPT pattern under more frequent droughts, and to know if the current PPT pattern of dry-wet years will prevail. Only after that, we will be able to predict the course of the semiarid grassland as a source or sink of C under PPT pattern changes.

Appendix

Threshold-Delay Model equations

$$y_t = k \cdot y_{t-1} + \delta_t \qquad \text{Eq. A1}$$

were y_t is the variable response (*e.g.* NEE rate) at time t, k describes the reduction of the response variable over time.

$$\delta_t = Min\left[y_{\max} \times (1-k), \delta_t^* \times \left(1 - \frac{y_{t-1}}{y_{\max}}\right)\right] \qquad \text{Eq. A2}$$

where δ_t is the magnitude of the response following the PPT event, and y_{max} is the maximum potential value. The magnitude depends on the prior state (y_{t-1}). The maximum potential response δ_t is given by,

$$\delta_t^* = \left\{ \begin{array}{ll} \frac{\delta_{\max}}{R^U - R^L} \cdot (R_{t-\tau} - R^L) & R^L < R_{t-\tau} < R^U \\ 0 & R_{t-\tau} \le R^L \\ \delta_{\max} & R_{t-\tau} \ge R^U \end{array} \right\} \qquad \text{Eq. A3}$$

were δ_{max} is the maximum response that depends on the size of the PPT event, R^L is the low PPT threshold, R^U is the upper PPT threshold, Rt is the PPT event size at the time *t*, and τ is the time delay between the stimulus and the response.

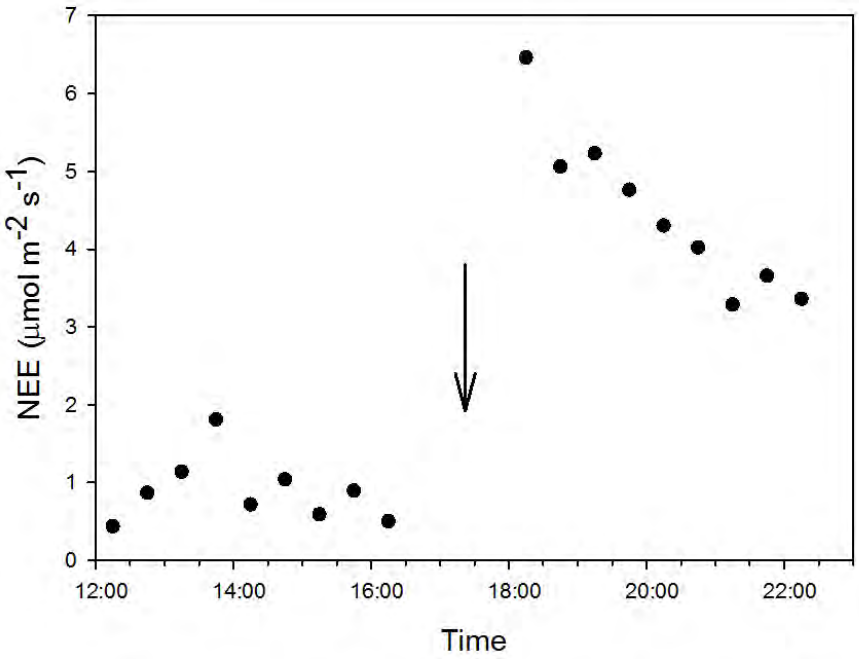

Figure A1. Dynamic of half an hour net ecosystem exchange (µmol m^{-2} s^{-1}) after a precipitation event of 8.12 mm. the arrow indicates the time of PPT event occurrence.

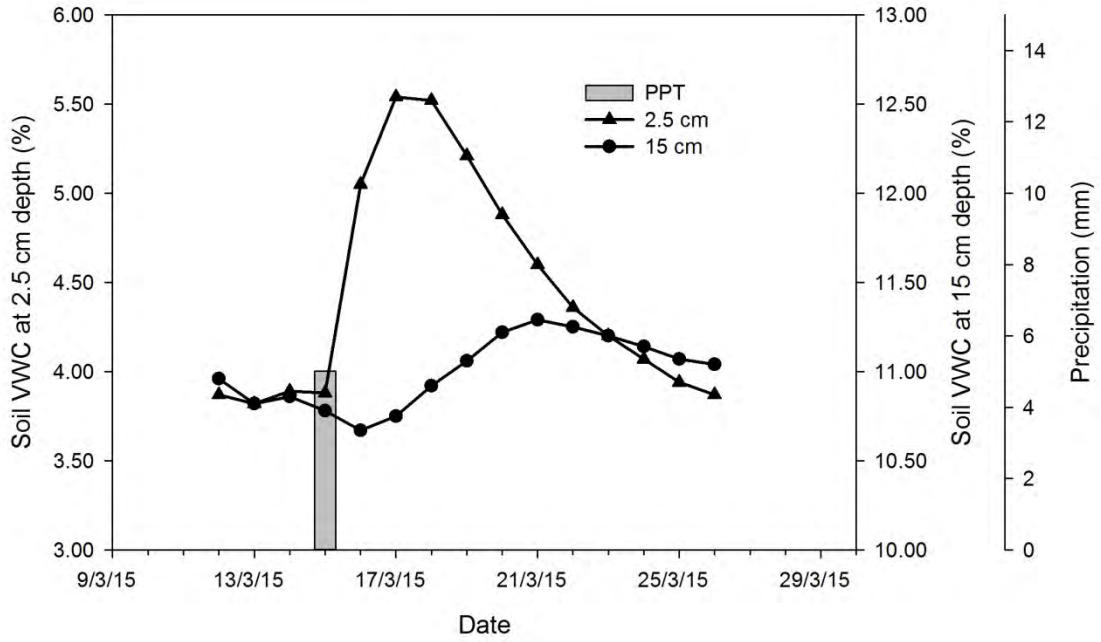

Figure A2. Dynamic of volumetric soil water content (VWC, v/v) at two depths (2.5 and 15 cm) after a small PPT event of 5 mm.

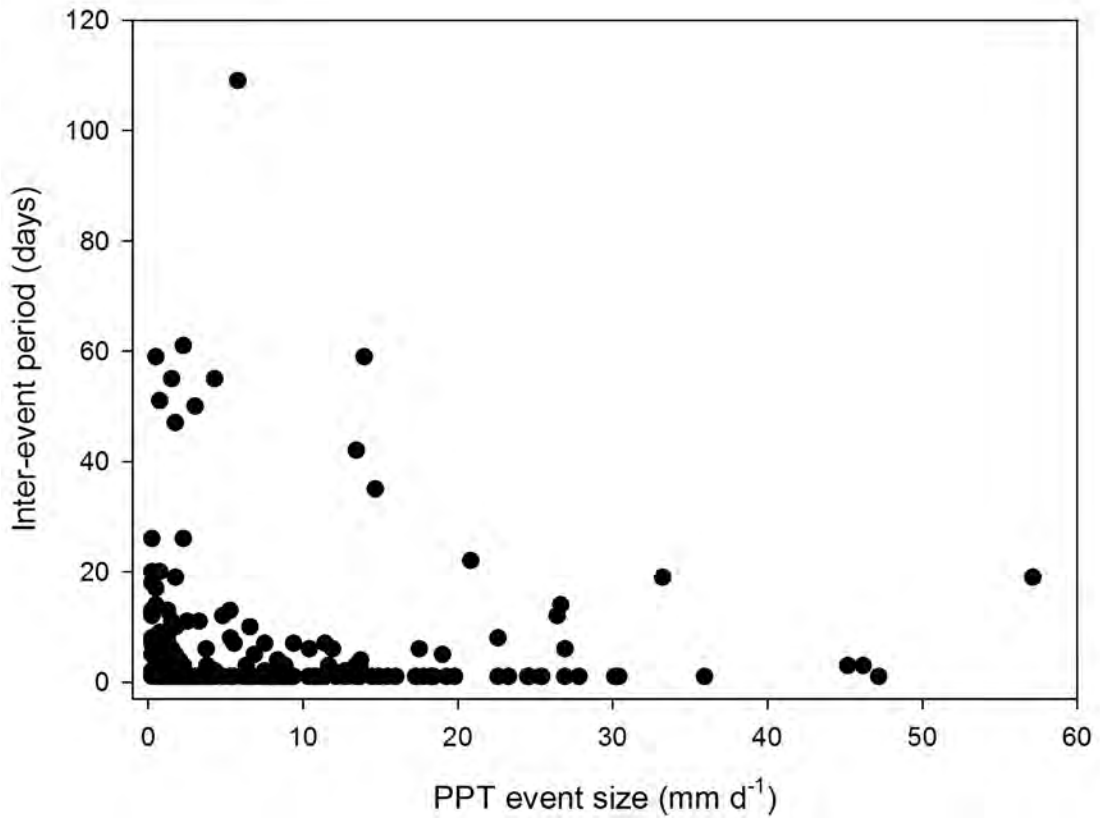

Figure A3. Bivariate relationship between precipitation event size (mm d^{-1}) and the inter-event period between PPT events (days).

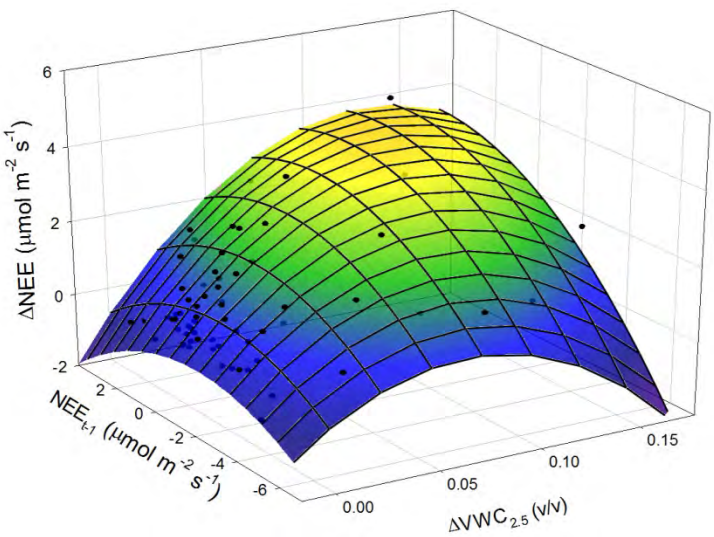

Figure A4. Bivariate relationship among the change of soil VWC at 2.5 cm depth, the previous C flux and the change of NEE after the PPT event adjusted to a quadratic function.

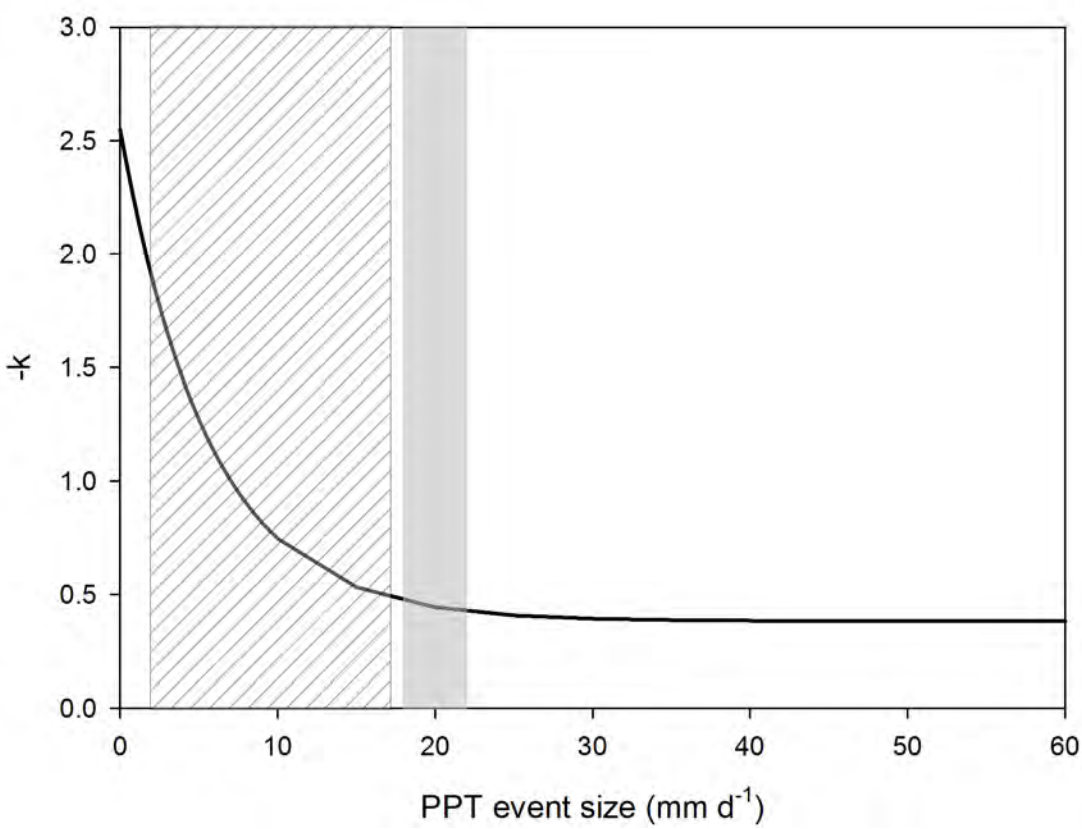

Figure A5. Extrapolation of decaying rates (-k) in the full range of observed PPT events (mm d^{-1}) through the exponential model –k = 0.3821+2.1674*EXP(-0.1785*PPT_event). Shadow section of the figure (diagonal lines) indicates the range of PPT event size used to calculate parameters of the model, and the gray area indicates the range of PPT event size where decaying rates reach a steady state.

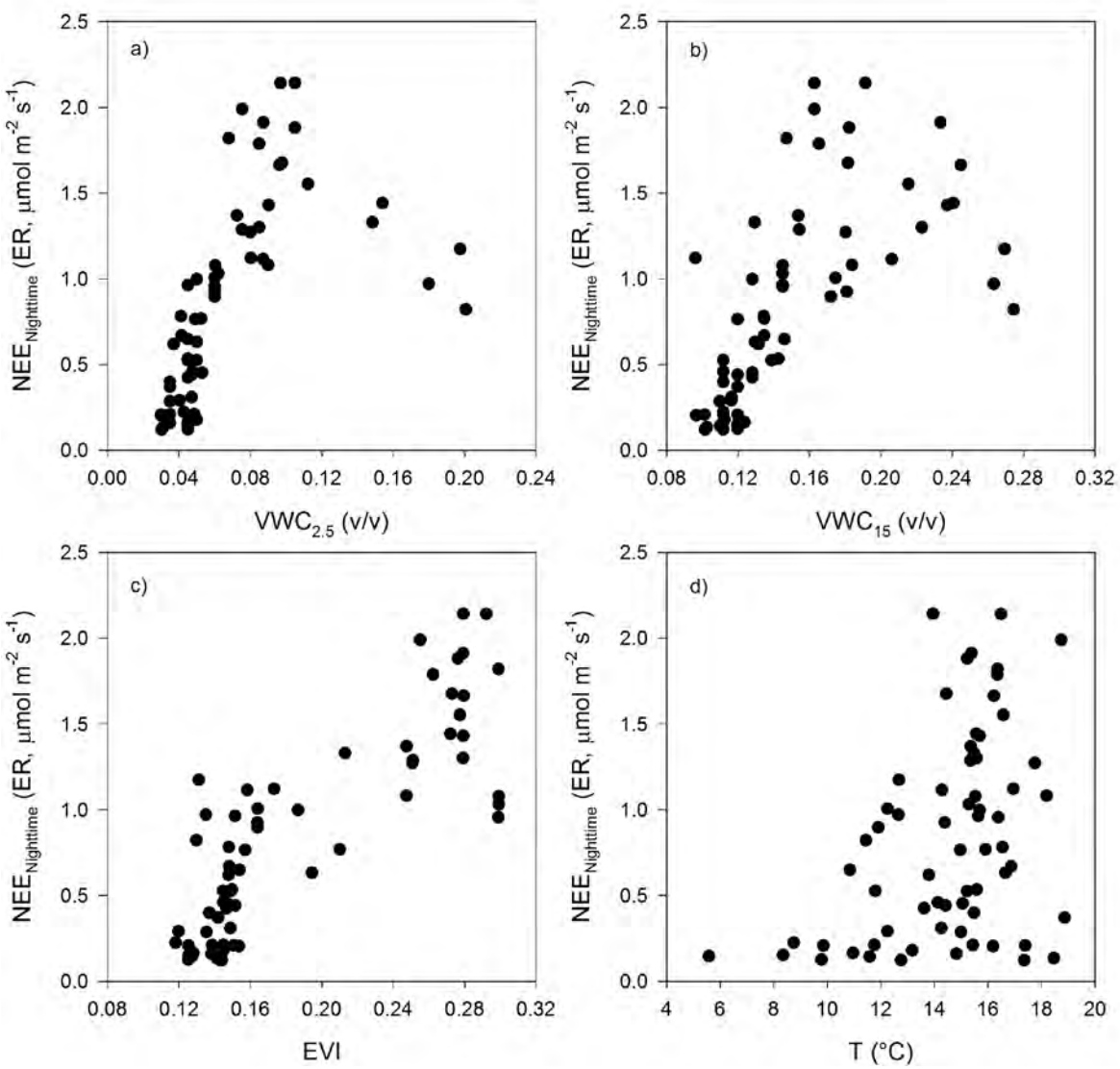

Figure A6. Relationship between nighttime-NEE derived ER and a) the soil volumetric water content at 2.5 cm depth ($VWC_{2.5}$, v/v), b) the soil volumetric water content at 15 cm depth (VWC_{15}, v/v), c) the enhanced vegetation index (EVI), and

d) the air temperature (T, °C).

Table A1. Calculated parameters of exponential decay models (NEE= y_0 + a * Exp(-k*t), means ± 1 SE) for the daytime NEE after a PPT event. Relationship between the PPT sulse size (mm) and the decaying rate of above regressions is presented in the last row with the same negative exponential equation form –k = y_0 + a * Exp(-b*PPT_event), where -k = -b.

PPT event (mm)	$NEE_{t=0}$ (µmol m^{-2} s^{-1})	y_0	a	-k	R^2
13.7	5.5	1.1163 ± 0.0478	4.3853 ± 0.117	0.5274 ± 0.0309	0.99
16.74	5.26	0.3509 ± 0.3148	4.6404 ± 0.4527	0.5028 ± 0.1277	0.95
6.86	2.474	0.0294 ± 0.0517	2.439 ± 0.119	0.9886 ± 0.1189	0.99
10.08	1.947	0.0937 ± 0.0433	1.8862 ± 0.1152	0.7977 ± 0.1109	0.97
2.52	1.3394	0.0265 ± 0.0417	1.3114 ± 0.0944	1.7682 ± 0.4217	0.98
PPT event * -k		0.3821 ± 0.0953	2.1674 ± 0.1381	0.1785 ± 0.0333	0.99

Table A2. Calculated coefficients of bivariate quadratic regressions of Eq. 2, where ΔNEE stands for the change in net ecosystem exchange (µmol m^{-2} s^{-1}), PPT_event is the PPT event size (mm), DSLE is the inter-event period (days), ΔVWC is the change of volumetric soil water content (v/v), prevNEE is the net ecosystem exchange (µmol m^{-2} s^{-1}) previous to the PPT event, and prevVWC is previous volumetric soil water content (v/v).

Model	Parm	Value	SE	t-value	95% confidence limits		P>|t|
ΔNEE X PPT_event X DSLE	a	-0.1739	0.1710	-1.0168	-0.5154	0.1677	0.3130
	b	0.1648	0.0216	7.6178	0.1216	0.2080	0.0000
	c	0.0388	0.0143	2.7164	0.0103	0.0673	0.0085
	d	-0.0031	0.0005	-6.9453	-0.0040	-0.0022	0.0000
	e	-0.0004	0.0001	-2.3979	-0.0007	-0.0001	0.0194
	f	0.0018	0.0007	2.6625	0.0004	0.0031	0.0098

ΔNEE X ΔVWC X PrevVWC	a	1.2896	0.3818	3.3782	0.5246	2.0547	0.0014
	b	-10.1752	6.3150	-1.6113	-22.8308	2.4804	0.1129
	c	68.5215	8.7771	7.8069	50.9319	86.1111	0.0000
	d	24.3958	21.7722	1.1205	-19.2367	68.0283	0.2674
	e	-265.8927	51.6391	-5.1491	-369.3799	-162.4055	0.0000
	f	-164.0469	42.4387	-3.8655	-249.0961	-78.9978	0.0003
ΔNEE X ΔVWC X PrevNEE	a	0.6098	0.1562	3.9044	0.2961	0.9235	0.0003
	b	55.7163	8.3033	6.7101	39.0387	72.3940	0.0000
	c	-0.1520	0.1079	-1.4090	-0.3687	0.0647	0.1650
	d	-260.9974	64.0923	-4.0722	-389.7305	-132.2643	0.0002
	e	-0.0467	0.0239	-1.9587	-0.0946	0.0012	0.0557
	f	3.2041	1.5562	2.0589	0.0784	6.3298	0.0447

References

Aguado-Santacruz, G.A., 1993. Efecto de factores ambientales sobre la dinámica vegetacional en pastizales de los Llanos de Ojuelos, Jalisco: un enfoque multivariable (MSc). Colegio de Postgraduados, Chapingo, México.

Austin, A.T., Yahdjian, L., Stark, J.M., Belnap, J., Porporato, A., Norton, U., Ravetta, D.A., Schaeffer, S.M., 2004. Water pulses and biogeochemical cycles in arid and semiarid ecosystems.Oecologia 141, 221–235. doi:10.1007/s00442-004-1519-1

Bates, J.D., Svejcar, T., Miller, R.F., Angell, R.A., 2006.The effects of precipitation timing on sagebrush steppe vegetation. J. Arid Environ. 64, 670–697. doi:10.1016/j.jaridenv.2005.06.026

Belnap, J., 2003. Microbes and microfauna associated with biological soil crusts. Biol. Soil Crusts Struct.Funct.Manag.167–174.

Bertolin, G.E., Rasmussen, J., 1969. Preliminary Report on the Study of the Precipitation on the Pawnee National Grasslands, Technical report (U.S. International Biological Program. Grassland Biome). Natural Resource Ecology Laboratory, Colorado State University, 34 p.

Birch, H.F., 1964.Mineralisation of plant nitrogen following alternate wet and dry conditions. Plant Soil 20, 43–49.

Borken, W., Matzner, E., 2009.Reappraisal of drying and wetting effects on C and N mineralization and fluxes in soils.Glob. Change Biol. 15, 808–824. doi:10.1111/j.1365-2486.2008.01681.x

Bowling, D.R., Grote, E.E., Belnap, J., 2011.Rain pulse response of soil CO_2exchange by biological soil crusts and grasslands of the semiarid Colorado Plateau, United States. J. Geophys. Res. 116, G03028.doi:10.1029/2011JG001643

Christensen, J.H., B. Hewitson, A. Busuioc, A. Chen, X. Gao, I. Held, R. Jones, R.K. Kolli, W.-T. Kwon, R. Laprise, V. Magaña Rueda, L. Mearns, C.G. Menéndez, J. Räisänen, A. Rinke, A. Sarr and P. Whetton, 2007: Regional Climate Projections. In: Climate Change 2007: The Physical Science Basis. Contribution of Working Group I to the Fourth Assessment Report of the Intergovernmental Panel on Climate Change [Solomon, S., D. Qin, M. Manning, Z. Chen, M. Marquis, K.B. Averyt, M. Tignor and H.L. Miller (eds.)]. Cambridge University Press, Cambridge, United Kingdom and New York, NY, USA.

Collins, S.L., Sinsabaugh, R.L., Crenshaw, C., Green, L., Porras-Alfaro, A., Stursova, M., Zeglin, L.H., 2008. Pulse dynamics and microbial processes in aridland ecosystems: Pulse dynamics in aridland soils. J. Ecol. 96, 413–420. doi:10.1111/j.1365-2745.2008.01362.x

COTECOCA, (Comisión Técnico Consultiva para la Determinación de Coeficientes de Agostadero), 1979. Coeficientes de agostadero de la República Mexicana. Estado de Jalisco. SARH-Subsecretaría de Ganadería, México, D. F.

Concostrina-Zubiri, L., Huber-Sannwald, E., Martínez, I., Flores, J.F., Reyes-Agüero, J.A., Escudero, A., Belnap, J., 2014. Biological soil crusts across disturbance-recovery scenarios: effect of grazing regime on community dynamics. Ecol. Appl. 24, 1863–1877.

Crawford, C.S., Gosz, J.R., 1982. Desert Ecosystems: Their Resources in Space

and Time. Environ. Conserv. 9, 181–195.

Degens, B.P., Sparling, G.P., 1995. Repeated wet-dry cycles do not accelerate the mineralization of organic C involved in the macro-aggregation of a sandy loam soil. Plant Soil 175, 197–203. doi:10.1007/BF00011355

Delgado-Balbuena, J., |Arredondo, J.T., Loescher, H.W., Huber-Sannwald, E., Chavez-Aguilar, G., Luna-Luna, M., Barretero-Hernandez, R., 2013. Differences in plant cover and species composition of semiarid grassland communities of central Mexico and its effects on net ecosystem exchange. Biogeosciences 10, 4673–4690.doi:10.5194/bg-10-4673-2013

Easterling, D.R., Meehl, G.A., Parmesan, C., Changnon, S.A., Karl, T.R., Mearns, L.O., 2000. Climate Extremes: Observations, Modeling, and Impacts. Science 289, 2068–2074.

Farrar, J.F., Smith, D.C., 1976. Ecological physiology of the lichen Hypogymniaphysodes. III. The importance of the rewetting phase. New Phytol. 77, 115–125. doi:10.1111/j.1469-8137.1976.tb01505.x

Fierer, N., Schimel, J.P., 2002. Effects of drying–rewetting frequency on soil carbon and nitrogen transformations.Soil Biol. Biochem. 34, 777–787.

García, E., 2003. Distribución de la precipitación en la República Mexicana. Bol. Inst. Geogr. UNAM, Investigaciones Geográficas 50, 67–76.

Halverson, L.J., Jones, T.M., Firestone, M.K., 2000. Release of Intracellular Solutes by Four Soil Bacteria Exposed to Dilution Stress. Soil Sci. Soc. Am. J. 64, 1630. doi:10.2136/sssaj2000.6451630x

Hao, Y., Wang, Y., Mei, X., Cui, X., Zhou, X., Huang, X., 2010.The sensitivity of temperate steppe CO2 exchange to the quantity and timing of natural interannual rainfall. Ecol. Inform. 5, 222–228. doi:10.1016/j.ecoinf.2009.10.002

Haynes, R.J., Swift, R.S., 1990. Stability of soil aggregates in relation to organic constituents and soil water content. J. Soil Sci. 41, 73–83. doi:10.1111/j.1365-2389.1990.tb00046.x

Heisler-White, J.L., Knapp, A.K., Kelly, E.F., 2008. Large precipitation events increase aboveground net primary productivity in semi-arid grasslands.

Oecologia 158, 129 – 140.

Solomon, S., D. Qin, M. Manning, Z. Chen, M. Marquis, K.B. Averyt, M. Tignor and H.L. Miller (eds.), 2007, Climate change 2007: The physical science basis: contribution of Working Group I to the fourth assessment report of the Intergovernmental Panel on Climate Change. Cambridge University Press, Cambridge, New York, 996 p.

Huxman, T.E., Snyder, K.A., Tissue, D., Leffler, A.J., Ogle, K., Pockman, W.T., Sandquist, D.R., Potts, D.L., Schwinning, S., 2004a.Precipitation pulses and carbon fluxes in semiarid and arid ecosystems.Oecologia 141, 254–268. doi:10.1007/s00442-004-1682-4

Huxman, T.E., Cable, J.M., Ignace, D.D., Eilts, J.A., English, N.B., Weltzin, J., Williams, D.G., 2004b. Response of net ecosystem gas exchange to a simulated precipitation pulse in a semi-arid grassland: the role of native versus non-native grasses and soil texture. Oecologia 141, 295–305. doi:10.1007/s00442-003-1389-y

Jarvis, P., Rey, A., Petsikos, C., Wingate, L., Rayment, M., Pereira, J., Banza, J., David, J., Miglietta, F., Borghetti, M., Manca, G., Valentini, R., 2007. Drying and wetting of Mediterranean soils stimulates decomposition and carbon dioxide emission: the “Birch effect.” Tree Physiol. 27, 929–940.

Killham, K., Firestone, M.K., 1984. Proline transport increases growth efficiency in salt-stressed Streptomyces griseus. Appl. Environ. Microbiol. 48, 239–241.

Kim, D.-G., Vargas, R., Bond-Lamberty, B., Turetsky, M.R., 2012. Effects of soil rewetting and thawing on soil gas fluxes: a review of current literature and suggestions for future research. Biogeosciences 9, 2459–2483.doi:10.5194/bg-9-2459-2012

Knapp, A.K., Beier, C., Briske, D.D., Classen, A.T., Luo, Y., Reichstein, M., Smith, M.D., Smith, S.D., Bell, J.E., Fay, P.A., Heisler, J.L., Leavitt, S.W., Sherry, R., Smith, B., Weng, E., 2008. Consequences of More Extreme Precipitation Regimes for Terrestrial Ecosystems.BioScience 58, 811–821. doi:10.1641/B580908

Knapp, A.K., Fay, P.A., Blair, J.M., Collins, S.L., Smith, M.D., Carlisle, J.D., Harper, C.W., Danner, B.T., Lett, M.S., McCarron, J.K., 2002. Rainfall Variability, Carbon Cycling, and Plant Species Diversity in a Mesic Grassland.Science 298, 2202–2205. doi:10.1126/science.1076347

Knapp, A.K., Hoover, D.L., Wilcox, K.R., Avolio, M.L., Koerner, S.E., La Pierre, K.J., Loik, M.E., Luo, Y., Sala, O.E., Smith, M.D., 2015. Characterizing differences in precipitation regimes of extreme wet and dry years: implications for climate change experiments. Glob. Change Biol. 21, 2624–2633. doi:10.1111/gcb.12888

Knapp, A.K., Smith, M.D., 2001. Variation among biomes in temporal dynamics of aboveground primary production. Science 291, 481–484. doi:10.1126/science.291.5503.481

Kormann, R., Meixner, F., 2001. An Analytical Footprint Model For Non-Neutral Stratification. Bound.-Layer Meteorol. 99, 207–224. doi:10.1023/A:1018991015119

Lado-Monserrat, L., Lull, C., Bautista, I., Lidon, A., Herrera, R., 2014.Soil moisture increment as a controlling variable of the “Birch effect”.Interactions with the pre-wetting soil moisture and litter addition. Plant Soil 379, 21–34. doi:10.1007/s11104-014-2037-5

Lal, R., 2004. Carbon Sequestration in Dryland Ecosystems. Environ. Manage. 33, 528–544. doi:10.1007/s00267-003-9110-9

Lauenroth, W.K., Sala, O.E., 1992. Long-Term Forage Production of North American Shortgrass Steppe. Ecol. Appl. 2, 397–403. doi:10.2307/1941874

Loik, M., Breshears, D., Lauenroth, W., Belnap, J., 2004. A multi-scale perspective of water pulses in dryland ecosystems: climatology and ecohydrology of the western USA. Oecologia 141, 269–281. doi:10.1007/s00442-004-1570-y

Maliva, R., Missimer, T., 2012. Aridity and Drought, in: Arid Lands Water Evaluation and Management, Environmental Science and Engineering. Springer Berlin Heidelberg, pp. 21–39.

Marañón-Jiménez, S., Castro, J., Kowalski, A.S., Serrano-Ortiz, P., Reverter, B.R., Sánchez-Cañete, E.P., Zamora, R., 2011. Post-fire soil respiration in relation

to burnt wood management in a Mediterranean mountain ecosystem.For. Ecol. Manag. 261, 1436–1447. doi:10.1016/j.foreco.2011.01.030

Medina-Roldán, E., Arredondo Moreno, J.T., García Moya, E., Huerta Martínez, F.M., 2007. Soil water content dynamics along a range condition gradient in a shortgrass steppe. Rangel. Ecol. Manag. 60, 79–87. doi:doi: 10.2111/05-219R2.1

Medina-Roldán, E., Huber-Sannwald, E., Arredondo, J.T., 2013. Plant phenotypic functional composition effects on soil processes in a semiarid grassland. Soil Biol. Biochem. 66, 1–9. doi:10.1016/j.soilbio.2013.06.011

Miller, A.E., Schimel, J.P., Meixner, T., Sickman, J.O., Melack, J.M., 2005. Episodic rewetting enhances carbon and nitrogen release from chaparral soils. Soil Biol. Biochem. 37, 2195–2204. doi:10.1016/j.soilbio.2005.03.021

Muñoz-Flores, L., Riego-Ruiz, LR., Arredondo-Moreno, JT., Luna-Luna, M., Argüello-Astorga, GR. and Huber-Sannwald, E. 2014. How grazing and fire regime influence soil biogeochemical cycling in a native grassland in central Mexico. The first global soil biodiversity conference: assessing soil biodiversity and its role for ecosystem services, Dijon, France, 2 – 5 December, 2014

Noy-Meir, I., 1973. Desert Ecosystems: Environment and Producers. Annu. Rev. Ecol. Syst. 4, 25–51.

Ogle, K., Reynolds, J.F., 2004. Plant responses to precipitation in desert ecosystems: integrating functional types, pulses, thresholds, and delays. Oecologia 141, 282–294. doi:10.1007/s00442-004-1507-5

Parton, W., Morgan, J., Smith, D., Del Grosso, S., Prihodko, L., LeCain, D., Kelly, R., Lutz, S., 2012.Impact of precipitation dynamics on net ecosystem productivity.Glob. Change Biol. 18, 915–927. doi:10.1111/j.1365-2486.2011.02611.x

Placella, S.A., Brodie, E.L., Firestone, M.K., 2012. Rainfall-induced carbon dioxide pulses result from sequential resuscitation of phylogenetically clustered microbial groups. Proc. Natl. Acad. Sci. 109, 10931–10936. doi:10.1073/pnas.1204306109

Reichmann, L.G., Sala, O.E., Peters, D.P.C., 2013. Water controls on nitrogen transformations and stocks in an arid ecosystem. Ecosphere 4, art11. doi:10.1890/ES12-00263.1

Reichstein, M., Falge, E., Baldocchi, D., Papale, D., Aubinet, M., Berbigier, P., Bernhofer, C., Buchmann, N., Gilmanov, T., Granier, A., Grünwald, T., Havránková, K., Ilvesniemi, H., Janous, D., Knohl, A., Laurila, T., Lohila, A., Loustau, D., Matteucci, G., Meyers, T., Miglietta, F., Ourcival, J.-M., Pumpanen, J., Rambal, S., Rotenberg, E., Sanz, M., Tenhunen, J., Seufert, G., Vaccari, F., Vesala, T., Yakir, D., Valentini, R., 2005. On the separation of net ecosystem exchange into assimilation and ecosystem respiration: review and improved algorithm. Glob. Change Biol. 11, 1424–1439. doi:10.1111/j.1365-2486.2005.001002.x

Robertson, T.R., Bell, C.W., Zak, J.C., Tissue, D.T., 2009. Precipitation timing and magnitude differentially affect aboveground annual net primary productivity in three perennial species in a Chihuahuan Desert grassland. New Phytol. 181, 230–242. doi:10.1111/j.1469-8137.2008.02643.x

Sala, O.E., Lauenroth, W.K., 1982. Small rainfall events: An ecological role in semiarid regions. Oecologia 53, 301–304. doi:10.1007/BF00389004

Schimel, J.P., Bennett, J., 2004. Nitrogen mineralization: challenges of a changing paradigm. Ecology 85, 591–602.

Thomey, M.L., Collins, S.L., Vargas, R., Johnson, J.E., Brown, R.F., Natvig, D.O., Friggens, M.T., 2011. Effect of precipitation variability on net primary production and soil respiration in a Chihuahuan Desert grassland. Glob. Change Biol. 17, 1505–1515. doi:10.1111/j.1365-2486.2010.02363.x

Turner, B.L., Haygarth, P.M., 2001. Biogeochemistry.Phosphorus solubilization in rewetted soils.Nature 411, 258.doi:10.1038/35077146

Unger, S., Máguas, C., Pereira, J.S., David, T.S., Werner, C., 2012.Interpreting post-drought rewetting effects on soil and ecosystem carbon dynamics in a Mediterranean oak savannah. Agric. For. Meteorol. 154–155, 9–18. doi:10.1016/j.agrformet.2011.10.007

Unger, S., Máguas, C., Pereira, J.S., David, T.S., Werner, C., 2010. The influence

of precipitation pulses on soil respiration – Assessing the “Birch effect” by stable carbon isotopes. Soil Biol. Biochem. 42, 1800–1810. doi:10.1016/j.soilbio.2010.06.019

Van Gestel, M., Merckx, R., Vlassak, K., 1993.Microbial biomass and activity in soils with fluctuating water contents. Geoderma 56, 617–626. doi:10.1016/0016-7061(93)90140-G

Wu, H., Hayes, M.J., Weiss, A., Hu, Q., 2001. An evaluation of the Standardized Precipitation Index, the China-Z Index and the statistical Z-Score. Int. J. Climatol. 21, 745–758. doi:10.1002/joc.658

Wu, Z., Dijkstra, P., Koch, G.W., Peñuelas, J., Hungate, B.A., 2011. Responses of terrestrial ecosystems to temperature and precipitation change: a meta-analysis of experimental manipulation: META-ANALYSIS OF EXPERIMENTAL MANIPULATION. Glob. Change Biol. 17, 927–942. doi:10.1111/j.1365-2486.2010.02302.x

Xu, L., Baldocchi, D.D., Tang, J., 2004. How soil moisture, rain pulses, and growth alter the response of ecosystem respiration to temperature. Glob.Biogeochem. Cycles 18, n/a–n/a. doi:10.1029/2004GB002281

General conclusions

Arid and semiarid ecosystems are hot spots of interannual variability of carbon fluxes at such a degree that drive the interannual variability of the global C sink. Similarly, our study site showed a large variation among years ((-21.6 ± 90.95 g C $m^{-2}y^{-1}$, μ ± S.D.). A longer monitoring assessment should be carried out before we could define the role of the semiarid grassland as a sink or source of C. However, this ecosystem is likely to be C neutral in the long term. On the other hand, we identified air temperature and photosynthetic photon flux density (PPFD) as the main diurnal drivers, whereas soil moisture and vegetation dynamics controlled NEE at seasonal scales. More importantly we identified that the role of the semiarid grassland as source or sink of C depends widely on precipitation but in a more complex relationship to PPT amount and frequency. The importance of the amount and the frequency of PPT was revealed at different time scales. Timing and amount of daily PPT are relevant for the short term C pulses, thus small PPT events after long inter-event periods favor large C pulses into the atmosphere. The seasonal PPT distribution in one year largely determines the annual C uptake of the grassland. These results highlight the interconnectedness of synoptic scale meteorological processes affecting C uptake processes at ecosystem scale (i.e. polar fronts that cause winter PPT with summer monsoons).

More attention should be paid to changes in seasonal PPT patterns promoted by climate changes in arid and semiarid ecosystems, rather than only annual amount of PPT in the growing season. That is especially important since forecasted reductions of winter precipitation in Mexico at the end of this century might trigger larger C release than expected by mean annual PPT reduction. Adverse climatic conditions in the future will threaten even more the persistence of the semiarid grassland in Mexico under the current degraded conditions that have resulted from overgrazing and agricultural practices.